DESIGN OF AND DECENTRALIZED PATH PLANNING FOR PLATOONS OF MINIATURE AUTONOMOUS UNDERWATER VEHICLES

by

CALEB ALLEN SYLVESTER

A thesis submitted to the Faculty of
Virginia Polytechnic Institute and State University
in partial fulfillment of the requirements for the degree of

MASTER OF SCIENCE
in
ELECTRICAL ENGINEERING

Dr. Daniel Stilwell, Chair
Dr. William Baumann
Dr. Krishnan Ramu

15 September 2004
Blacksburg, Virginia

DESIGN OF AND DECENTRALIZED PATH PLANNING FOR PLATOONS OF MINIATURE AUTONOMOUS UNDERWATER VEHICLES

Caleb Allen Sylvester

ABSTRACT

Many successful control schemes for land-based or air-based groups, or platoons, of autonomous vehicles cannot be implemented in underwater applications because of their dependence upon high-bandwidth communication. In current strategies for controlling groups of autonomous underwater vehicles (AUVs), platoon size remains limited by communication bandwidth requirements. So, there is great need for advances in low-bandwidth control techniques for arbitrarily large platoons of AUVs.

This thesis presents a new approach to multiple vehicle control. The concepts described herein enable an arbitrarily large platoon to be controlled while utilizing minimal inter-vehicle communication. Specifically, this thesis examines a sufficient condition on platoon commands in order for a low-bandwidth decentralized controller to exist. Knowing from this sufficient condition the necessary general form of platoon commands, a number of higher-order statistics were tested. This thesis describes and analyzes their utility as platoon commands. In addition to these theoretical developments, this thesis presents the practical design needs for the Virginia Tech miniature autonomous underwater vehicle as well as their resolution.

Contents

List of Figures

List of Tables

Chapter 1

Introduction

The Virginia Tech miniature autonomous underwater vehicle has been developed by the Autonomous Systems and Controls Lab (ASCL) of Virginia Polytechnic Institute and State University. Research and development objectives of the ASCL include: to develop and exhaustively field-test a low-cost, small, autonomous underwater vehicle; and to develop control algorithms suitable for adaptive sampling and managing arbitrarily sized platoons of multiple cooperating AUVs.

To these ends the ASCL has made sizable progress. The current vehicle costs less than six thousand dollars, is 32 inches long by 3.75 inches in diameter, has a mass of less than five kilograms, and is currently capable of being deployed in a variety of dynamic environments (quarries, large lakes, rivers) in which it can autonomously execute prescribed missions. In the ways of control strategies, the ASCL has developed navigation strategies for single vehicles equipped only with economic, off-the-shelf navigation instrumentation. It has also developed methods for an AUV to determine local water currents in order to incorporate current effects into heading control and path planning [1]. Currently, real-life communications issues are beginning to be considered, an understanding of which is important as the ASCL looks to soon expand experimental capabilities to multiple vehicles.

Two other keys to expansion are addressed by this thesis: AUV construction and generalizable platoon control. This thesis' first main contribution is the mechanical design considerations, including design objectives, fabrication notes, and lessons learned. The second main contribution is an investigation of decentralized, low-bandwidth control of an arbitrarily large platoon of autonomous robots. Redundant manipulator techniques have been shown to be highly effective in their application to the problem of cooperative control. This technique produces stable results and robust control and eliminates the need for much communication.

The remainder of this thesis is organzied as follows. Chapter Two describes how each AUV com-

ponent meets certain design requirement. Chapter Three presents the foundation of this thesis, the adoption of redundant manipulator techniques to multi-vehicle control, and then discusses other attempts to achieve multi-robot cooperation. Chapter Three concludes by stating a sufficient condition required of platoon commands for a decentralized, low-bandwidth controller to result. Chapter Four explains several types of command functions and the emergent vehicle and platoon behaviors that they produce - approximations of specific probability distribution functions, central and spatial moments, and Hu's invariant moments. Chapter Five closes with concluding remarks about the findings in Chapter Four. Appendices include the process of constructing a VT miniature autonomous underwater vehicle (Appendix A), mechanical drawings of parts contracted to be professionally machined (Appendix B), and vendors and prices of required parts (Appendix C).

Chapter 2

Parts Required by the VT Miniature Autonomous Underwater Vehicle

2.1 Introduction

All components and support structures composing the VT miniature AUV fall into one of three categories. The first consists of thirteen high-precision machined parts. These are fabricated by a professional machinist. The second consists of low-cost off-the-shelf components; and the third is comprised of custom made parts fabricated from readily available materials by members of the ASCL. This portion of the thesis reviews the specifications and intended uses of each component in the vehicle. The process of constructing the AUV is fully presented in Appendix A. The author executed each of these steps in order to build the current VT miniature AUV. Pertinent mechanical drawings (for parts contracted for machining) are included in Appendix B. All vendor and pricing information is provided in Appendix C.

2.2 Components

Figure 2.1 displays the *propellor* currently employed by the VT miniature AUV. It has a 5" diameter and a 2" pitch. A propellor's pitch is measured in units of distance and indicates the distance travelled after one propellor revolution. So, for a given propellor diameter, there exist several pitch configurations of the blades. Appropriate diameter and pitch are selected according to vehicle shape and size, power limitations on the AUV, desired mission length, desired mission types, and the size, mass, and mounting configuration of payload sensors. Note that there are differences between 2- and 3-blade configurations.

Since the AUV is only 3.75" in diameter, the propellor must not have too large a diameter or else it would catch on objects or debris that would otherwise not hinder its movement. Figure 2.1 shows that the propellor's diameter is less than the AUV's greatest width - the distance between the tips of any two fins - and only 1.25" greater than the vehicle's diameter, so a 5" diameter meets the size requirement on the propellor. Since the vehicle's ability to dive depends not only on fin positions but also on propellor thrust, the propellor is required to provide as much thrust as possible. Another member of the ASCL tested four propellors and found the 5" diameter, 2" pitch propellor to provide the most thrust.

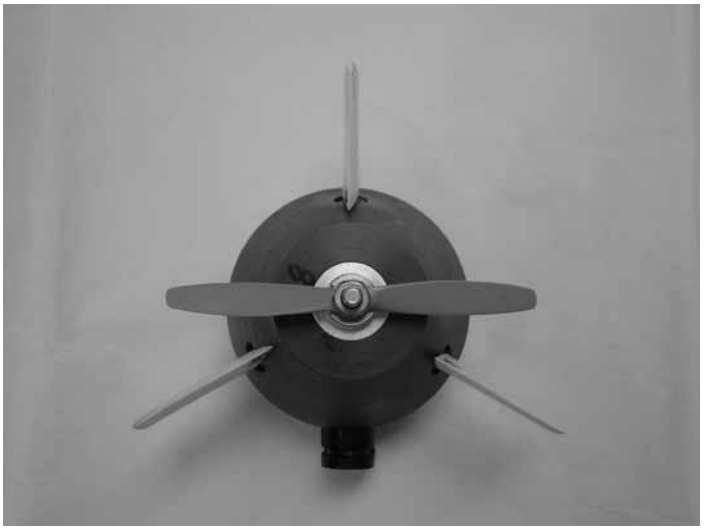

Figure 2.1: Propeller profile: 2 blade, 5 inch diameter

The *driveshaft* was designed by the author (primarily) and another member of the ASCL. The exterior portion of the driveshaft is shown on the right in Figure 2.6, having the propellor mounted to it. A mechanical drawing of the driveshaft appears in Appendix B. It must connect the propellor to the DC brushless motor inside the AUV. The driveshaft is required to be strong, corrosion resistant, and resistant to long-term wear. Stainless steel is used to meet all three of these objectives. There are three main characteristics of the driveshaft that define its functionality and durability, each of which denotes specific sections of the driveshaft. The sternmost section is made to have a 1/4-20 thread, which provides the propellor and the propellor's securing nut and clamp a secure surface to screw onto. The middle section must maintain a high integrity rotary seal between the surface of the driveshaft and two o-rings (o-rings are stationary, driveshaft rotates in one direction), so the driveshaft is made to have a maximum surface finish of 32 rms (micro-inches of surface roughness). Lastly, the bow most section consists of a flat spot cut into the cylindrical driveshaft. This flat spot serves as a stable surface

into which a set screw can be driven.

The requirement of a solid connection between the driveshaft and the DC motor is met by three parts: the driveshaft coupler, the dogbone (Figure 2.3), and the motor coupler (Figure 2.2). The author designed both of these couplers (the latter is simply a larger version of the former); their mechanical drawings are in Appendix B. The *driveshaft coupler* connects to the flat spot on the bow most end of the driveshaft. The driveshaft coupler is shown mounted to the driveshaft in (Figure 2.5) in the picture to the right. The *motor coupler* connects to the shaft of the DC motor. For its strength and resistance to corrosion and deformation, stainless steel is used to make both components. These pieces are required not to slip along or revolve about the driveshaft or the DC motor shaft. To prevent slippage, the couplers have keyed inner diameters that allow the respective shafts to enter the couplers only to a certain depth. A set screw prevents revolution about the driveshaft and motor shaft. These couplers must also support and securely hold the dogbone piece between them, so both have keyed slots into which the dogbone fits.

Figure 2.2: Two motor couplers, showing set screw holes

The *dogbone* piece is displayed in Figure 2.3. The dogbone must be highly resistant to deformation in order to maintain a sturdy connection along the drivetrain. The author selected this specific dogbone piece because it is (believed to be) made of stainless steel. It is 83 mm long; the driveshaft and motor coupler dimensions were based partially on the availability of this length of dogbone. The dogbone has small wings on each end that fit into the slots on the couplers.

The *DC motor* is a 24V servo motor made by Shinano Kenshi. Its rated speed and power are 3000 RPM and 40W.

Figure 2.3: Dogbone shown next to slots into wich it mounts on motor coupler

The driveshaft mounts in a component called the *driveshaft housing*, which the author designed (see Appendix B). The driveshaft housing cannot be too heavy (as its location in the tail section enables it to easily create a moment on the AUV) and is required to be corrosion resistant. Aluminum construction meets both of these needs. This housing is also responsible for holding two o-rings and two bearings for the driveshaft. The housing contains two o-ring grooves, both of which have a 32 rms surface finish and dimensions specified for the appropriate o-rings to maintain water tight rotary seals with the 32 rms surface finish of the driveshaft. The o-rings are BUNA-010 quad rings.

Each end of the driveshaft housing is fitted with a *stainless steel ball bearing*. Since the o-rings in the driveshaft housing do not bear the load of maintaining perfect driveshaft rotation, bearings are used to keep the driveshaft lodged securely in the housing. They keep the shaft from pitching or yawing within the housing. The author selected a stainless steel bearing because of its strength, durability, and resistance to corrosion. Compared to nylon bearings, the stainless steel component has a much more durable low-friction spin, which is necessary for reliable long-term use. One side of the bearing is shielded from dirt; the other side is left open to make convenient the application of lubricating and cleaning agents.

The driveshaft housing and its contents are mounted in the rear of the *tail section* of the vehicle, shown in Figure 2.5. Though in cooperation with one other ASCL graduate student, the author was primarily responsible for designing the tail. A mechanical drawing of the tail is in Appendix B. The main requirement of the tail is that its material be strong enough to support not only the objects known to be mounted in the tail (e.g., fins), but also components made necessary by future mission

requirements. To meet this requirement, non-cellcore PVC is used to make the tail because its density, and consequently its strength, are greater than that of cellcore PVC. Cellcore PVC, known simply as PVC, is less dense than the non-cellcore type because air is injected in the PVC, creating tiny air bubbles throughout. The non-cellcore variety is desirable because it is strong enough to maintain high integrity threads and hole shapes. Specifically, the tail piece supports the driveshaft housing, all three finshaft housings, the bulkhead connector, the GPS and RF antennas, and the static o-ring seal with the hull. It also supports the weight of the remaining vehicle, as all electronics, motors, batteries, etc. ultimately mount to the tail section. Figure 2.4 shows the set of brackets to which the internal components of the vehicle mount and how these brackets screw into the tail.

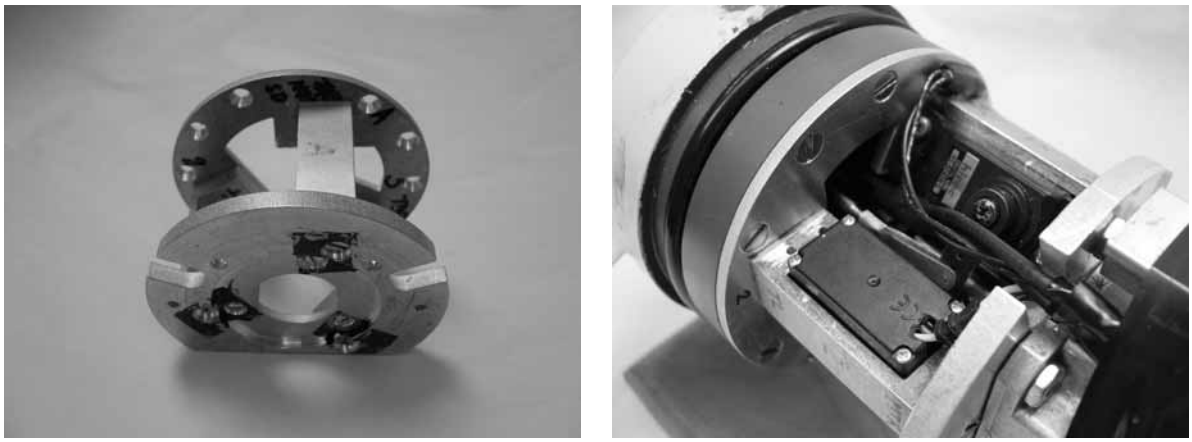

Figure 2.4: Set of brackets to which electronics mount; their mounting to tail

The following description of the tail section provides details of its design features. Mounting certain components in the tail requires the following 16 sets of holes or cuts. The first is the driveshaft housing hole. The second, third, and fourth compose an evenly spaced 360 degree array of fin mounting holes. The fifth is the hole for a bulkhead connector on the bottom of the AUV. The area around this hole is surrounded by a flat spot shaved into the cylindrical circumference of the tail. The flat spot supplies a flush surface against which the bulkhead connector can create a dependable seal. The sixth cut is an o-ring groove required for a static hull seal. This groove has a 32 rms surface finish and has dimensions specified for statically sealing a 3.5" opening. The o-ring used to seal the hull is a BUNA-010 o-ring. Based on the desired inner hull diameter, the necessary o-ring is determined by the *Parker O-Ring Handbook, 2001 Edition*. The seventh cut is the diameter of the portion of the tail (referred to as the plug) that fits into the hull (referred to as the bore). The *Parker O-Ring Handbook* specifies the clearance between the plug and the bore. However, inaccuracy in the manufacture of the hull's inner diameter create slightly small and/or slightly elliptical diameters. To compensate, a professional

machinist makes the tail to meet bore and plug specifications and then custom fits each tail section to a certain hull, trimming slightly the plug diameter if necessary. This custom trimming does not degrade sealing integrity because the o-ring groove diameter is not changed. Finally, the last nine holes are drilled and tapped (made to have threads) for 3/8 inch 6-32 screws. These holes are spaced so as to evenly distribute the stress endured by the PVC in supporting the remaining AUV components (Figure 2.5).

Figure 2.5: Tail section details

The tail hosts an evenly spaced array of three fin mounting holes (Figure 2.1). Each of these holes contains a *finshaft housing*. Denoted by the letter A in (Figure 2.5), this view shows a finshaft housing mounted in the tail with a fin inserted in the housing. The author and one other ASCL graduate student designed the finshaft housing. A mechanical drawing of the finshaft housing is in Appendix B. This piece is made of aluminum in order to reduce the weight of the tail and to be corrosion resistant. The main design requirement of the finshaft housings is that they *not* have o-rings mounted inside. These housings are considerably smaller than the driveshaft housing, so actually getting very small o-rings inside these pieces would be *very* difficult. And these o-rings require routine maintenance, so o-rings are mounted on the finshafts, which are removed quite easily. The finshaft housings are specified by their appropriate fit within and spacing around the tail, their inner diameter, and the 32 rms surface finish of the inner diameters.

The finshaft housing supports the *finshaft*, which was designed by the author and one other ASCL graduate student. The finshaft is displayed in both its mechanical drawing in Appendix B and in Figure 2.7. The finshaft must be able to withstand substantial forces from striking objects in the AUV's task space. The strength of stainless steel meets this requirement and actually provides enough flexibility for the fins to bend and to be bent into realignment. The finshaft has three main characteristics,

each of which correlates to specific sections of the finshaft. Since the finshaft must connect securely to a servo motor, the finshaft's innermost end has a flat spot cut into it, which matches with a set screw. The finshaft's middle section has in it two small o-ring grooves with a 32 rms surface finish. These maintain a watertight oscillating seal (the finshaft housing rotates in both positive and negative directions relative to the o-rings). The o-rings are BUNA-006 quad rings. Lastly, the exterior section consists of a rough surfaced, squared, T-shaped length of steel. Previous finshafts were simply thin, smooth, cylindrical rods that did poorly to adhere to fin material. To make sure the plastic fins do not slip off of the finshaft, the new finshaft is much larger, T-shaped, and rough surfaced. The finshaft must be kept from slipping in and out of its housing. The flat spot and set screw keep the shaft from sliding to the outside of the AUV; there is a lip along the shaft prevents it from sliding down into the vehicle (Figure 2.7).

Fins (see Figure 2.6) must be repeatability and quickly made (in case a new fin has be made during a deployment). They must also be hard (so they do not tear or deflect) but easily reshaped with a knife (because of needing to fit along the uniquely sloped circumference of the tail). A Polytek Development Corporation plastic meets these objectives. It is the congealed mixture of two liquid agents: one a plastic and one a hardener. The mixture is easy to work with and takes only about two minutes to begin to set and 30 minutes to cure. A former ASCL graduate student built a mold that is used to produce one fin at a time. The mold is small, so it can be taken anywhere, and the selected plastic produces durable but easily reshaped fins.

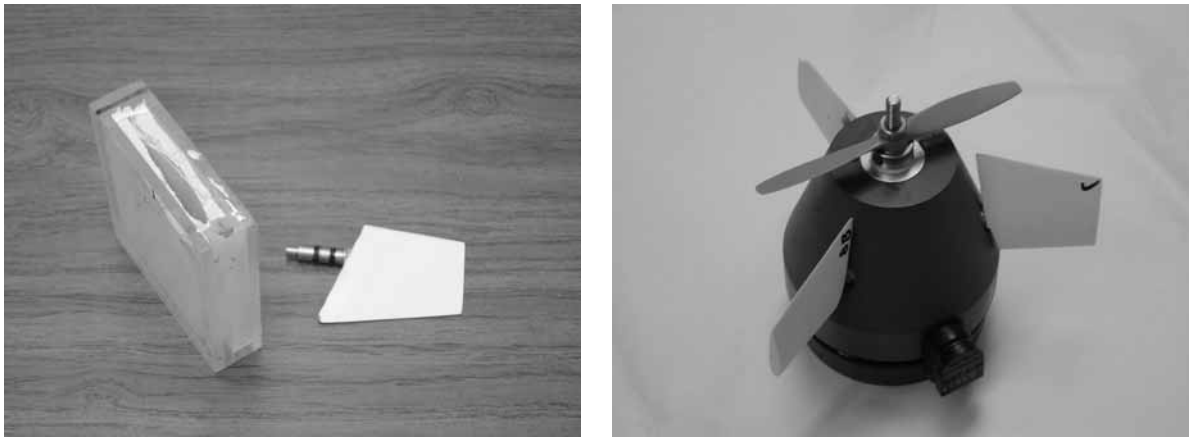

Figure 2.6: Fin details

Shown in Figure 2.7, the *fin crank* is the last component related to the fin arrangement. It was designed by the author and one other ASCL graduate student; its mechanical drawing is shown in Appendix B. The fins are connected to servo motors by rods called linkages. The fin crank must

reliably connect the linkages to the finshafts, must not deform, and must enable the fins to respond quickly and precisely to servo actuation. To keep from deforming and wearing, it is made of stainless steel. The crank holds a set screw that matches the finshaft's flat spot, thus keeping the crank from revolving about the finshaft. The security provided by the steel and the set screw guarantee that the fins respond appropriately to actuation. Figure 2.7 shows the fin crank as it properly mounts to the fin shaft.

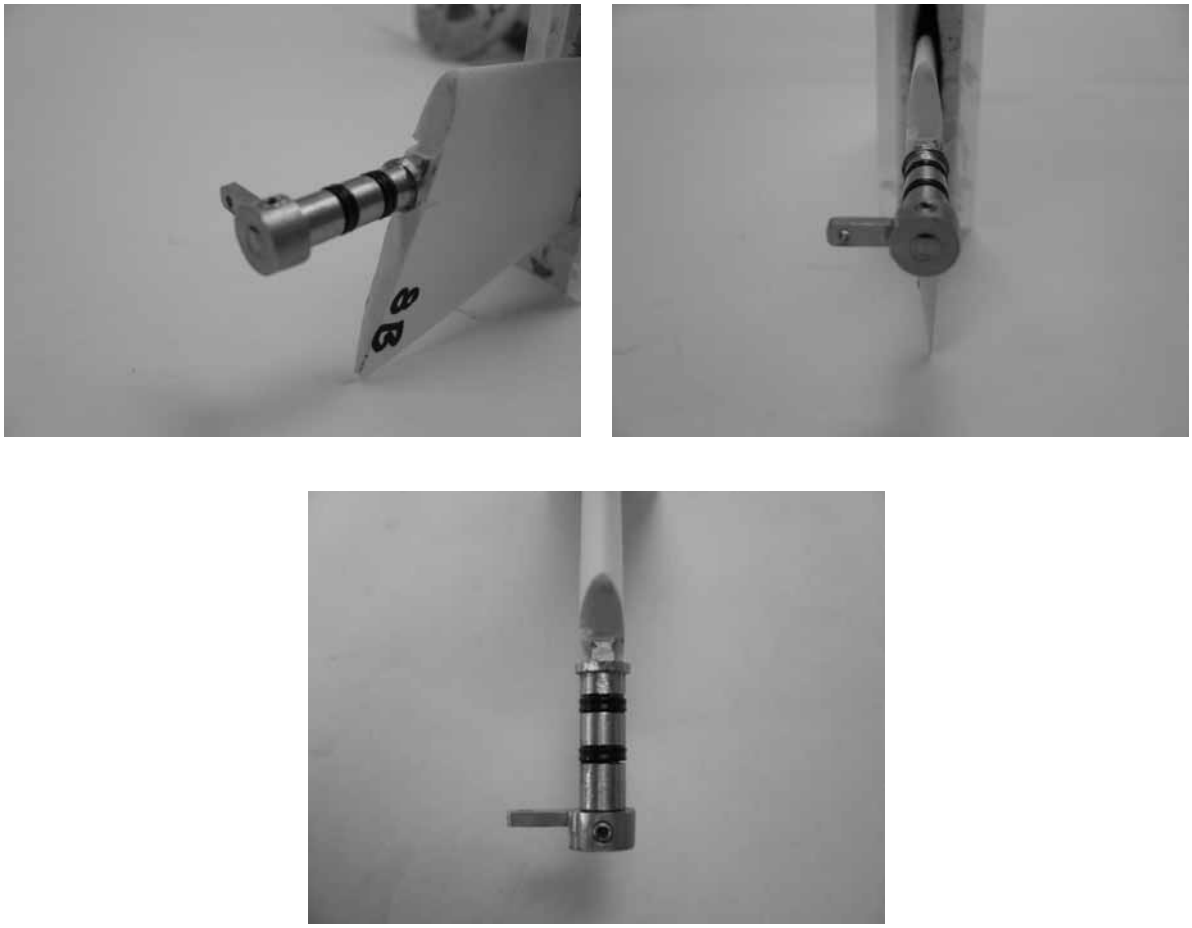

Figure 2.7: Fin crank details

A *bulk head connector* attaches to the bottom of the AUV (Figure 2.1). This connector is required to have a size and form compatible with the AUV, to have enough electrical connections for all externally connected electronics, to provide a reliable connection to the vehicle, and to be at least moist mateable (which means that it requires some lubrication to connect and can be connected while still wet but cannot be connected and disconnected while fully submerged). The 10 pin, moist mateable SeaCon brand bulkhead connector was selected for its combination of size, form factor, electrical connections, and mateability. Only four of the pins are used, so the 10-pin model can be utilized if ever more power

or sensory resources are attached to the AUV's exterior. The connector has an o-ring that sits flushly against the tail's flat spot and a threaded post that enters the tail. The connector is easily bound to the tail by a washer and nut on the tail's interior. Being 18" long, the connector's ten wires easily route to connectors in the AUV. Figure 2.5 shows the bulkhead connector as well as the wires entering the AUV.

The ASCL fabricates its own *servo linkages*, which connect the fins to their corresponding actuators. The author designed the linkage mechanism, which is shown in Figure A.5 in Appendix A. These linkages are required to deform as little as possible, to have an adjustable length, to connect with no slippage to both the fin crank and the servo arm, and to endure continual use over long periods of time. An AUV linkage is built from two different remote control class linkage models. The author selected these two linkage types because one provides necessary rigidity and the other provides a necessary type of connector. Linkage rigidity is derived from the primary linkage, which is made stiff by the overlaying of three layers of material (instead of the more typical two layers): a piano wire core is stabilized by a plastic sheath, the combination of which is reinforced by another stiffening sheath. This primary linkage already has a clevis (clip) on one end with a finely threaded connection to the linkage, so the variable length requirement is met by this feature of the primary linkage. The threaded clevis attaches to the servo arm so that length adjustments can be made conveniently each time the fin positions need to be manually calibrated. The secondary clevis is useful because it is stationary, as opposed to the adjustable primary clevis, so it is connected to the fin crank in the much less accessible rear of the tail. The secondary clevis fits tightly in the fin crank; the primary clevis fits with very little slip in the servo arm, so slippage is minimzed and each fin's response remains quick and accuurate.

One *digital servo* controls each fin linkage and fin. The author researched digital servos and provided sizing and technical information necessary to make the selection of the HS-5245MG, made by HiTec. Digital servos are used because they actuate and hold their position with much more accuracy than analog servos. The AUV needs the most precise and fastest actuation possible, which digital servos supply. The servos must generate high amounts of torque because of previously unsatisfactory performance of lower torque models and the possibility of encountering debri blockages or strong hydrodynamic forces on the fins. Another restriction upon servo selection was that the chosen configuration for mounting servos in the AUV was size prohibitive. The HS-5245MG sufficiently balances the needs for high torque and low volume. The HS-5245MG also has high quality metal gears, a dual ball bearing for bearing loads on the shaft, and a metal arm. Metal gears are more rugged than nylon (or resin) gears; and the metal arm is important because it does not deflect and wear like the nylon arms.

Servo trays hold the servos in place (Figures 2.8). The author devised the idea for and the mounting configuration of the servo trays. The author and another ASCL graduate student designed this component. The mechanical drawing for the servo tray is in Appendix B. Each tray is required to fit snugly around a servo in order to keep the servo from twisting and shifting. And the combination of all three servo trays is required to create a strong support structure between the tail section and the front portions of the vehicle. The snug fit requirement is met by machining the trays to proper dimensions. The strength of the support structure is achieved by the manner of screwing the trays to the servo and motor brackets (Figure 2.8). Since there remains a need to keep this portion of the vehicle from being too heavy, aluminum is used to make the servo trays. Though aluminum is softer than steel, the configuration of the three servo trays offers a great deal of structural integrity to the vehicle (Figure 2.8).

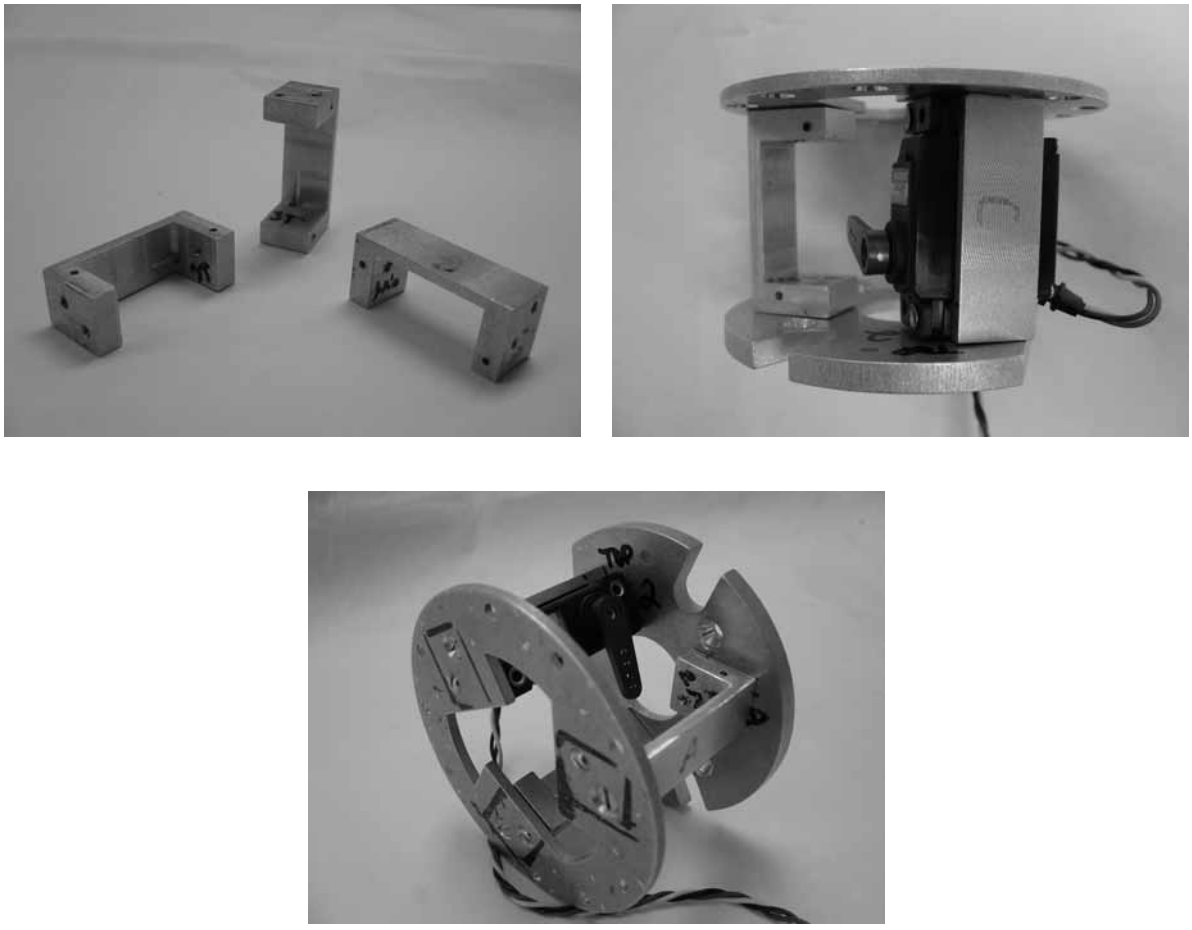

Figure 2.8: Servo tray details

The servo trays connect to the *servo bracket* (Figure 2.9) on the tail side and to the motor bracket (Figure 2.10) on the nose side (Figure 2.8). Both of these brackets serve significant purposes in the

structural integrity of the vehicle. The author and one other ASCL graduate student designed these brackets; their mechanical drawings are in Appendix B. To keep from adding excessive weight to the tail, both brackets are made of aluminum. The thickness of these brackets makes them strong enough to hold screws with high integrity and to contribute much strength to the tray/bracket structure shown in Figure 2.8. The servo bracket must connect to the tail section without damaging the tail's soft PVC, so an arrangement of nine screws is used to distribute the strain on the PVC. The servo bracket's nine holes must match perfectly the tail's nine holes. Also, the servo bracket must have not only enough surface area for the servo trays to mount to, but also enough material removed from its center for the drivetrain, servo linkages, bulkhead connections, and GPS and RF antennas, to pass through it without interfering with one another. All of these requirements are met by the unique shape of the servo bracket, which is displayed in Figure 2.9.

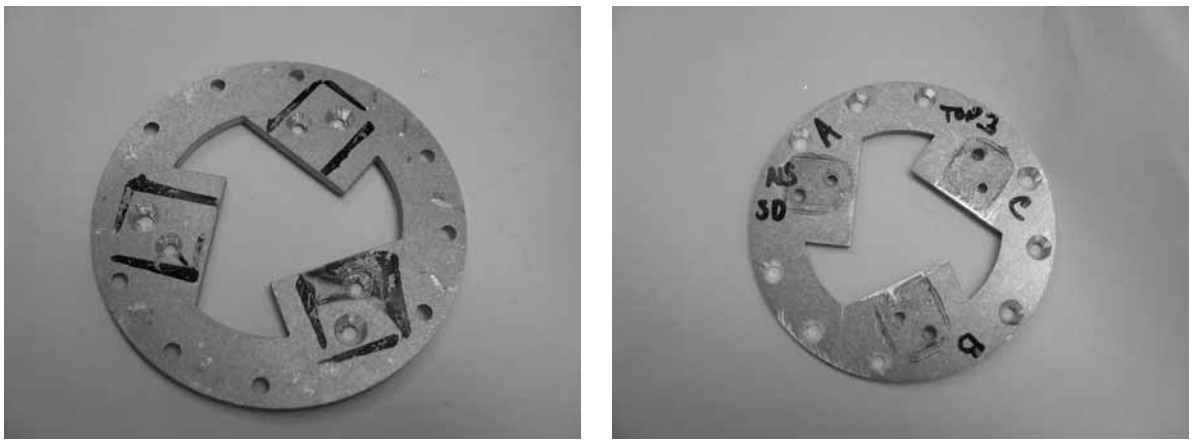

Figure 2.9: Servo bracket details

The author and another ASCL graduate student designed the *motor bracket*, displayed in Figure 2.10 and its mechanical drawing in Appendix B. There are five main requirements of the motor bracket. The first is that it have a keyed fit with the face of the motor, which ensures that the motor shaft is on the center axis of the vehicle as long as the motor bracket is attached in proper alignment to the servo trays. The second requirement is that there be sufficient material for all of the servo trays to securely connect to the motor bracket. The third is that it have four correctly placed holes by which to symmetrically attach the motor. The motor bracket must also supply enough stability to securely hold the rails on which all of the AUV electronics are mounted. So, in combination with a small connecting piece of aluminum called the rail brace, the motor bracket supports the rails and all of the electronics. And lastly, the motor bracket must not fully block the entire cross-sectional area of the vehicle's inner diameter because wires must pass between the tail and the electronics section of the vehicle. The holes

and the face mounting surface for the motor are displayed in Figure 2.10.

Figure 2.10: Motor bracket details

The current VT miniature AUV was required to be shorter than previous ASCL vehicles. Part of the solution to shorten the vehicle was to change the manner in which electronics are mounted inside. The previous vehicle employed aluminum rails that extended along the sides of the AUV, which provided room enough for circuit boards to be mounted in stacks of two. A vertical rail system was chosen for the latest vehicle in order to stack more than two cards. The rails are plumb with one another and extend along the top and bottom of the AVU, from the motor bracket to the nose. Aligning the rails vertically and inserting vertical supports along the length of the vehicle allows cards to attach to the vertical supports and to be layered in compact stacks. The *rails* are required to be low profile in order to minimize their space requirement. They must also resist deformation but consist of material that is relatively easily machined. Once the vertical rail system was conceptualized, the author designed the rail and rail support configuration and designed and selected the necessary parts and materials. Each rail is a piece of aluminum stock, 3/4" wide by 1/8" thick. The low-profile 1/8" thicknes keeps the rails from taking too much vertical space. And though the aluminum is thin, the 3/4" width is sufficient to keep the rails from flexing from side to side. Deformation in the vertical direction is prevented by the vertical supports. Being such thin aluminum, the pieces selected are easily drilled with holes and cut to length. Six support screws are set along the length of the rails; they are appropriately spaced for the sizes of necessary circuit cards. The author selected stainless steel 6-32 screws for mounting circuit boards and to create a sturdy AUV body. Figure 2.11 shows the nose end of the rails, which is secured by a final support screw and a special aluminum brace used to brace the open nose end.

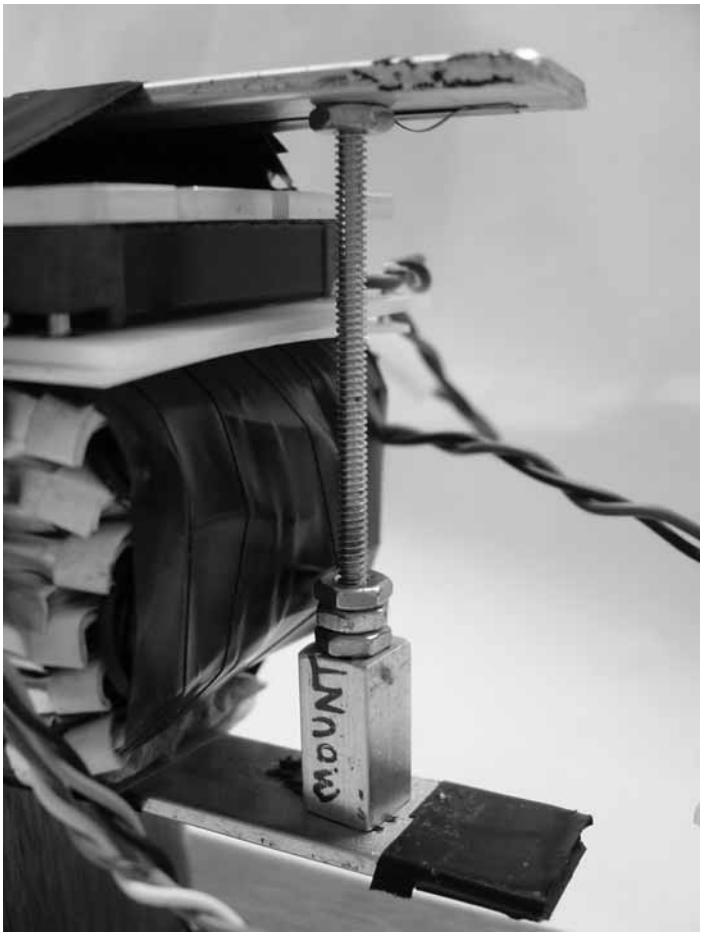

Figure 2.11: Rail details

The rails are connected to the motor bracket by two *rail braces*. The author designed the rail brace, which can be viewed in Figure 2.12 or in its mechanical drawing in Appendix B. The rail braces hold the rails perpendicularly to the motor bracket (Figure 2.12). By connecting the rail brace to the motor bracket, and the rail to the rail brace, the rail is ultimately supported by the motor bracket. Since the space available for such connection is limited, the rail braces must be small. They must also connect to the rails in such a way that the rails do not shift or slip along the surface of the rail braces. They must also be light weight. The brace is optimally sized to allow the rails to run along the very edge of hull's inner diameter, which leaves the maximum amount of space for stacking electronics. If the rail and rail brace are connected with only one screw, the rail is able to rotate about the screw. To prevent this, the brace has two screw holes that are matched with holes drilled in the rail. Aluminum is used to make the rail braces because it is light. Figure 2.12 shows where the braces connect to the motor bracket.

To minimize vehicle length, electronics must be mounted compactly (Figure 2.13). The author

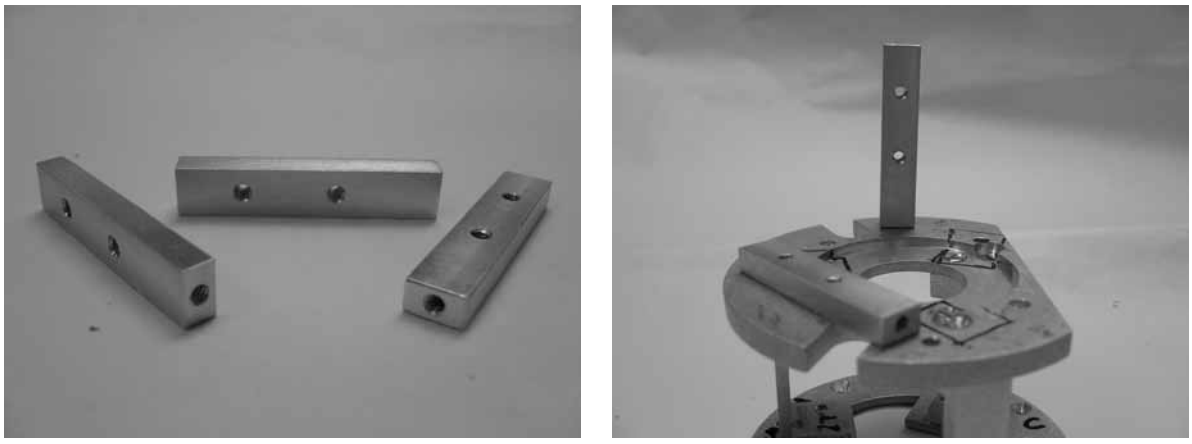

Figure 2.12: Rail brace details

devised the mounting strategy and selected materials that meet mounting requirements. The prescribed strategy allows cards to be tightly stacked but requires an intermediate connection between the support screws and the circuit boards because of how closely components are placed to the edges of some of the cards and because the cards have designated mounting holes at their corners, not their centers. So, the intermediate connection to the support screws must connect to these corners. The bridging material must be as light as possible and very easily shaped and fit into small spaces. And the connectors must be kept from slipping up or down along the support screws. A 1mm or 1.5mm thick modeling plastic called styrene is used here. It is very light and can be cut with scissors or scored and shaped with a utility knife. Thin 6-32 nuts are used to keep the cards from slipping along the support screws. Considering the length, width, and maximum height of each circuit card (as well as especially tall or wide components on specific boards), the author used a model arrangement of cards to designate the placement of each circuit card in order to minimize AUV length and to reserve space between stacks for manipulating screwdrivers, pliers, wrenches, etc. One unforeseen advantage of this mounting strategy is that cards may be pitched up or down, which may allow for an even better use of space.

The *hull* of the AUV is required to be light weight in order to keep the vehicle within the weight budget for being positively bouyant, to have as high a manufacturing tolerance as possible, and to have a smooth surface finish for o-ring seals. In meeting these three needs - light weight, circularity, and smooth finish - acrylic tube was found to satisfy all three. Specifically, the acrylic tube selected has a 3.5" inner diameter, 1/8" wall thickness, and 3.75" outer diameter. The manufacturing tolerance on the tube is ± 0.03" with imperfect circularity, which means that tail sections (and nose sections) as they are initially produced by a professional machinist do not always fit in the selected acrylic tube. So, each tail section is custom cut to fit into a specific section of acrylic tube. The author coordinated

Figure 2.13: Card mounting, close-up view displays styrene cards and nuts securing them along support screws

with professional machinists to make sure that seal specifications were met.

The *nose* section (2.14) was designed by the author and one other ASCL graduate student. The mechanical drawing of the nose section is in Appendix B. The nose must sustain a large threaded hole in which the pressure sensor is mounted. Like the tail, the nose's o-ring must sufficiently seal the AUV. And the nose is required to have a hydrodynamically efficient shape. Non-cellcore PVC is used to make the nose because it can support the pressure sensor. Professional machinists perform the same custom trimming of the nose diameter that is required for each tail section. The nose is shown, with its pressure sensor hole displayed, in Figure 2.14.

All payload sensors must be attached to the hull of the AUV, so the mounting solution must be convenient, repeatable, dependable, and hydrodynamically efficient (Figure 2.15). The author designed and built the sensor mounting system, selected the necessary materials. The solution consists of a set of aluminum rails, flexible straps, and small buckles to align and hold sensors to the AUV. To keep the cylindrical bodies of the AUV and sensor from slipping about one another, a pair of aluminum rails holds the sensor at all times along the center of the vehicle's bottom. These rails are permanently attached to the AUV and eliminate the sensor's yaw and slippage along the bottom portion of the vehicle. Another

Figure 2.14: Nose details

such rail can be used to prevent the sensor from slipping towards the nose. The sensor's connection to the bulkhead connector prevents slippage towards the tail. The straps are made from polyurethane and are used with a low-profile, plastic buckle, both of which are positively buoyant. The straps are only for single use, but the buckles may be used repeatedly with new sections of strapping. Being thin and relatively low-profile, both the straps and buckles are satisfactorily hydrodynamically efficient.

The GPS and RF antenna mounting solutions are shown in Figure 2.16. Figure A.1, in Appendix A, shows the RF antenna hole prior to being filled with waterproofing silicon sealant. The author designed and built both of these antenna mounts. The solutions for mounting these antennas must adequately address each antenna's form factor and waterproofing options. Also, mounting apparatuses may not be completely rigid structures. When struck by some potentially destructive force, they must be able to flex or break in such a way as to prevent damage to the seals around them.

The RF antenna must be fixed in the tail section so that the metal coaxial connection between the cable (inside the AUV) and the antenna (outside the AUV) is waterproofed. Given a sufficiently narrow hole drilled in the tail, the dimensions of the cable and antenna are such that the cable keeps the antenna from pulling out of the AUV and the antenna keeps the cable from pulling into the AUV (they form a barbell shaped connection). These same dimensions require the milled square shown in Figure A.1 in order to screw and unscrew the coax connection in the event that it needs maintenance. To waterproof the connection, this entire milled portion is filled with silicon sealant. The antenna is quite flexible, and the coax connector is slightly smaller than the hole in the tail, so once the assembly is waterproofed with pliable silicon sealant, the RF antenna assembly is sufficiently flexible to meet the

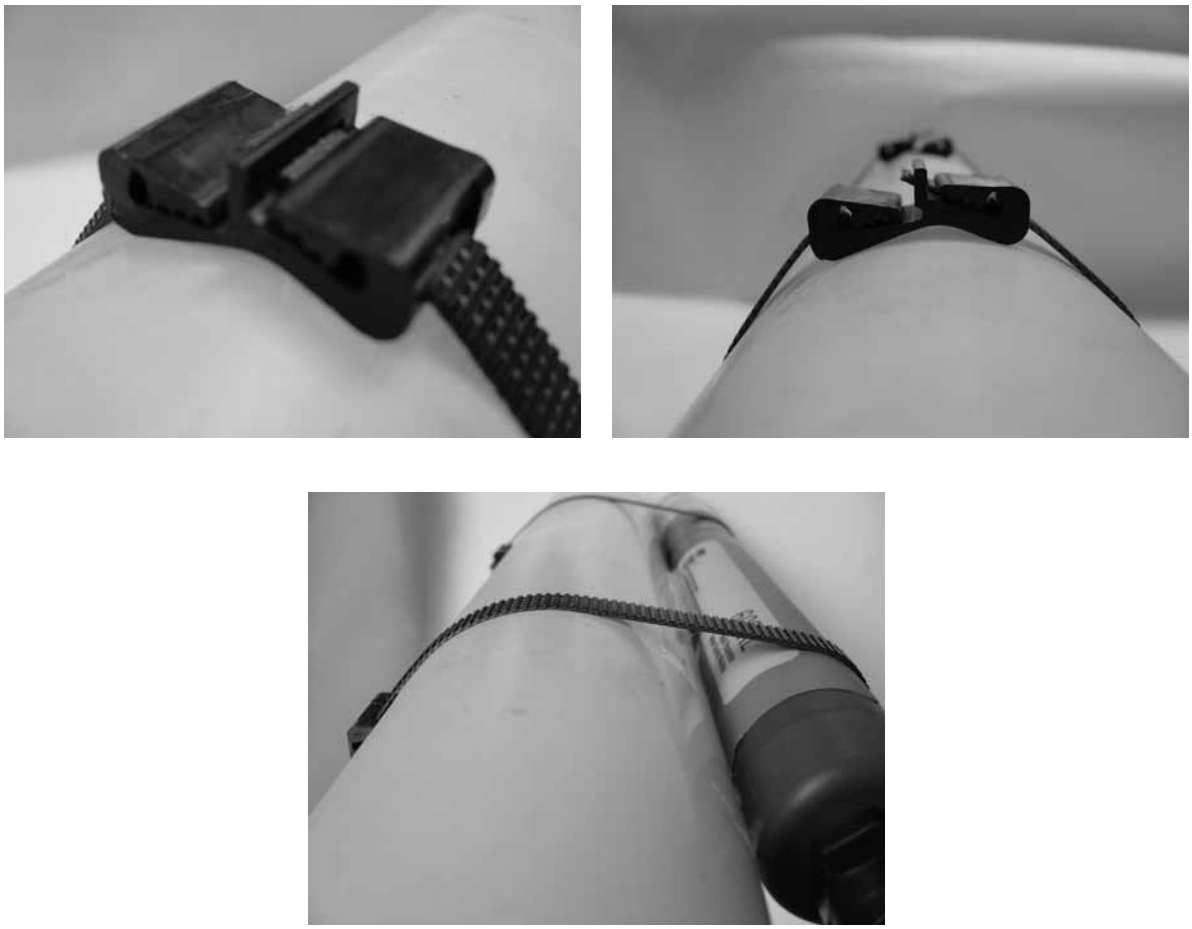

Figure 2.15: Payload mounting apparatus, buckle and strap profiles

requirement of not being too rigid.

Since the GPS antenna does not stand stiffly like the RF antenna, and since signal reception depends upon the antenna being parallel to the body of the AUV, a unique mast and shelf are required to correctly orient the GPS antenna. This shelf is designed so that the shelf and antenna will break away from the mast if struck with enough force. To keep from having to drill and seal another hole in the tail, the mast is simply bound to the hull with a steel clamp. A small hole is drilled in the tail so that the GPS cable may pass from the inside of the vehicle to the antenna. This hole is waterproofed with a very flexible sealant that actually allows the GPS antenna to swing freely about without compromising the watertight seal.

Appendix A specifically describes the step-by-step process of how to build the VT miniature autonomous underwater vehicle.

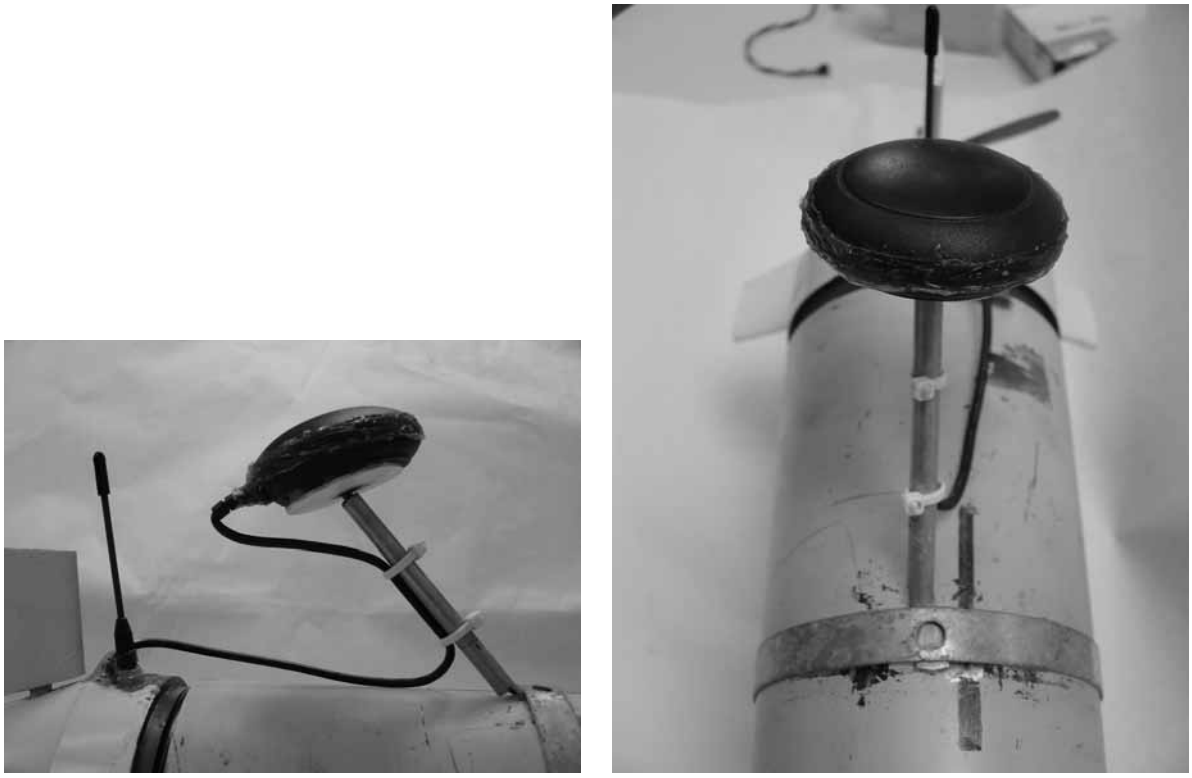

Figure 2.16: RF and GPS; GPS top view

Chapter 3

Communication Strategies for Platoon Cooperation

3.1 Introduction of Platoon Cooperation Problem

Groups of cooperating robots are highly valuable in a wide range of applications. However, achieving multi-vehcicle cooperation can be difficult. Since available communication bandwidth limits the number of robots that can communicate with one another, it is necessary to derive low communication solutions requiring minimal or no inter-vehicle communication. Indeed, there has yet been developed a low-communication solution that can be generalized to an arbitrarily large platoon of autonomous robots. From pairs of slow-moving holonomic robots in safe environments, to groups of nonholonomic vehicles teaming in large and unpredictable environments, several control schemes cast light on how to accomplish low-bandwidth communication among cooperating, small, low-cost autonomous vehicles.

Section 3.2 of this chapter presents how redundant manipulator techniques can be applied to platoons of autonomous robots. Section 3.3 presents a review of other work in the field. A sufficient condition for an arbitrarily large platoon of autonomous robots to have a decentralized, low-communication controller is presented in Section 3.4. Finally, the last section addresses collision and obstacle avoidance, which are achieved by way of a gradient projection method.

3.2 Low-Bandwidth Communication: Adopting Redundant Manipulator Techniques to the Cooperation Problem

The results shown here are not at all restricted to underwater vehicle applications. Indeed, the proposed approach to trajectory-generation treats the vehicles as point-masses, and there is no need to assume the vehicle dynamics are that of an air vehicle, ground vehicle, or underwater vehicle. Each vehicle is assumed to have a local controller for trajectory tracking. Excepting when a vehicle must deviate from its computed trajectory for locally-determined reasons, such as obstacle or collision avoidance, no inter-vehicle communication takes place. Only broadcast communications are assumed; which consist of an external system broadcasting necessary information to the entire platoon via one signal that is received by all of the vehicles. There are no requirements for point-to-point communications or nearest neighbor registration. This trajectory generation algorithm is computed in real-time by each vehicle using information that can be determined by sensors onboard the vehicle and by information broadcast by the exogenous system. Thus this approach permits changes in the environment, as sensed locally by each vehicle, to be incorporated into the path planning algorithm [2].

Consider a platoon composed of r vehicles. The position of each vehicle is denoted by vector $q_i \in \mathbb{R}^p$ for $i = 1, \ldots, r$. This work considers motion in the plane for which $p = 2$. The vector of vehicle positions is denoted $q = [q_1^T, q_2^T, \cdots, q_r^T]^T \in \mathbb{R}^{pr}$. Since only the trajectory of each vehicle is of interest, not low-level control, vehicles are assumed to be point masses with dynamics

$$\dot{q}_i(t) = u_i(t), \qquad q_i(0) = q_i^o, \qquad t \geq 0 \tag{3.1}$$

where $i = 1, \ldots, r$, q_i^o is a constant, and $u_i(t) \in \mathbb{R}^p$ is a control input. The dynamics of the entire platoon are denoted

$$\dot{q}(t) = u(t), \qquad q(0) = q^o, \qquad t \geq 0 \tag{3.2}$$

where $u(t) = [u_1^T(t), \cdots u_r^T(t)]^T$, $q = [q_1^T(t), \ldots, q_r^T(t)]^T$, and $q^o = [q_1^o, \cdots, q_r^o]^T$.

This approach to controlling a platoon of vehicles is based on the concept of controlling the *platoon*, not the individual vehicles. While the global behavior of the platoon is regulated, the individual vehicles' behaviors are not. Indeed, the local behavior of each vehicle is not known until the closed-loop system is simulated. This is contrary to the numerous other platoon control approaches where low-level behaviors are explicitly designed, and global "emergent" behaviors remain unknown until the system is simulated.

As the goal is to regulate the platoon, a suitable measure of the platoon performance is required. Any function of the platoon that can be exogenously measured will suffice. Such functions are referred

to as *platoon functions* and denoted $h(q) = [h_1(q), \cdots, h_l(q)]^T \in \mathbb{R}^l$. The principal contribution of this work, presented in Section 3.4, is a sufficient condition on the platoon function $h(q)$ such that the corresponding controller has a decentralized structure. For the purposes of illustration, a specific example is presented that was originally presented in [2]. This example platoon function is given by

$$h(q) = \begin{bmatrix} \mu_1 \\ \sigma_1^2 \\ \mu_2 \\ \sigma_2^2 \end{bmatrix} \tag{3.3}$$

where

$$\mu_1 = \frac{1}{r}\sum_{i=1}^{r} q_{i1} \qquad \sigma_1^2 = \frac{1}{r-1}\sum_{i=1}^{r}(q_{i1} - \mu_1)^2 \tag{3.4}$$

$$\mu_2 = \frac{1}{r}\sum_{i=1}^{r} q_{i2} \qquad \sigma_2^2 = \frac{1}{r-1}\sum_{i=1}^{r}(q_{i2} - \mu_2)^2 \tag{3.5}$$

and $q_i = [q_{i1}, q_{i2}]^T \in \mathbb{R}^2$ is the position of vehicle i in the horizontal plane. The choice of $h(q)$ in (3.3) represents the average position of the vehicles in the plane and the distribution of the vehicle positions about the average. The chosen communication topology relies on an exogenous system that is able to measure $h(q)$ and then broadcast it and any other required information back to the platoon.

A velocity-based control system that regulates the platoon function $h(q)$ is derived in the following manner: given a platoon function trajectory, $h(q(t))$, its derivative with respect to time is written

$$\dot{h}(q(t)) = J(q(t))\dot{q}(t)$$

where $J(q) = \frac{\partial}{\partial q}h(q)$ is the partial derivative of $h(q)$ with respect to q. Let $J^\dagger(q)$ be the pseudoinverse of $J(q)$, defined as $J^\dagger = J^T(JJ^T)^{-1}$, then

$$\dot{q}(t) = J^\dagger(q(t))\dot{h}(q(t)) \tag{3.6}$$

Suppose $h(t)$ is the solution of the stable first-order system

$$\dot{h}(t) = k_1\left(h^d(t) - h(t)\right) \tag{3.7}$$

where $k_1 > 0$ is a scalar constant and $h^d(t)$ is the desired platoon function trajectory, then the platoon state is governed by

$$\dot{q}(t) = k_1 J^\dagger(q(t))(h^d(t) - h(q(t))) \tag{3.8}$$

Stability of the platoon about the trajectory $h^d(q(t))$ with the feedback controller in (3.8) results from assuming a stable first-order system in (3.7) (under the assumption that the individual vehicles can

be velocity-controlled), as is typical in redundant manipulator control [3]. It is also assumed that the Jacobian J has full rank. For the platoon function example (3.3), J has full rank in all but two conditions: J is singular when all of the vehicles form a straight line in any of the dimensions composing q. Note that a feedforward velocity term $\dot{h}^d(t)$ can be incorporated in (3.8) to more accurately track $h^d(t)$ by reducing steady-state error to constant velocity trajectories [4].

The decentralized structure of the control law (3.8), assuming platoon function (3.3), is displayed through direct computation. The control law (3.8) is expanded, using the relationships (3.4) and (3.5), to show that the commanded velocity for each vehicle is

$$\dot{q}_i(t) = k_1 \begin{bmatrix} 1 & \frac{(q_{i1}(t)-\mu_1(t))}{2\sigma_1^2(t)} & 0 & 0 \\ 0 & 0 & 1 & \frac{(q_{i2}(t)-\mu_2(t))}{2\sigma_2^2(t)} \end{bmatrix} (h^d(t) - h(q(t))) \tag{3.9}$$

for $i = 1, \ldots, r$. See that the control for vehicle i depends only on its current state and the measured and commanded platoon performance functions $h(q)$ and h^d. To implement the control law locally (in a decentralized manner), each vehicle requires access to: q_i, which can be measured locally; $h(q)$ and h^d, which are broadcast from an exogenous system; and μ_1, μ_2, σ_1^2, and σ_2^2, which are components of $h(q)$. Since this is a velocity-based control law, it is assumed that each vehicle implements a local controller for tracking the trajectory generated by (3.9).

The structure of the control law (3.9) implies the following:

1. Each vehicle requires locally measured data and data that is broadcast from the exogenous system.

2. Every vehicle requires the same data from the exogenous system.

3. The communication required is independent of the number of vehicles in the platoon. So, no matter the platoon size, communication requirements do not increase with heightened platoon order.

For platoons of at least three vehicles (each having two degrees of freedom), the desired function h^d can be achieved by any of an infinite number of possible configurations. This redundancy is resolved using the pseudoinverse of the Jacobian. The platoon function h^d is achieved, but the exact formation emerges. Thus, the complex problem of planning coordinated motions of a large number of cooperating vehicles becomes one of allowing the formation to emerge based on the system dynamics and the desired platoon functions. It is important to note that control based on the pseudoinverse produces the minimum velocity vector for the entire platoon at each instant of time. Unfortunately, this property cannot be generalized to a claim of global optimality [3].

In simulation, since the vehicle trajectories are generated by controlling velocity, the commanded mean and variance are continuous to ensure a realistic acceleration profile.

An underlying yet critical assumption in this approach is that the platoon function $h(q)$ can be measured by an exogenous system. Thus the choice for $h(q)$ is dependent upon available sensing modalities. In the worst case, when no such sensing modality is available, each vehicle would report its current position to the exogenous system, and the exogenous system would then compute $h(q)$ and broadcast needed signals back the platoon. This worst-case scenario represents a significant increase in communication requirements. However, the broadcast communication from the exogenous system back to the platoon remains independent of the number of vehicles in the platoon, and represents a reduction in communication requirements over approaches that require direct communication with each vehicle.

3.3 Previous Approaches to Platoon Cooperation

Loosely speaking, a *holonomic* robotic manipulator is one for which returning to the original joint states means that the end effector returns to its original position. Specifically, holonomic systems are formulated such that returning to an initial joint-coordinate position guarantees that the position and orientation of the end-effector return to their original values [5]. A *nonholonomic* system is one that is not holonomic. For example, returning the AUV's propellor speed and fin angles to zero after running at non-zero values for any period of time does not gaurantee the vehicle's return to its original position.

Control methods for platoons of cooperating robotic vehicles have been studied extensively, using tools from both systems theory and computer science [6], [7]. In [6], a decentralized control scheme is developed for the cooperation of multiple robots. Each robot consists of a PUMA type robotic arm (which has a six degree of freedom wrist-like gripper) attached to a holonomic mobile base that moves the PUMA arm around the work space. Jacobian control is used to coordinate the joint movements of each PUMA arm. The group's task is to grasp and transport some object. Each robot employs a decentralized controller for which it has real-time access to only its own state information. At any given time, a robot can only infer information about the other robots' grasp forces through the team's combined action on the object.

In [7], a systems theoretic approach is developed to control a group of robots to cooperatively hunt and capture targets. A model-based controller determines the group formation necessary for holonomic robots to capture a target. The decentralized system requires each robot to calculate its own trajectory based on local relative-position feedback. Each robot senses its relative position to four types of objects:

1) visible targets, 2) a prescribed set of other robots, 3) collision imminent robots, and 4) obstacles. This model-based controller is a hybrid system comprised of a feedback control law and a reactive control framework. The feedback control law requires that each robot possess local relative position feedback (sensed or communicated). Each robot also has a vector called a *formation vector* that is derived from two things: the target location and the robot's relative separation from a set of assigned robots in the group. A set of mission specific constraints determines each robot's formation vector. The formation vector is one of four terms that generate each vehicle's trajectory; the remainder of which are 2) attraction to other robots, 3) attraction to the target, and 4) repulsion from other robots, obstacles, and the target. The overall group formation is derived from the set of all the robots' formation vectors [7].

Compared to controlling underwater vehicles, model-based control and hybrid schemes like the one in [7] are sensor and communications intense. For the robots to receive their necessary relative position feedback data, they must be interconnected by an extensive combination of sensors and high-bandwidth communication. The hybrid scheme also requires a second mapping step, two mappings compared to the single mapping required by the redundant manipulator approach. The robots in [7] first map from their surrounding environment to their formation vector; then the formation vectors map to the troop formation. A disadvantage of this two-step process is that as long as each robot determines its formation vector independently of all other robots, there is no guarantee that an appropriate mapping from local environments to formation vectors (the first map) will exist for every mission. So, for a certain initial mapping, there may not exist a second map from formation vectors to troop formation. This is significant because the single mapping characteristic of the redundant manipulator approach displays all singularities in the Jacobian matrix.

Communication bandwidth can be a factor in limiting the number of vehicles that cooperate to achive a given task. Many communications architectures have been directly or indirectly investigated for controlling cooperating autonomous vehicles. Approaches range from systems that require no communications [8] and rely solely on so-called *behavior-based* methods, to those that rely on large-bandwidth, explicit communications [4], as well as systems relying on varying levels of implicit and explicit communication [9, 10]. Current work focuses on multi-vehicle control systems for which very little communication is required, but for which the performance of the system can be assessed using systems-theoretic concepts (e.g., stability) [2].

Stated in [8] are the requirements for and effects of different amounts of communication between robots organized in small groups. The conclusion is that communication can significantly improve per-

formance for some mission types, but inter-robot communication seems unnecessary for other missions. Evidence further indicates that in cases where communication does aid in mission accomplishment, the lowest level of communication is almost as effective as the more complex type. Focus was placed on three tasks: *foraging*, *consuming*, and *grazing*. Three types of inter-robot communication were studied: *none*, *state*, and *goal*. *None* is just that, no direct communication between agents. This form assumes every robot's reliance solely on its own perception of the environment; it requires each robot to be able to distinguish between other robots, targets, and obstacles. *State* communication refers to the transmission of state information by way of animal-like methods, such as a deer waving its tail and running in order to signal danger to other deer. The authors also point out that communication is not always an *intentional* act, as information can be gathered by passive observation. A robot does not have to explicitly transmit its state to any one or set of robots. Rather, it can simply allow others to observe its state. And *goal* communication entails the transmission and reception of specific mission-oriented data. Goal and state communication require for their implementation deliberate, explicit signaling and reception of data. However, data that may inform a robot's controller may also be available through *implicit communication* [8]. For example, when one robot is able to observe another robot's status - though the observing agent may suffer a great sensing responsibility - cooperation enhancing communication is established. For AUVs, implicit information could include acoustic or magnetic signatures that indicate vehicles' proximity to one another.

Large-bandwidth explicit communications are necessary in the decentralized scheme shown in [4]. By insightfully stating the issues pertaining to the control and cooperation of robots, the authors provide a control scheme that offers the flexibility required for behavioral integration and simultaneously relies on well-established system-theoretic robot control methods. Stating the remarkable similarity between a redundant robotic manipulator and a platoon of autonomous vehicles, it is shown in [4] shows how to use redundant manipulator control techniques to answer questions of platoon control and formation synthesis. Like a redundant robotic arm, a platoon of autonomous vehicles typically possesses more degrees of freedom than are required to achieve desired functions of platoon geometry, such as center of mass or variance of the platoon elements [2]. The focus of [4] is placed on groups of mobile robots not constrained by rigid kinematic relationships. Given that a redundant system accomplishes some primary task, the redundancy is used to also resolve the demands of lower priority tasks, or secondary tasks. This formulation of the platooning problem enables the synthesis of a variety of tasks using redundancy-based controllers [4].

The redundancy-based controllers in [4] are classified as either of two traditional control techniques

for redundant manipulators: *task prioritization* or the *gradient descent technique*. *Task prioritization* is a method by which a secondary task is defined in identical, globally descriptive terms just like the primary task. Defined so, the secondary task has its own Jacobian and is projected onto the null space of the primary task Jacobian. Such projection takes advantage of the system's redundancy and ensures that both the secondary and primary tasks are accomplished as long as the second does not interfere with the first. Given a secondary task based on a system function $f_2(q)$ and associated Jacobian $J_2(q)$, the task prioritization controller is given by

$$E = K(f^d(q) - f(q)) + \dot{f}^d(q) \tag{3.10}$$

$$E_2 = K_2(f_2^d(q) - f_2(q)) + \dot{f}_2^d(q) \tag{3.11}$$

$$\dot{q} = J^\dagger E + \tilde{J}_2^\dagger(E_2 - J_2 J^\dagger E) + (I - J^\dagger J)(I - \tilde{J}_2^\dagger \tilde{J}_2)v \tag{3.12}$$

where $f^d(q)$ and $f_2^d(q)$ are the desired task variables, K and K_2 are control gains, $J^\dagger$ is the Moore-Penrose pseudoinverse given by $J^T(JJ^T)^{-1}$, $(I - J^\dagger J)$ is the projection operator onto the null space of the Jacobian, and $\tilde{J}_2 = J_2(I - J^\dagger J)$ [4].

Unlike the employment of globally descriptive Jacobian matrices, *gradient projections* do not require a Jacobian matrix or a specific, globally descriptive task value. Rather, what is projected onto the null space of the primary Jacobian is some task gradient that describes the need for a certain set of vehicles to adhere to a locally necessitated secondary task. The standard velocity-based gradient projection controller is given by

$$\dot{q}^d = J^\dagger(K(f^d(q) - f(q)) + \dot{f}^d(q)) + (I - J^\dagger J)v \tag{3.13}$$

These two approaches comprise the basis for redundant manipulator control and allow for the synthesis of a variety of tasks. In [4], the four tasks and their controller terms are described as follows.

1. a primary Jacobian pseudoinverse control term given by (3.13), a standard velocity-based gradient projection controller:

$$\kappa_1 = J^\dagger E = J^\dagger K(f^d(q) - f(q)) + \dot{f}^d(q) \tag{3.14}$$

2. a gradient projection obstacle avoidance term:

$$\kappa_2 = (I - J^\dagger J)v_{obstacle} \tag{3.15}$$

3. a task-priority-based heading control term for unit i:

$$\kappa_3 = \tilde{J}_2^\dagger(K_2(f_2^d(q) - f_2(q)) - J_2 J^\dagger E) \tag{3.16}$$

4. a null space optimization term for unit i (gradient projection):

$$\kappa_4 = K_{optimum}(I - J^{\dagger}J)(I - \tilde{J}_2^{\dagger}\tilde{J}_2)v_{optimum} \tag{3.17}$$

where $K_{optimum}$ is a gain for the null space optimization task, $v_{obstacle}$ is an obstacle avoidance velocity vector, and $v_{optimum}$ is a null space optimization velocity vector. So, the complete controller is given by

$$\dot{q} = \kappa_1 + \kappa_2 + \kappa_3 + \kappa_4 \tag{3.18}$$

The latter two represent a set of many secondary tasks that could be synthesized in this redundant structure. This approach requires of any secondary task that it not be incompatible with the primary task and that it not degrade the performance of the obstacle avoidance algorithm. Since the obstacle avoidance gradient approaches infinity at collision points, some secondary tasks may be implemented without fear of collision even if they locally conflict with the obstacle avoidance routine. So, to guarantee obstacle avoidance, all secondary task vectors must be guaranteed to be bounded [4].

The use of all four of the above enumerated controlled terms provides two main benefits. First, explicitly planned trajectories and specified platoon formations are not required. And secondly, the controller offers much inherent flexibility in the actual achievement of controller specifications. Mainly detracting, however, from the utility of this structure is its requirement of large bandwidth explicit communications. Gradient projections force every member of the platoon to know the local description of any vehicle with a non-zero secondary task term. This means that for obstacle avoidance, heading control, and/or vehicle optimization to be successfully implemented, any vehicle that customizes its trajectory in order to meet even one secondary task must somehow convey its spatial and velocity vectors to the entire platoon since this data is necessary for all other vehicles to calculate their trajectories. In underwater applications sustaining only low-bandwidth communications, this formulation becomes very difficult to implement, especially since there would most likely be great need for the system response to be highly sensitive.

In [9], a mixture of implicit and explicit communication is used to derive an optimal controller that allows a team of mobile robots to grip and transport an object around a horizontal workspace. Each robot is bound by nonholonomic velocity contraints that do not readily fit into a pseudoinverse structure relating force to acceleration. However, a pseudoinverse-based optimal controller is formulated that successfully accounts for the mobile robots' nonholonomic constraints. The work starts by drawing a parallel between a team of robots conveying a mutually held load and multiple manipulator configurations that benefit from the increased dexterity of multi-fingered robotic hands, the additional

load-bearing capacity of multi-robot systems, and the enhanced ability of multi-legged vehicles to traverse uneven terrain. Unlike the scenario in [4], this load-bearing strategy is constrained by closed kinematic chains (which occur whenever multiple manipulators make contact with a single object) and redundant actuation. Robots maintain rigid attachment to a pallet (the group geometry is constant throughout the load's manipulation) and specified motions are generated by forces applied by the robots. The supervisory controller finds the optimal distribution of forces among the robots while also accounting for the robots' nonholonomic constraints. Given a vector of desired robot accelerations, a modified pseudoinverse is used to find the minimum norm solution of forces applied by each robot. Specifically, a reduced form of the system matrix will satisfy the robots' nonholonomic constraints while the i^{th} robot's forces are determined by the following three sets of data: the commanded acceleration of the i^{th} robot, *all* locally measured distances to other robots (which are constant, and therefore easily known, in the rigid attachment configuration), and the world coordinate velocities of *all* the other robots. Introducing redundancy to the system matrix provides for the resolution of nonholonomicity problems in the rigid attachment of robots. Even though every robot's velocity vector is required to be communicated to the rest of the group, this formulation of rigid attachments improves upon the communication requirements of unattached robots that are required to maintain fixed relative distances to one another. Such a platoon structure demonstrates the high value of easily obtained, implicitly communicated information combined with still necessary explicit communication [9].

In [10], focus is placed on controlling distrubuted mobile robots that are subject to the physical constraints of mass, nonholonomic effects, and sensors' physical realities. Line and circle algorithms are developed to improve upon line and circle formation methods that previously existed only for idealized robots (point masses able to instantaneously move in any direction, equipped with perfect range sensors). The proposed solutions solve the problem of organizing a group of mobile robots with a nondescript and random initial formation into a geometric pattern, such as a circle, without using a centralized controller. A potential field algorithm is used for both motion control and the avoidance of vehicle collisions. Successful assembly of these formations depends heavily on effective implicit communications. Tactile (bumper), infrared, and ultrasonic sensors provide sufficient vision to determine all relative distances necessary for formation assembly. Explicit communication is required by the best circle algorithm, which ensures that each robot knows a time constant that is determined empirically during the simulated platooning motions [10]. Unfortunately, this work provides formation algorithms that remain centered approximately about the original formation's center, so neither the achieved line nor circle actually translates a space with any sort of searching or mapping task.

Control techniques for redundant robotic manipulators, based on a generalized inverse of the non-square manipulator Jacobian, are well-represented in the literature [3, 11], with applications that range from joint torque minimization of a traditional robotic arm [12] to force allocation for the legs of a walking robot [13]. The utility of such control techniques for coordinating a platoon of autonomous robots was recognized in [14, 4]. This thesis shows that, within the framework of redundant manipulator control techniques, many platoon tasks can be met by decentralized control and very little inter-vehicle communication. This technique enables platoons composed of a potentially large number of vehicles to be coordinated with very limited communications bandwidth [2].

In [11], pseudoinverse control is shown to be a robust method for controlling the velocity of each joint in a redundant robotic arm. Given a robotic arm with an end effector, Jacobian control involves an external description of the end effector's motion in rectilinear coordinates as it is related to the internal motions of each degree of freedom (joint) in the system. The pseudoinverse control method is couched in terms of the singular value decomposition (SVD) representation. And in the underdetermined case (the case when the Jacobian has fewer rows than columns, or fewer externally measured end effector descriptions than degrees of freedom), there will be an infinite number of solutions for the state vector as long as the Jacobian's rank is equal to its number of rows. The SVD analysis shows that the underdetermined subspace of a system matrix can be identified and that the pseudoinverse provides the minimum norm solution to the state vector. Since the pseudoinverse finds the minimum norm solution, instantaneous power is minimized; and since nearness to singularities is characterized by high joint velocities, the pseudoinverse causes the system to avoid singularities. It is very important to note that the null space of the Jacobian, or the set of homogeneous solutions to the state vector, is rejected as a state vector in the underdetermined case. The homogeneous solutions are the joint velocities that produce no end effector motion. So, the velocities produced by the pseudoinverse have no component that does not contribute to the motion of the end effector. The system's redundancy and resulting homogeneous solutions are shown to improve performance. At the cost of losing the minimum norm solution, homogeneous solutions can be included in the solution so as to optimize additional performance criterion. The criterion (or possibly multiple criteria) must not prohibit the robot from accomplishing the end effector task. Meeting an additional criterion by including homogeneous solutions in the velocity vector requires a trade-off between minimum energy and optimization of additional performance requirements [11].

While redundant manipulator techniques are applicable to multi-vehicle systems in various domains, such as land and air vehicles, the motivation for current research arises from the requirements of un-

derwater vehicles. Severely limited communication bandwidth underwater inhibits the coordinatation of multiple underwater vehicles. This prevents promising control techniques in air or ground applications from being directly adapted to underwater operations. The literature on reported experiments with platoons of underwater vehicles is very limited. One notable instance was described in [15]. Leader-follower control was demonstrated using Odyssey vehicles with a modified ultra-short baseline transponder. Though the control algorithm for the follower vehicles was somewhat ad hoc, the system displayed significant robustness. Multi-vehicle control laws based on potential functions are reported in [16]. These ideas are further developed in [17], along with descriptions of planned experimental activities [2].

Shown in [15], accurate acoustic sensing provided the basis for successful leader-follower control manifested in two MIT (Massachusetts Institute of Technology) Odessey IIB class vehicles (AUVs). Controlling AUV spacing, or even locally communicating position data, requires externally referenced navigation systems like acoustic modems. Previous work by some of the same investigators shows that a pair of AUVs can share a single transponder network only if they time multiplex their interrogations. They also showed that performance degrades as more vehicles are added to the network [15]. (These networks consist of transponders that are attached to the ocean floor prior to a mission, then recollected after a mission.) In [15], a homing and docking technology and technique are generalized to a leader/follower pair of AUVs. The leader uses its ultra-short baseline (USBL) instrumentation to supply a global reference beacon to the follower vehicle, which maintains a desired relative azimuth to the leader's acoustic beacon. In terms of multiple followers, the trailing set of AUVs is limited in this case to a single vehicle, which controls two spatial parameters relative to its leader: a dead reckoned azimuth and a depth separation that prevents the two from colliding. Notably, there is flexibility in vehicle spacing because there is no specified vehicle separation along the aligned azimuth. Acceptable separation is achieved and is dependent upon the vehicle's relative velocities. And collision avoidance is accomplished by more of a hardwired, ad hoc approach that provides no generality for enlarging the platoon.

In [18] and [16], model-based algorithms are developed for coordinating and cooperating underwater vehicles. These works present a robust multi-vehicle solution to gradient descent or climbing (the tracking of decreasing or increasing, respectively, gradients of some spatially distributed signal). It has been shown in [16] that, under assumptions of a linear controller, a single AUV finds the gradient source only if its initial straight line trajectory intersects the source. Earlier work shown in [18] demonstrates how critical it is to know near neighbor behavior in order to robustly perform. So, the authors propose

that this approach requires multiple vehicles and implicit inter-vehicle communication since a single vehicle has only limited success in finding and climbing the gradient. More specifically, [16] presents stability proofs for and generalizable platoon formations of one, two, and three vehicles. Effecacy of the AUV pair in [18] is based on modeling the AUV pair as a rigidly connected system of two point masses. No inter-vehicle communication is allowed, but each vehicle is assumed to possess the capability to observe the other vehicle's position. Further assumption necessitates that the vehicles be able to maintain a prescribed inter-vehicle spacing, which is achieved by modeling and controlling the pair as a rigid object with translational and rotational energies. In [16], however, such a restriction is replaced by the use of artificial potential fields, which ensure the maintanence of an optimized platoon formation by generating appropriate repulsion and attraction forces between vehicles. Employing inter-vehicle linear spring potentials (as opposed to the more fully descriptive nonlinear spring potentials), these potentials still require the same implicit communication strategies as the formulation of rigidly connected bodies.

Spatially regulated teams of AUVs in both [18] and [16] will find the source as long as all closed-loop decentralized controllers can access the following information: the global position and orientation of each vehicle *and* the relative position and orientation of each vehicle's nearest neighbor. The relative position and orientation data are fundamental to a group's coordination while the global data are necessary for sampling and gradient tracking missions. Global data is gathered from a long baseline acoustic modem; relative data is gathered via inter-vehicle sensing from a custom designed optical system consisting of a 2D-position sensitive device (PSD) and an array of blinking LEDs.

Presented in [17] is the highly interesting AUV research conducted in the Monterey Bay in California during the summer of 2003. In adherence to the objectives of the Autonomous Ocean Sampling Network II (AOSN-II) project, collaborative research was conducted to demonstrate the value of model-based, remote adaptive sampling networks of AUVs in predicting marine science phenomena in Monterey Bay. Specifically, a team from Princeton University tested control strategies for groups of coordinated and cooperative autonomous SLOCUM gliders. The controller presented in [17] answers the general problem of adaptive sampling using fleets of AUVs by supplying a solution specific to the dynamics of SLOCUM gliders. Based on fleet control via potential fields (developed in [18] and [16]), [17] further specifies system constraints and fleet stability in the case of using gliders with limited maneuverability. The strategy integrates measurements from the gliders into a coordinated mission planner. These measurements consist of GPS updates and estimated gradients of the signals being tracked. The group seeks quality data, changes its spatial distribution so as to alter the resolution of its sensing, rotates and reconfigures so as to maximize its sensing coverage, and maintains commanded group formations

throughout the mission. The SLOCUM gliders have a limited ability to communicate, so the feedback of sensor and position data is intermittent. Dependence on this discontinuous data makes difficult the task of fleet coordination, but the system is robust to even two to three hour steps between updates. Measurements are used every two hours to recalculate each glider's path for coordinated sampling patters, cooperative gradient climbing, or some other task. The distinction between coordinated control and cooperative control is this. *Coordinated control* refers to inter-vehicle relationships and uses gliders' GPS reports and local current estimates measured every two hours to maintain prescribed paths, formations, and patterns. *Cooperative control* refers to the group's maneuvering in response to the dynamic environment and further specifies paths, formations, and patterns in response to the group's sensor data, GPS data, and water current estimates [17]. For example, coordination ensures that three AUVs maintain a triangular formation with certain inter-vehicle spacing; cooperation ensures that this triangular formation moves in a circular path to sample some chemical seeping from a vent in the ocean floor.

Being focused on formation control, formation stability and optimization are studied and presented in [17]. Specifically, vehicles set at the vertices of inscribed polygon shapes comprise a set of formations that are optimal for estimating gradients in the presence of noise. Line formations can produce directional derivaties along the line containing all of the aligned vehicles; and sufficiently frequent sampling allows for estimation of the gradient in the direction of motion (as long as the vehicles are not following one another in a single file line). Given instantaneous sensor measurements, a formation of at least three vehicles is necessary to compute gradients in the plane of descent (or ascent). Rough estimation of second-order derivatives is possible if four or five vehicles assemble such that for $n = 4, 5$, $(n-1)$ vehicles form an inscribed polygon and one maintains a position in the center of the polygon. Additionally, six gliders can contribute to a least-squares estimate of the second-order derivatives of the gradient [17].

The contributions of [18], [16], and [17] are valuable for comparison to this thesis because they present sophisticated and effective algorithms for controlling groups of AUVs. Consider first the artificial potential approach in [17]. This method produces quite an informative stability analysis of multi-vehicle formations and sheds much light on optimum arrangements of AUVs for different mission types, thus serving as the foundation for the most useful and well-developed adaptive sampling system in operation to date. The main similarity between the artificial potential and redundant manipulator approaches is their theoretical scalability to a large number of vehicles. However, though both methods utilize decentralized controllers in each AUV, the manipulator approach does not con-

trol inter-vehicle spacing or orientation. Unlike the redundant manipulator approach, the customized formations achieved with artificial potentials mandate that each vehicle be in consistent contact with near neighbor vehicles and nearby virtual leaders. Consider how this approach with gliders is limited in practice by the following: 1) the necessity that each vehicle be aware of a mission-specific number of other vehicles (communication requirements), 2) vehicle-specific velocity contraints that make impossible the achievement of some formations, and 3) vehicle-specific problems with matching some fleet configurations with overwhelmingly strong local ocean currents. Comparatively, the redundant manipulator approach provides the following benefits when implemented on a more fully actuated vehicle than the SLOCUM glider (e.g., the ASCL AUV): it does not require inter-vehicle awareness or communication except for locally necessary collision avoidance, it allows for many platoon configurations excepting three known singularities, and it provides independence of strong local currents via highly dynamic actuation of the AUV.

3.4 Generalizations: Trajectory Planning for an Arbitrarily Sized Platoon

The mean and variance example in Section 3.2 illustrates the basic concepts of decentralized path planning using redundancy resolution. Now consider a characterization of other suitable platoon functions. A class of platoon functions that yield decentralized controllers is characterized by using a sufficient condition on the partial derivatives of $h(q)$. The investigation of such a condition was initiated by Dr. D. J. Stilwell. As variations on h were postulated by either the author or D. J. Stilwell, the author determined the resulting controller form and communication requirements. D. J. Stilwell summarized the work and formulated the following theorem.

Theorem 3.4.1 *Consider the platoon function* $h(q) = [h_1(q), \ldots, h_l(q)]^T$ *and suppose there exist scalar functions* $g_1(q), \ldots, g_s(q)$ *such that the partial derivative of* $h(q)$ *can be expressed*

$$\frac{\partial h_i}{\partial q_j} = f_{ij}(q_j, g_1(q), \ldots, g_s(q)) \tag{3.19}$$

for all $1 \leq j \leq r$ *and* $1 \leq i \leq l$*, and where* s *is independent of the dimension of* q*. Then the exogenous system need broadcast no more than* $s + \frac{l(l+3)}{2}$ *scalar variables.*

For notational convenience, define $g(q) = [g_1(q), \ldots, g_s(q)]^T$. Then

$$J(q) = \frac{\partial h(q)}{\partial q} = \begin{bmatrix} f_{11}(q_1, g(q)) & \cdots & f_{1r}(q_r, g(q)) \\ \vdots & \ddots & \vdots \\ f_{l1}(q_1, g(q)) & \cdots & f_{lr}(q_r, g(q)) \end{bmatrix}$$

Also define the $l \times l$ symmetric matrix $J^B(q) = (J(q)J^T(q))^{-1}$.

$$(J(q)J^T(q))^{-1} = \begin{bmatrix} J^B_{11}(q) & \cdots & J^B_{1l}(q) \\ \vdots & \ddots & \vdots \\ J^B_{l1}(q) & \cdots & J^B_{ll}(q) \end{bmatrix}$$

Using this notation and recalling that the control signal for the platoon is $\dot{q}(t) = k_1 J^\dagger(q(t))(h^d(t) - h(q(t)))$, the local controller for each vehicle is

$$\dot{q}_i(t) = k_1 \sum_{j=1}^{l} \sum_{k=1}^{l} f^T_{ki}(q_i(t), g(q(t))) J^B_{kj}(q(t))(h^d(t) - h(q(t))) \tag{3.20}$$

for all $1 \leq i \leq r$. The signal $q_i(t)$ is measured locally by vehicle i. Signals that are not measured locally and must be broadcast by the exogenous system are $J^B(q)$, which has $\frac{l(l+1)}{2}$ independent entries, the vector $(h^d(t) - h(q(t)))$, which has has l independent entries, and $g(q)$, which has s independent entries. Thus each local controller requires that $s + \frac{l(l+3)}{2}$ scalar variables be broadcast from the exogenous system.

3.5 Vehicle Autonomy

Since the control law in Section 3.4 regulates the platoon as a whole, the trajectory requirements of an individual vehicle (e.g., collision avoidance) may not be satisfied. Thus, each vehicle must have limited autonomy to adjust its trajectory based on local information.

For a platoon composed of a sufficient number of vehicles, there are an infinite number of vehicle positions that satisfy a given value of the platoon function h^d. Thus it is possible for the vehicles to move while the measured platoon function $h(q)$ remains constant. Let $v_i(t)$, $i = 1, \ldots, r$, be a desired secondary velocity of vehicle i based on local information, to be coupled in some manner to the nominal velocity for satisfying h^d as determined by (3.8). The corresponding secondary velocity vector for the entire platoon is denoted

$$v = \begin{bmatrix} v_1 \\ \vdots \\ v_r \end{bmatrix}$$

Note again that this velocity vector is distinct from the velocity determined from the control law (3.8), and is intended to satisfy secondary objectives while the platoon still achieves the desired platoon functions h^d. Other uses for a secondary velocity vector in controlling a platoon have been explored in [14, 4].

By projecting v onto the null space of J, the components of v that do not alter the platoon function are determined. The projection of v onto the null space of J is expressed as

$$(I - J^\dagger J)v \tag{3.21}$$

The control law (3.8) is combined with (3.21), yielding

$$\dot{q}(t) = k_1 J^\dagger(q(t))(h^d(t) - h(q(t))) + k_2(I - J^\dagger(q(t))J(q(t)))v(t) \tag{3.22}$$

where $k_2 > 0$ is a scalar constant. Note that the secondary velocity vector v is only satisfied insofar as it does not affect the primary objective h^d, and may not be achieved at all in certain circumstances.

Under the same sufficient condition on $h(q)$ as in Theorem 3.4.1, (3.22) is expanded to display the control law for each vehicle,

$$\begin{aligned}\dot{q}_i(t) = k_1 \sum_{j=1}^{l}\sum_{k=1}^{l} f_{ki}^T(q_i(t), g(q(t)))J_{kj}^B(q(t))(h^d(t) - h(q(t))) \\ + k_2 v_i(t) - k_2 \sum_{k=1}^{l}((\sum_{j=1}^{l} f_{ji}(q_i(t), g(q(t)))J_{jk}^B(q(t)))(\sum_{j=1}^{r} f_{kj}(q_j, g(q))v_j))\end{aligned} \tag{3.23}$$

As required for the controller (3.20), an exogenous system must transmit at most $s + \frac{l(l+3)}{2}$ scalar variables. In addition, if v_i, the secondary velocity for vehicle i is non-zero, then vehicle i must transmit its desired secondary velocity and current position to the remainder of the platoon. In other words, if a vehicle desires to deviate from the path determined by (3.20) in a direction v_i, it must transmit v_i and q_i to the remainder of the platoon. Otherwise, vehicle i transmits nothing. Since the overarching desire is to reduce communication requirements, it is expected that missions would be designed to minimize broadcast transmissions from an individual vehicle.

3.5.1 Vehicle Autonomy Illustration

The control law (3.20) is illustrated using $h(q)$ defined in (3.3). In a similar manner to the analysis of (3.8), the control law (3.22) is computed,

$$\begin{aligned}\dot{q}_i(t) = k_1 &\begin{bmatrix} 1 & \frac{(q_{i1}(t)-\mu_1(t))}{2\sigma_1^2(t)} & 0 & 0 \\ 0 & 0 & 1 & \frac{(q_{i2}(t)-\mu_2(t))}{2\sigma_2^2(t)} \end{bmatrix} \big(h^d(t) - h(t)\big) \\ - k_2 &\begin{bmatrix} \frac{q_{i1}(t)-\mu_1(t)}{(r-1)\sigma_1^2(t)} \sum_{j=1}^{r} (q_{j1}(t) - \mu_1(t)) v_{j1}(t) \\ \frac{q_{i2}(t)-\mu_2(t)}{(r-1)\sigma_2^2(t)} \sum_{j=1}^{r} (q_{j2}(t) - \mu_2(t)) v_{j2}(t) \end{bmatrix}\end{aligned} \tag{3.24}$$

To implement (3.24), vehicle i requires $q_i(t)$, which is measured locally, and h^d and $h(q)$, which are broadcast by the exogenous system. The additional required terms μ_1, μ_2, σ_1^2, and σ_2^2 are components of $h(q)$. If vehicle j chooses a nonzero secondary velocity vector, then every vehicle in the platoon also requires v_j and q_j. It is anticipated that missions will be designed so that v_j is typically zero and does not need to be broadcast by vehicle j.

The vector v_i is determined locally by vehicle i. The maximum distance at which the obstacle is detected is denoted $d_{\max}$. The vector from the vehicle to object j in world coordinates is p_{ij}. The relative angle between the vehicle's heading and object j is denoted θ. As it was formulated in [2], the vector v_{ij} is computed using an artificial potential field,

$$v_{ij} = \begin{cases} -(\frac{\pi}{2} - \theta) k_2 \frac{(d_{\max} - \|p_{ij}\|)}{\|p_{ij}\|^2} p_{ij}, & \text{if } |\theta| < \frac{\pi}{2} \text{ and } \|d\| < d_{\max} \\ 0, & \text{otherwise} \end{cases}$$

This is an ad hoc scheme where v_{ij} points away from the object with a magnitude proportional to likelihood that the vehicle's path will intersect the object but also approaches infinity as the distance to impact decreases to zero. Suppose there are n detected objects, then

$$v_i = \sum_{j=1}^{n} v_{ij}$$

represents the summation of the obstacle avoidance vectors.

Although the vehicles must navigate about an obstacle, the platoon achieves the objectives in $h(q)$. By design, as one vehicle makes navigation corrections due to the obstacle, all other vehicles make small navigation corrections so that the platoon function $h(q)$ is satisfied [2].

Chapter 4

Further Investigation of Low Bandwidth Platooning Solutions

4.1 Introduction

After studying the existence and synthesis of the decentralized velocity controller for platoon mean and variance, two questions of generalization remain of special interest. The first consideration is how $h(q)$ might be defined so that the platoon assumes some specified probability distribution of position data or some unique formation. All potential platoon functions will be chosen to meet Theorem 3.4.1, thus ensuring that a low-bandwidth controller exists. The second consideration is the optimum dimension of $h(q)$. Performance objectives may be met by a certain family of functions defining $h(q)$, to which adding higher order functions of the same family or other types of functions may or may not enhance performance.

The following analysis and simulations show how higher-order platoon statistics provide no improvement on the simplicity, utility, performance, and predictability of the original platoon function (3.3). Excepting some evident platoon shaping functions, neither approximations of specific probability distribution functions, nor central and spatial moments, nor Hu's invariant moments make improvement upon the original platoon function.

4.2 The Moment Theorem and Approximating Probability Density Functions

The *characteristic function* of a random variable is by definition the integral

$$\Phi_x(\omega) = \int_{-\infty}^{\infty} f(x)e^{j\omega x}\,dx \tag{4.1}$$

If $j\omega$ is changed to s, then the resulting integral

$$\Phi(s) = \int_{-\infty}^{\infty} f(x)e^{sx}\,dx \tag{4.2}$$

is the *moment generating function* of the random variable x. As (4.1) indicates, $\Phi_x(\omega)$ is the Fourier transform of $f(x)$. Hence the properties of characteristic functions are essentially the same as the properties of Fourier transforms. Further, Moment Theorem is stated as follows.

Theorem 4.2.1 *Differentiating* (4.2) *n times yilds*

$$\Phi^{(n)}(s) = E(x^n e^{sx}) \tag{4.3}$$

and

$$\Phi^{(n)}(0) = E(x^n) = m_n \tag{4.4}$$

So, the derivatives of (4.2) *evaluated at the origin equal the moments of x. Expanding* $\Phi(s)$ *into a series near the origin and using* (4.4) *produces*

$$\Phi(s) = \sum_{n=0}^{\infty} \frac{m_n s^n}{n!} \tag{4.5}$$

This equality is valid only if all moments are finite and the series converges absolutely near s = 0. Since f(x) can be determined in terms of $\Phi(s)$, (4.5) *shows that, under the stated conditions, the density of a random variable is uniquely deteremined if all of its moments are known. Finally, knowledge of other moments provides additional information that can be used to distinguish between two densities with the same mean and variance [19].*

Based on this theorem, initial focus was placed on comprising $h(q)$ of enough higher-order moments to approximate probability density functions of interest. To determine the viability of these higher-order moment definitions, a general multi-moment definition of the platoon function has been developed. Its presentation here describes the implications of commanding moments of any order.

4.2.1 Higher-Order Moments: Communication Requirements

Theorem 4.2.2 *The k^{th} moment of a random variable x, $\phi_k(x) = E\left[x^k\right]$, is defined for any k according to different probability distribution functions of x. The unbiased estimate of $\phi_k(x)$ is $\hat{\phi}_k(x)$, which can be calculated at any time as*

$$\hat{\phi}_k(x) = E\left[\phi_k(x)\right] \tag{4.6}$$

$$= E\left[E\left[x^k\right]\right] \tag{4.7}$$

$$= \frac{1}{r}\sum_{i=1}^{r} x_i^k \tag{4.8}$$

Suppose that the platoon function $h(q)$ is composed in the xy plane of the first k estimates of x and y such that

$$h(q(t)) = \begin{bmatrix} \hat{\phi}_1(x) \\ \vdots \\ \hat{\phi}_k(x) \\ \hat{\phi}_1(y) \\ \vdots \\ \hat{\phi}_k(y) \end{bmatrix} \tag{4.9}$$

then the local controller for each vehicle is

$$\dot{q}_i(t) = k_1 J^{\dagger}\left(q_i(t), \hat{\phi}_1(x), ..., \hat{\phi}_{2k-2}(x), \hat{\phi}_1(y), ..., \hat{\phi}_{2k-2}(y)\right)\left[h^d(q(t)) - h(q(t))\right], \tag{4.10}$$

such that each vehicle need know only q_i, h^d, and the 1^{st} through $(2k-2)^{th}$ unbiased estimates of x and y.

The moments $\phi_j(x)$ and $\phi_j(y)$, $j = 1, 2, ..., k$, comprise the commanded platoon function $h^d(q)$ and are defined accordingly for different probability distribution functions of the platoon's position data. The sample statistics $\hat{\phi}_j(x)$ and $\hat{\phi}_j(y)$ are calculated at each time interval according to (4.6).

Proof: For a k-moment evaluation of the two-dimensional xy space, $h(q(t)) \in \mathbb{R}^{2k}$. The Jacobian $J(q) = \frac{\partial}{\partial q}h(q)$ is the partial derivative of $h(\cdot)$ with respect to q. $J(q) \in \mathbb{R}^{2k\times 2r}$,

$$J = \begin{bmatrix} \frac{\partial \hat{\phi}_1(x)}{\partial x_1} & \frac{\partial \hat{\phi}_1(x)}{\partial y_1} & \cdots & \frac{\partial \hat{\phi}_1(x)}{\partial x_r} & \frac{\partial \hat{\phi}_1(x)}{\partial y_r} \\ \vdots & \vdots & \vdots & \vdots & \vdots \\ \frac{\partial \hat{\phi}_k(x)}{\partial x_1} & \frac{\partial \hat{\phi}_k(x)}{\partial y_1} & \cdots & \frac{\partial \hat{\phi}_k(x)}{\partial x_r} & \frac{\partial \hat{\phi}_k(x)}{\partial y_r} \\ \frac{\partial \hat{\phi}_1(y)}{\partial x_1} & \frac{\partial \hat{\phi}_1(y)}{\partial y_1} & \cdots & \frac{\partial \hat{\phi}_1(y)}{\partial x_r} & \frac{\partial \hat{\phi}_1(y)}{\partial y_r} \\ \vdots & \vdots & \vdots & \vdots & \vdots \\ \frac{\partial \hat{\phi}_k(y)}{\partial x_1} & \frac{\partial \hat{\phi}_k(y)}{\partial y_1} & \cdots & \frac{\partial \hat{\phi}_k(y)}{\partial x_r} & \frac{\partial \hat{\phi}_k(y)}{\partial y_r} \end{bmatrix} \tag{4.11}$$

which is evaluated as

$$J = \begin{bmatrix} \frac{1}{r} & 0 & \frac{1}{r} & 0 & \ldots & \frac{1}{r} & 0 \\ \frac{2}{r}x_1 & 0 & \frac{2}{r}x_2 & 0 & & \frac{2}{r}x_r & 0 \\ \frac{3}{r}x_1^2 & 0 & \frac{3}{r}x_2^2 & 0 & \ldots & \frac{3}{r}x_r^2 & 0 \\ \vdots & \vdots & \vdots & \vdots & \ldots & \vdots & \vdots \\ \frac{k}{r}x_1^{k-1} & 0 & \frac{k}{r}x_2^{k-1} & 0 & \ldots & \frac{k}{r}x_r^{k-1} & 0 \\ 0 & \frac{1}{r} & 0 & \frac{1}{r} & \ldots & 0 & \frac{1}{r} \\ 0 & \frac{2}{r}y_1 & 0 & \frac{2}{r}y_2 & \ldots & 0 & \frac{2}{r}y_r \\ 0 & \frac{3}{r}y_1^2 & 0 & \frac{3}{r}y_2^2 & \ldots & 0 & \frac{3}{r}y_r^2 \\ \vdots & \vdots & \vdots & \vdots & \ldots & \vdots & \vdots \\ 0 & \frac{k}{r}y_1^{k-1} & 0 & \frac{k}{r}y_2^{k-1} & \ldots & 0 & \frac{k}{r}y_r^{k-1} \end{bmatrix} \tag{4.12}$$

The product $JJ^T \in \mathbb{R}^{2k \times 2k}$ has the form

$$JJ^T = \begin{bmatrix} \frac{1}{r} & \frac{2}{r}\hat{\phi}_1(x) & \ldots & \frac{k}{r}\hat{\phi}_{k-1}(x) & 0 & 0 & \ldots & 0 \\ \frac{2}{r}\hat{\phi}_1(x) & \frac{4}{r}\hat{\phi}_2(x) & \ldots & \frac{2k}{r^2}\hat{\phi}_k(x) & 0 & 0 & \ldots & 0 \\ \frac{3}{r}\hat{\phi}_2(x) & \frac{6}{r}\hat{\phi}_3(x) & \ldots & \frac{3k}{r}\hat{\phi}_{k+1}(x) & 0 & 0 & \ldots & 0 \\ \vdots & \vdots & \ldots & \vdots & \vdots & \vdots & \ldots & \vdots \\ \frac{k}{r}\hat{\phi}_{k-1}(x) & \frac{2k}{r}\hat{\phi}_k(x) & \ldots & \frac{kk}{r}\hat{\phi}_{2k-2}(x) & 0 & 0 & \ldots & 0 \\ 0 & 0 & \ldots & 0 & \frac{1}{r} & \frac{2}{r}\hat{\phi}_1(y) & \ldots & \frac{k}{r}\hat{\phi}_{k-1}(y) \\ 0 & 0 & \ldots & 0 & \frac{2}{r}\hat{\phi}_1(y) & \frac{4}{r}\hat{\phi}_2(y) & \ldots & \frac{2k}{r}\hat{\phi}_k(y) \\ 0 & 0 & \ldots & 0 & \frac{3}{r}\hat{\phi}_2(y) & \frac{6}{r}\hat{\phi}_3(y) & \ldots & \frac{3k}{r}\hat{\phi}_{k+1}(y) \\ \vdots & \vdots & \ldots & \vdots & \vdots & \vdots & \ldots & \vdots \\ 0 & 0 & \ldots & 0 & \frac{k}{r}\hat{\phi}_{k-1}(y) & \frac{2k}{r}\hat{\phi}_k(y) & \ldots & \frac{kk}{r}\hat{\phi}_{2k-2}(y) \end{bmatrix} \tag{4.13}$$

Evident is the requirement to calculate higer-order moments than those contained in $h(q(t))$. The number of additional moments is $(2k-2-k)=(k-2)$ and they are required to determine the product JJ^T.

The clearest way to describe the general form of $(JJ^T)^{-1}$ is to employ the following definition of a matrix inverse. Suppose $A \in \mathbb{R}^{2k\times 2k}$. Set $n=2k$ so that $A \in \mathbb{R}^{n\times n}$. If the inverse of A exists, then it is defined as A^{-1},

$$A^{-1} = \frac{adjA}{detA} \tag{4.14}$$

where $adjA$ is the adjugate of A and $detA$ is the determinant of A.

For the sake of clarity, define $B=(JJ^T)^{-1}$ so that $B \in \mathbb{R}^{n\times n}$,

$$B = \begin{bmatrix} b_{11} & b_{12} & ... & b_{1k} & 0 & ... & 0 \\ b_{21} & b_{22} & ... & b_{2k} & 0 & ... & 0 \\ \vdots & \vdots & ... & \vdots & \vdots & ... & \vdots \\ b_{k1} & b_{k2} & ... & b_{kk} & 0 & ... & 0 \\ 0 & 0 & ... & 0 & b_{(k+1)(k+1)} & ... & b_{(k+1)n} \\ \vdots & \vdots & ... & \vdots & \vdots & ... & \vdots \\ 0 & 0 & ... & 0 & b_{n(k+1)} & ... & b_{nn} \end{bmatrix} \tag{4.15}$$

Since B is constructed by evaluating $det(JJ^T)$ and $adj(JJ^T)$, B is a function strictly of the sample statistics $\hat{\phi}_j(x)$ and $\hat{\phi}_j(y)$. More specifically, $b_{11},...,b_{kk} = f\left(\hat{\phi}_j(x)\right)$ and $b_{(k+1)(k+1)},...,b_{nn} = f\left(\hat{\phi}_j(y)\right)$. There are no terms of x_i or y_i in $B=(JJ^T)^{-1}$.

The final step in determining $J^\dagger \in \mathbb{R}^{2r\times 2k}$ is to multiply J^T by B. Each row of $J^\dagger = J^T B$ is thus described in terms of x_i or y_i, and b_j = the j^{th} column of B, $j=1,2,...n$.

$$J^\dagger = \begin{bmatrix} (x_1,b_1) & ... & (x_1,b_k) & 0 & ... & 0 \\ 0 & ... & 0 & (y_1,b_{k+1}) & ... & (y_1,b_n) \\ \vdots & ... & \vdots & \vdots & ... & \vdots \\ (x_r,b_1) & ... & (x_r,b_k) & 0 & ... & 0 \\ 0 & ... & 0 & (y_r,b_{k+1}) & ... & (y_r,b_n) \end{bmatrix} \tag{4.16}$$

The vector $(h^d - h) \in \mathbb{R}^{2k}$,

$$h^d - h = \begin{bmatrix} \phi_1(x) - \hat{\phi}_1(x) \\ \vdots \\ \phi_k(x) - \hat{\phi}_k(x) \\ \phi_1(y) - \hat{\phi}_1(y) \\ \vdots \\ \phi_k(y) - \hat{\phi}_k(y) \end{bmatrix} \tag{4.17}$$

Finally, the decentralized structure of the controller is maintained by the final operation, $J^\dagger(h^d - h)$, so that each row of $\dot{q}(t) = k_1 J^\dagger(h^d - h)$ is

$$\dot{q}(t) = k_1 f \begin{pmatrix} x_1, & \hat{\phi}_1(x), ..., \hat{\phi}_{2k-2}(x), & (\phi_1(x) - \hat{\phi}_1(x)), ..., (\phi_k(x) - \hat{\phi}_k(x)) \\ y_1, & \hat{\phi}_1(y), ..., \hat{\phi}_{2k-2}(y), & (\phi_1(y) - \hat{\phi}_1(y)), ..., (\phi_k(y) - \hat{\phi}_k(y)) \\ & \vdots \quad \vdots & \vdots \\ x_r, & \hat{\phi}_1(x), ..., \hat{\phi}_{2k-2}(x), & (\phi_1(x) - \hat{\phi}_1(x)), ..., (\phi_k(x) - \hat{\phi}_k(x)) \\ y_r, & \hat{\phi}_1(y), ..., \hat{\phi}_{2k-2}(y), & (\phi_1(y) - \hat{\phi}_1(y)), ..., (\phi_k(y) - \hat{\phi}_k(y)) \end{pmatrix} \tag{4.18}$$

This description of $\dot{q}(t)$ clearly shows that a decentralized controller exists for a generalized platoon function consisting of the first k unbiased estimates of x and y.

An h defined as in (4.9) requires for the local calculation of $\dot{q}_i(t)$ that each vehicle have access to not only the k estimates of each variable in h, but also the updated values of sample estimates $(k+1)$ through $(2k-2)$, an additional $(k-2)$ estimates (which, importantly, is less than $s + \frac{l(l+3)}{2}$). Compared to the original mean and variance control, this more general controller requires that more information be supplied to each vehicle. So, the list of necessary information for decentralized control has been lengthened. Local implementation of (4.18) specifically requires each vehicle to have access to the following:

1. $x_i(t)$ and $y_i(t)$, locally measured by each vehicle
2. $h(q(t))$ and $h^d(q(t))$, which are broadcast from the exogenous system
3. updated sample statistics $\hat{\phi}_{k+1}$, . . . , $\hat{\phi}_{2k-2}$ of both x and y, which must be broadcast from the exogenous system

This result imposes a new communication requirement on the system. The use of the mean and variance lent itself to a conveniently calculated controller that depended only upon the contents of h.

However, if the platoon function contains the first k moments of x and y, then in order for the system to track h^d, the exogenous system must calculate and broadcast $(k-2)$ additional estimates. It is obvious that the choice of k directly affects the system's communication requirements.

4.2.2 Higher-Order Moments: Approximating Arbitrary Distributions

The implication of (4.18) gives rise to the investigation of two questions - which probability distribution function should h define, and which value of k enables sufficient achievement of the commanded density function? Specifically, can a platoon's position data be transformed from one distribution to another, from a uniform to a normal distribution, for example? Results show that different h^d yield different results for changing a uniform distribution into a uniform, normal, or exponential distribution. Each effort is more specifically defined, explained, and demonstrated in the following sections.

As shown by (4.1) - (4.5), the theoretical value of a density's k^{th} moment may be found by differentiating the density's charateristic function k times and evaluating the derivative at the density's parameters. As an example, the mean and variance completely characterize any normal distribution. This is the method by which each h^d is formulated. The necessary parameters are chosen to be time-varying, so at each instant the time-varying theoretical k^{th} moment is calculated and used as a commanded statistic. Having already proven the minimal communication required of this structure, the hypothesis is that such a construction of h^d will generate a stable framework in which an arbitrarily sized platoon can alter the density function of its position data.

Commanding to a Uniform Distribution and Variations on the Platoon Function

The parameters of any uniform distribution are the bounding end points, a and b. The probability density function of a uniformly distributed random variable x is

$$f(x) = \frac{1}{a-b} \qquad x = [a, b] \tag{4.19}$$

and the k moments in $h^d(q)$ are defined by appropriately evaluating the uniform characteristic function

$$\frac{e^{jb\omega} - e^{ja\omega}}{j\omega(b-a)} \tag{4.20}$$

Such derivation produces the theoretical general moments of a uniformly distributed random variable x,

$$E[x^k] = \phi_k(x) = \frac{b^{k+1} - a^{k+1}}{(k+1)(b-a)} \tag{4.21}$$

The parameters a and b are shifted as functions of time in $h^d(q)$ so that $r = 100$ vehicles move from an initially unifiorm distribution characterized by $[a_{x,y}, b_{x,y}] = [0, 10]$ to a similar uniform distribution where $[a_x, b_x, a_y, b_y] = [80, 120, 60, 100]$. Figure 4.1 shows the platoon's movement when $h(q)$ is composed of $k = 1$, 2, 3, 4, 5 , or 6 moments (left to right). Figure 4.2 shows how well the platoon tracks the commanded uniform distribution by illustrating the response of the highest-order moment for each h tested. Figure 4.3 helps explain what the platoon function should consist of. Figure 4.4 displays the platoon's initial and final position histograms, which indicate the sufficiency of the controller in maintaining the uniformity of the position data.

Since pseudoinverse control produces the minimum velocity vector for each new trajectory, the case in which h consists only of μ_x and μ_y, the first general moments of x and y, not surprisingly yields straight paths for each vehicle. This h makes the platoon accountable to no other statistics that would mandate changes in each vehicle's distance from the average positions commanded by the first moment.

However, controlling higher-order moments in addition to $\phi_1(x)$ and $\phi_1(y)$ induces changes in the platoon variance and shape. Depending on which moments are controlled, different platooning phenomena emerge and can be interpreted by considering two things: known relationships between certain moments and how they may or may not dictate the platoon, and the fact that the pseudoinverse produces the minimum velocity vector. To start, consider the addition of only the second general moment so that $h^d(q) = [\phi_1(x), \phi_2(x), \phi_1(y), \phi_2(y)]^T$. Though the variance is not directly controlled, its defining elements are contained in the platoon function, as variance is defined for any random variable t as

$$\sigma_t^2 = E[t^2] - E^2[t] \tag{4.22}$$

Relenquishing direct control over σ_x^2 and σ_y^2 allows them to vary greatly as both ϕ_1 and ϕ_2 increase, but since variance is implicitly contained in h, the controller maintains an average position according to ϕ_1, accomplishes ϕ_2 according to the minimal velocities generated by the pseudoinverse, and draws the variance back to the value projected by (4.22). So, sweeping paths and sharp turns generated for $k > 1$ are the minimum velocity solutions to achieving both the commanded mean and certain higher-order moments of x and y and are the result of omitting specific variance commands from the controller. When $k > 2$ and the platoon remains stable, the definition of variance in (4.22) ensures that the variance profile does not change for a given parameter pair (a, b), no matter the selection of k (Figure 4.3). This fact will be used shortly to help classify types of platoon functions based on any order of general uniform moment.

Once sufficient conditions for stability and path viability are stated, more general predictions can be made about specific selections of h. First, though the Moment Theorem stated in (4.5) is a good

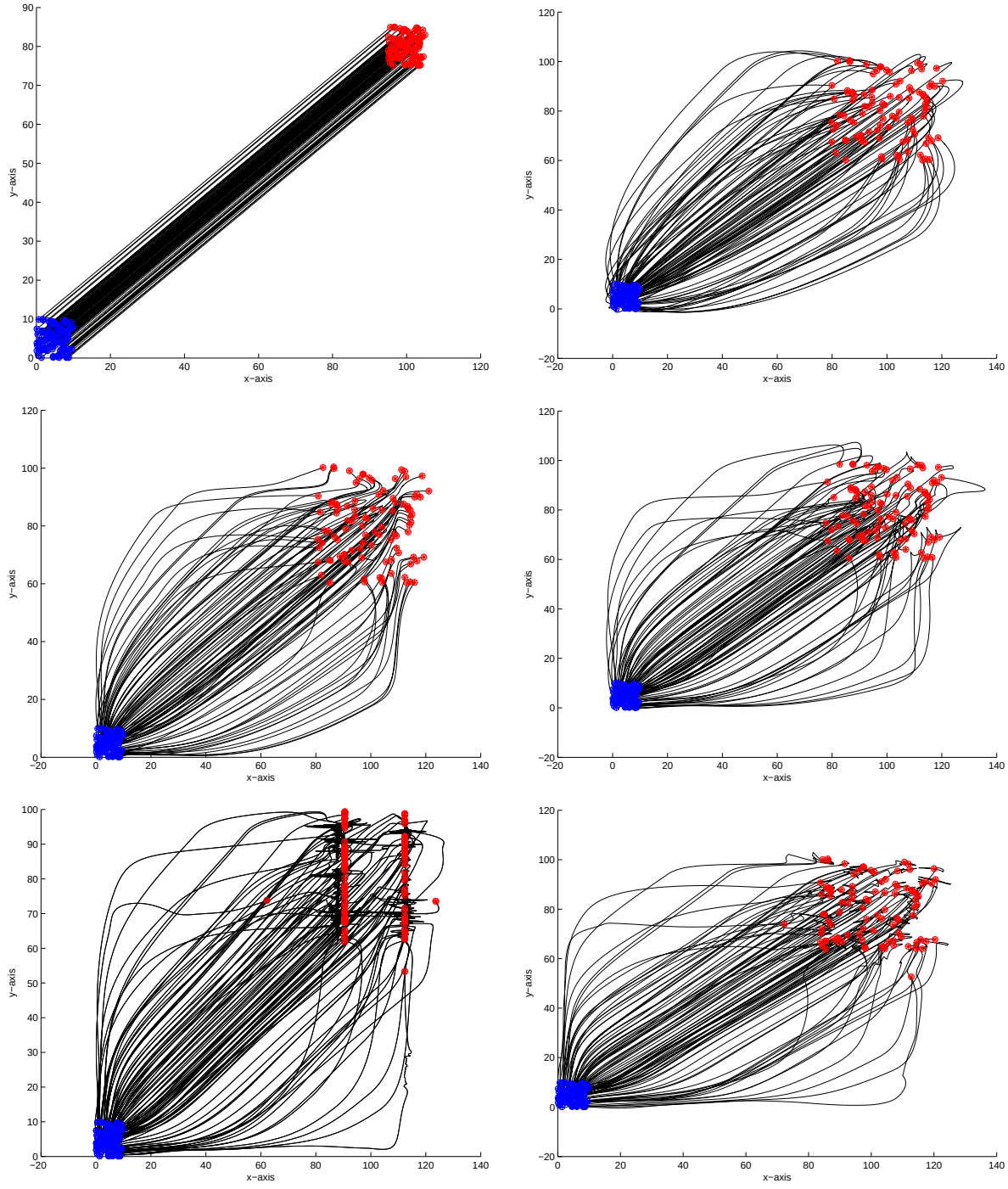

Figure 4.1: Movement of 100 vehicles over 1200 second period; $k = 1, 2, 3, 4, 5, 6$ (top left to bottom right)

starting point for the study undertaken by this thesis, it does not in this context wholly support the theory that arbitrarily selected distributions can be achieved for an arbitrarily sized group of autonomous vehicles. The higher-order general moments in (4.5) are considered by mathematicians to be statistically unstable [20], as even small changes in the value of a higher order moment can

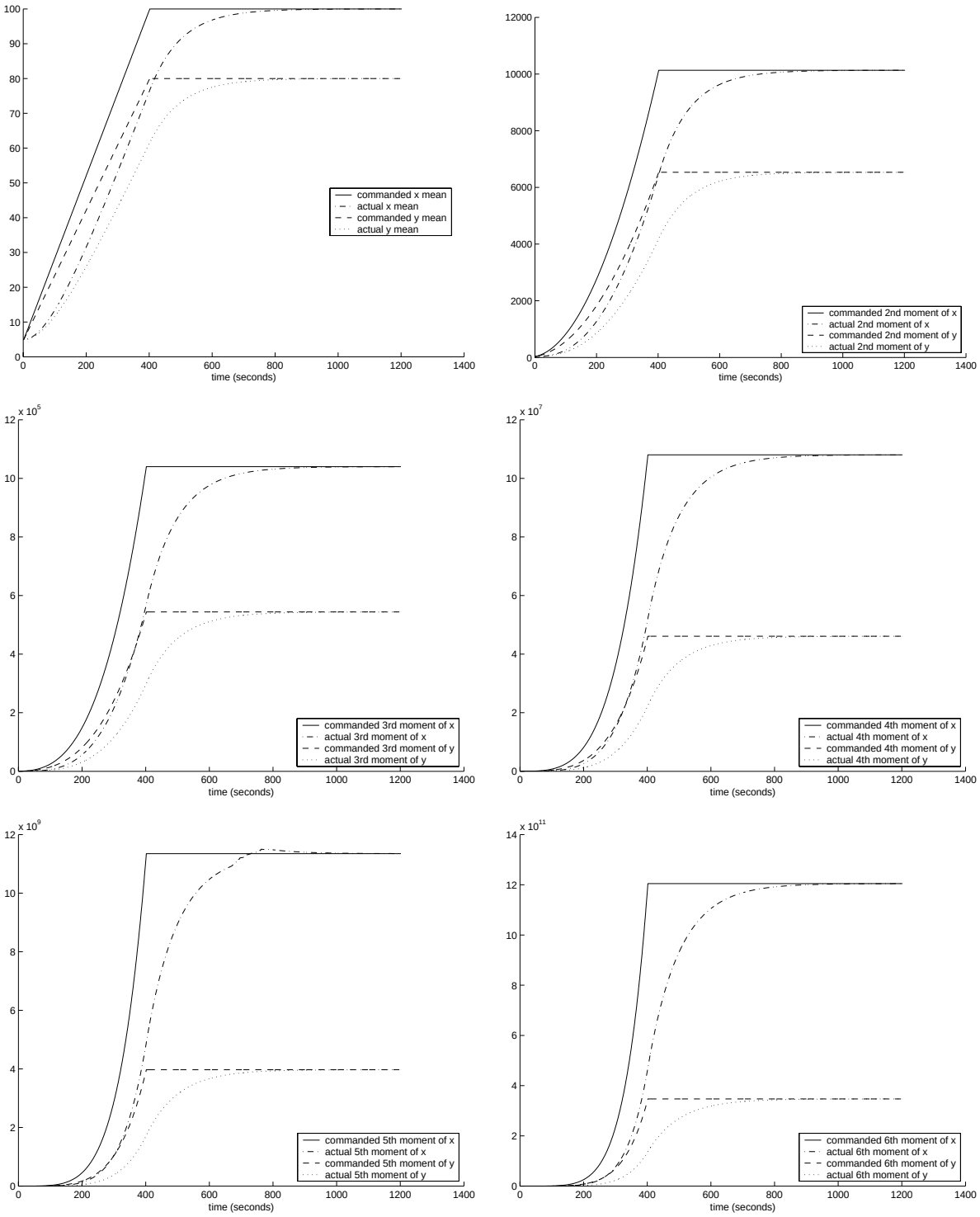

Figure 4.2: Tracking of highest-order moment in platoon function; $k = 1, 2, 3, 4, 5, 6$ (top left to bottom right)

unpredictably induce very significant changes in the distribution of data. In other words, two distinct probability distributions can have very similar higher-order moments. In the present context, such statistical changes induce drastic changes in platoon formation and unrealistic demands on vehicles'

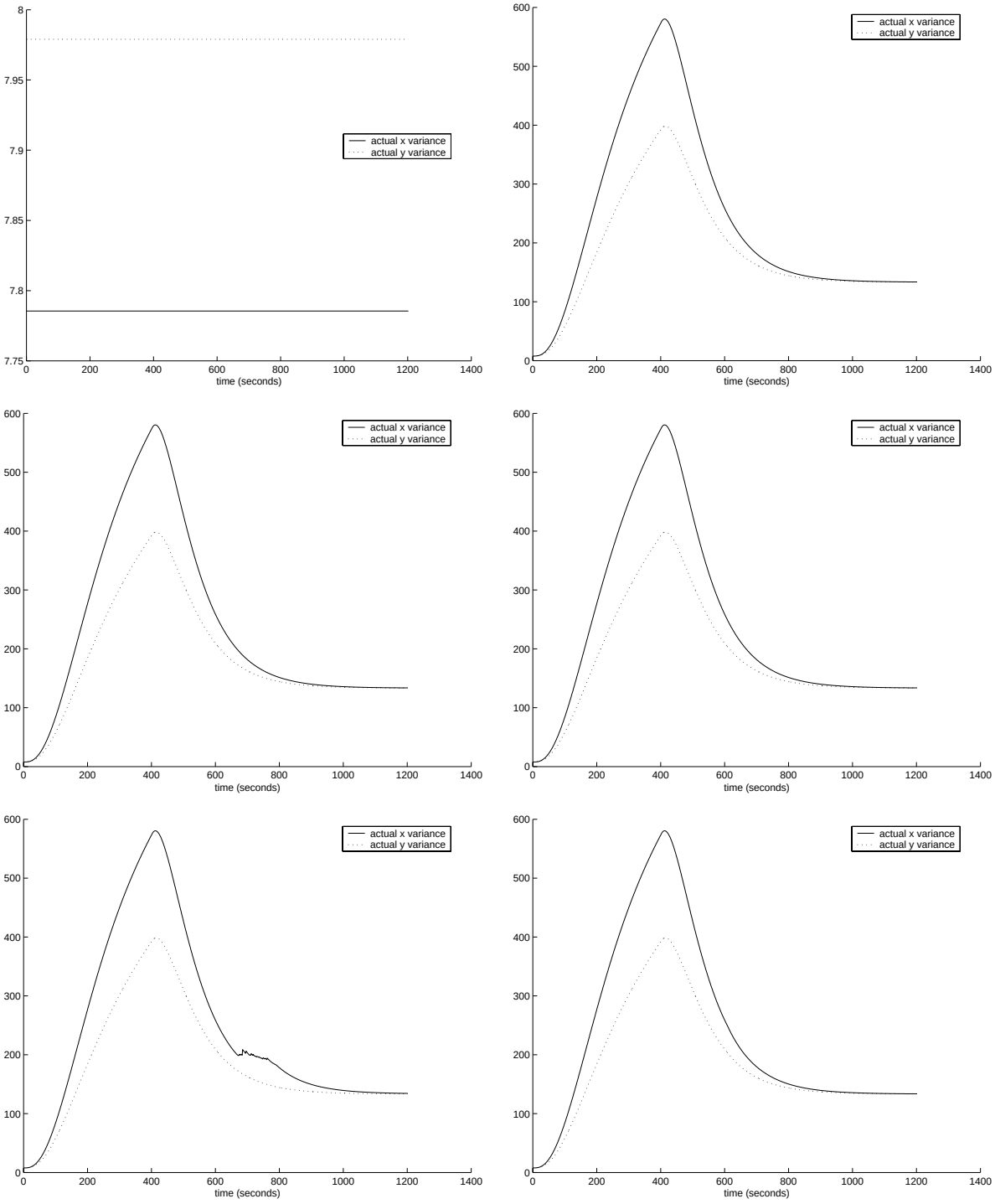

Figure 4.3: Actual variance; $k = 1, 2, 3, 4, 5, 6$ (top left to bottom right)

actuation capabilities. An example of this is the case of $k = 5$. The lower-left subplot of Figures 4.1, 4.2, 4.3, and 4.4 show the effects of this phenomena. Though the platoon becomes unstable (most clearly seen in 4.3), stability is regained in this case. The simulated result, however, is that velocities are one to two magnitudes too high and the platoon formation is no longer predictable. So, some higher-order moments (or combinations of them) could actually drive the platoon unstable. Others,

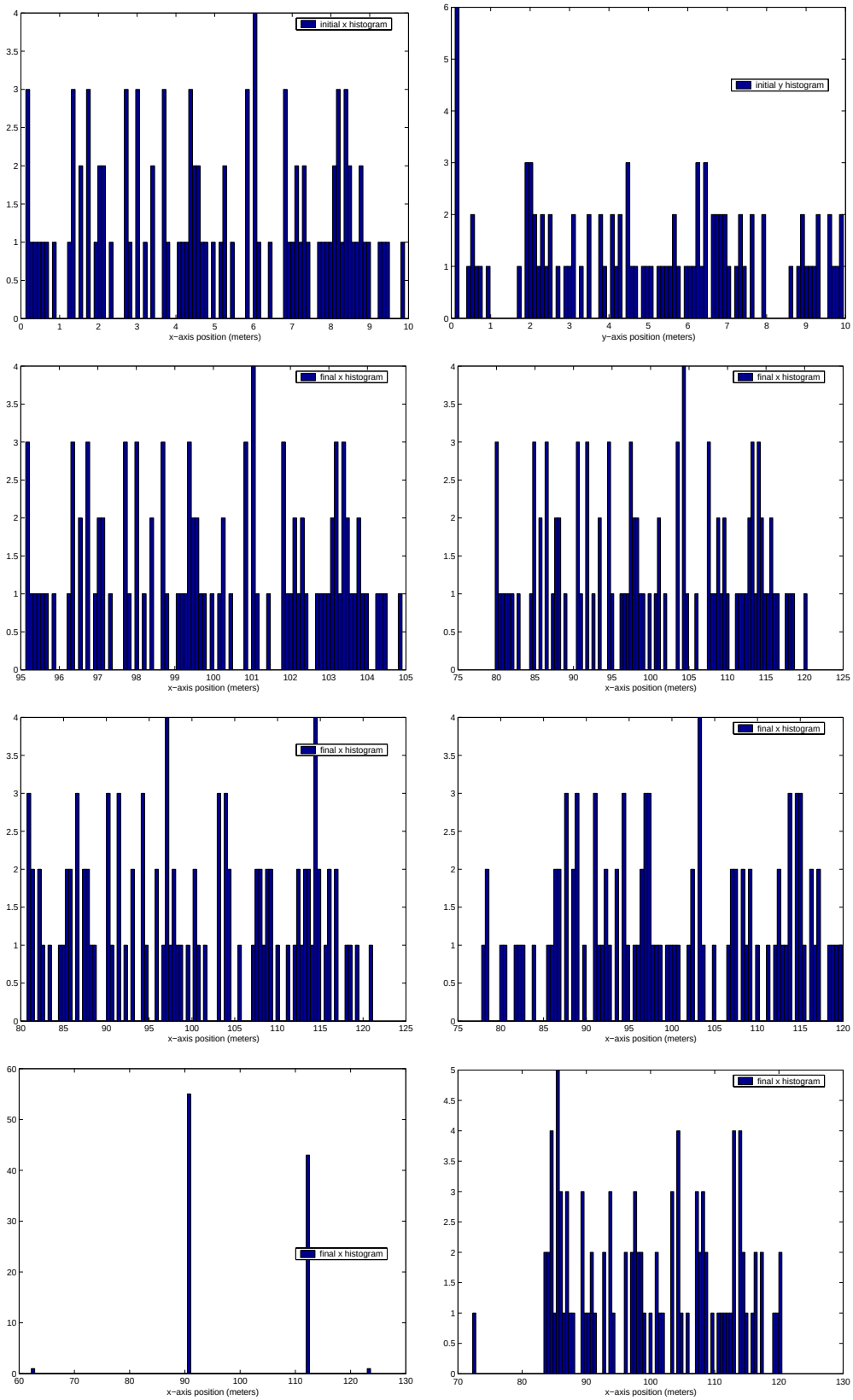

Figure 4.4: Initial (x and y) and final (x only) histograms showing uniformity of data; $k = 1$, 2, 3, 4, 5, 6 (top left to bottom right)

like in the case just shown, may not ultimately destabilize the platoon but at least generate unsuitable vehicle trajectories during a brief period of instability. For simplicity, this phenomena will henceforth be referred to as *statistical instability*.

So, this use of the Moment Theorem to maintain a uniform distribution of position data proves in two ways useful. First, it shows that for $h^d(q) = [\phi_1(x,y)]$ or $h^d(q) = [\phi_1(x,y), \phi_2(x,y)]^T$, uniformity is identically preserved. Simulation results also show that $h^d(q)$ defined by the first three *or* four moments produce very similar, nearly identically uniform densities of position data (Figure 4.4). For higher-order values of k and nonsequential combinations of moments (e.g., $h^d(q) = [\phi_1(x,y), \phi_3(x,y)]^T$), uniformity is completely lost. Figure 4.5 shows examples of such results.

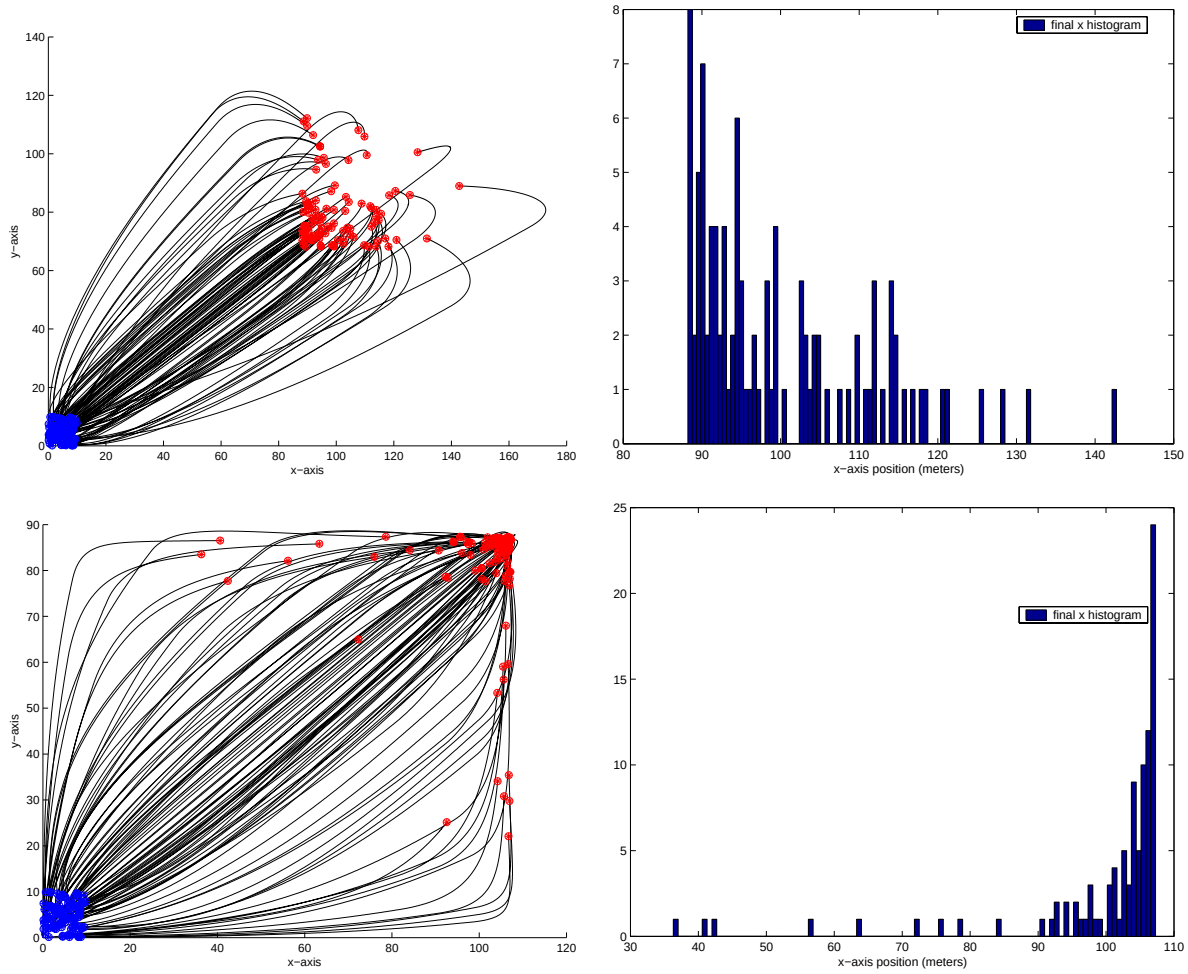

Figure 4.5: Examples of platoon functions for which uniform distribution is not achieved; $h^d(q) = [\phi_{1x,y}, \phi_{3x,y}]^T$, $[\phi_{2x,y}, \phi_{3x,y}]^T$

When $h^d(q)$ is defined by a set of theoretical moments of a uniform density, which are parameterized by commanded density bounds a and b according to (4.21), emergent platoon behaviors will demonstrate one of the four following phenomena.

1. If $h^d(q) = [\phi_1(x,y), \phi_2(x,y), \ldots, \phi_k(x,y)]^T$, where $k = 1, 2, ..., n$, uniform densities of x and y will emerge for lower-order moments only. Statistical instability of higher-order moments causes more complicated h definitions to destabilize the platoon or generate unviable trajectories. Figure 4.4 illustrates the validity of controlling select moments in order to maintain a uniform distribution.

2. If $h^d(q) = [\phi_1(x,y), \phi_k(x,y)]^T$, where $k = 2, ..., n$, then the platoon achieves the commanded mean and assumes a set of final vehicle positions that minimize the energy required to meet the requirements of $\phi_k(x,y)$. The higher the value of k, the larger the commanded moment's value will be. With an arbitrarily sized platoon, energy is better spent in sending a few vehicles to remote locations in order to track the commanded higher-order statistic, not moving the whole platoon, so this platoon function generates non-uniform formations with increasingly remote data points (to achieve $\phi_k(x,y)$) and decreasing platoon variance (to maintain $\phi_1(x,y)$ and to minimize energy expenditure). Observe in Figure 4.6 these two trends. Note especially the differences between these two results and that of defining $h^d(q) = [\phi_1(x,y), \phi_2(x,y)]^T$.

3. If $h^d(q) = [\phi_2(x,y), \phi_k(x,y)]^T$, where $k = 3, ..., n$, then the platoon achieves the same mean it would if it were directly commanded by the same parameters (a, b) used for h^d. It also replicates the tendancy of the previously described platoon function - the higher the order of the k^{th} moment, the greater the platoon's dependency upon outlying vehicle positions to achieve the commanded k^{th} moment. Also, the actual variance increase as k increases. See in Figure 4.7 these two trends. Note especially the differences between these two results and that of defining $h^d(q) = [\phi_1(x,y), \phi_2(x,y)]^T$.

4. If $h^d(q) = [\phi_k(x,y)]$, where $k = 1, 2, ..., n$, then the controller generates nearly straight line trajectories to track the single commanded moment, as opposed to the sharp and sometimes unviable turns produced by the previous three general platoon functions. Since no other platoon-level statistics must be achieved, each minimum velocity vector generated by the controller is manifested as a set of nearly smooth, straight paths. More specifically, for $k > 1$ since no average position is mandated in h^d, the platoon remains oriented to the original platoon location. This case shows the trend of higher-order moments to use outlying vehicle positions to achieve the commanded statistics, so as k increases, some vehicles travel long distances and a majority of vehicles are kept close to their origin. This is consistent with the generalized $h^d(q) = [\phi_1(x,y), \phi_k(x,y)]^T$ in item 2. In both cases, increasing k in h^d decreases the variance of x and y. Figure 4.8 illustrates

both of these tendancies.

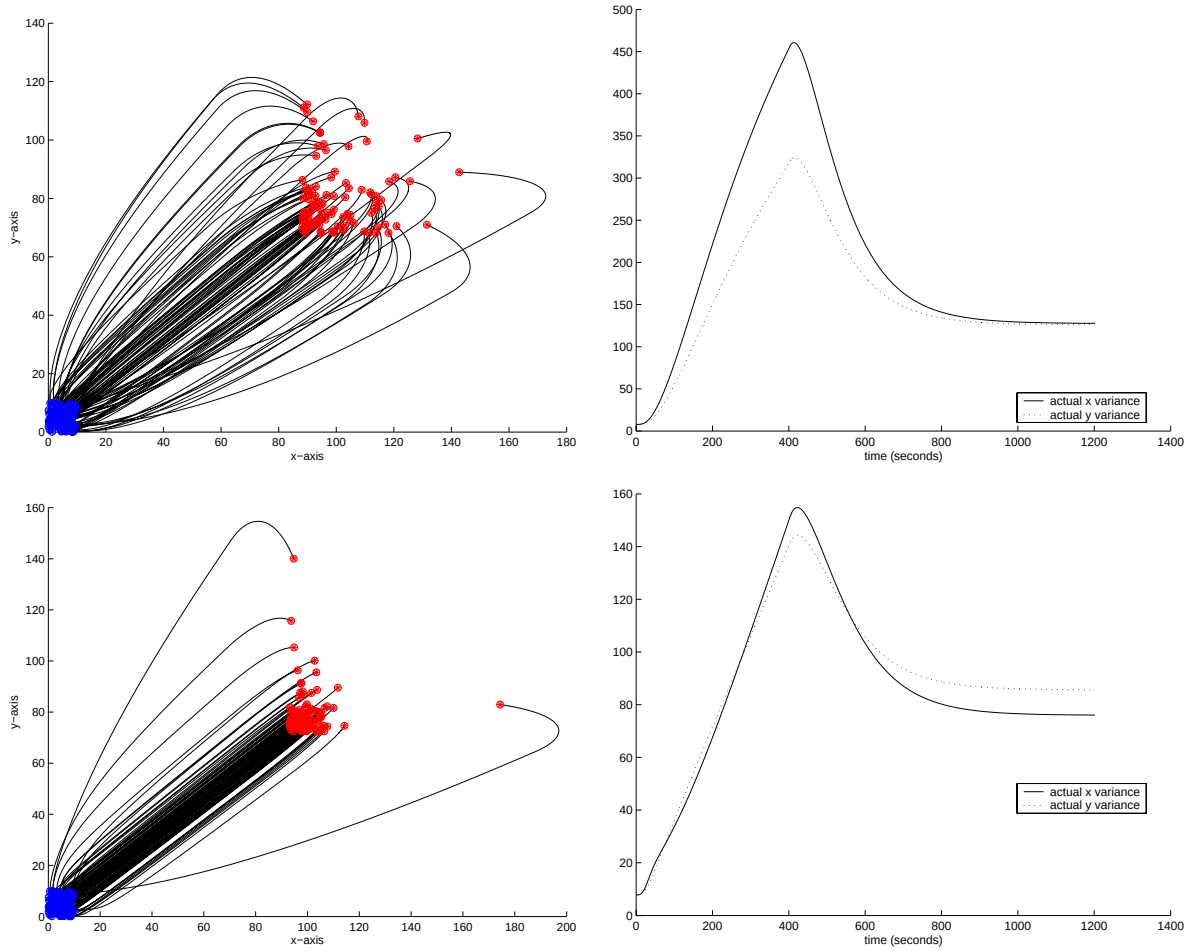

Figure 4.6: Trajectories and corresponding variance characteristics for $h^d(q) = [\phi_{1x,y}, \phi_{3x,y}]^T, [\phi_{1x,y}, \phi_{5x,y}]^T$, respectively

Finally, the communication strategy for this approach is simple. Command only the first general moment, the average, of the position data in order to mobilize a platoon that will implement locally optimal trajectories at each instant in time (Figure 4.1). Commanding the second moment is not the same as commanding the variance, so choosing not to directly control the variance allows it to fluctuate throughout a platoon's maneuver. This allowance is what causes the sweeping trajectories and sharp turns seen in the simulation results for higher-order definitions of h. This, combined with the fact that many of the vehicles' maneuvers are physically impossible is what makes the original formulation - $h^d(q) = \left[\mu_x, \sigma_x^2, \mu_y, \sigma_y^2\right]^T$ - better than any presented thus far. Though this platoon-level controller produces emergent behaviors at the vehicle level, its stable, straight line paths combined with collision avoidance capabilities actually make the emergent behaviors relatively predictable.

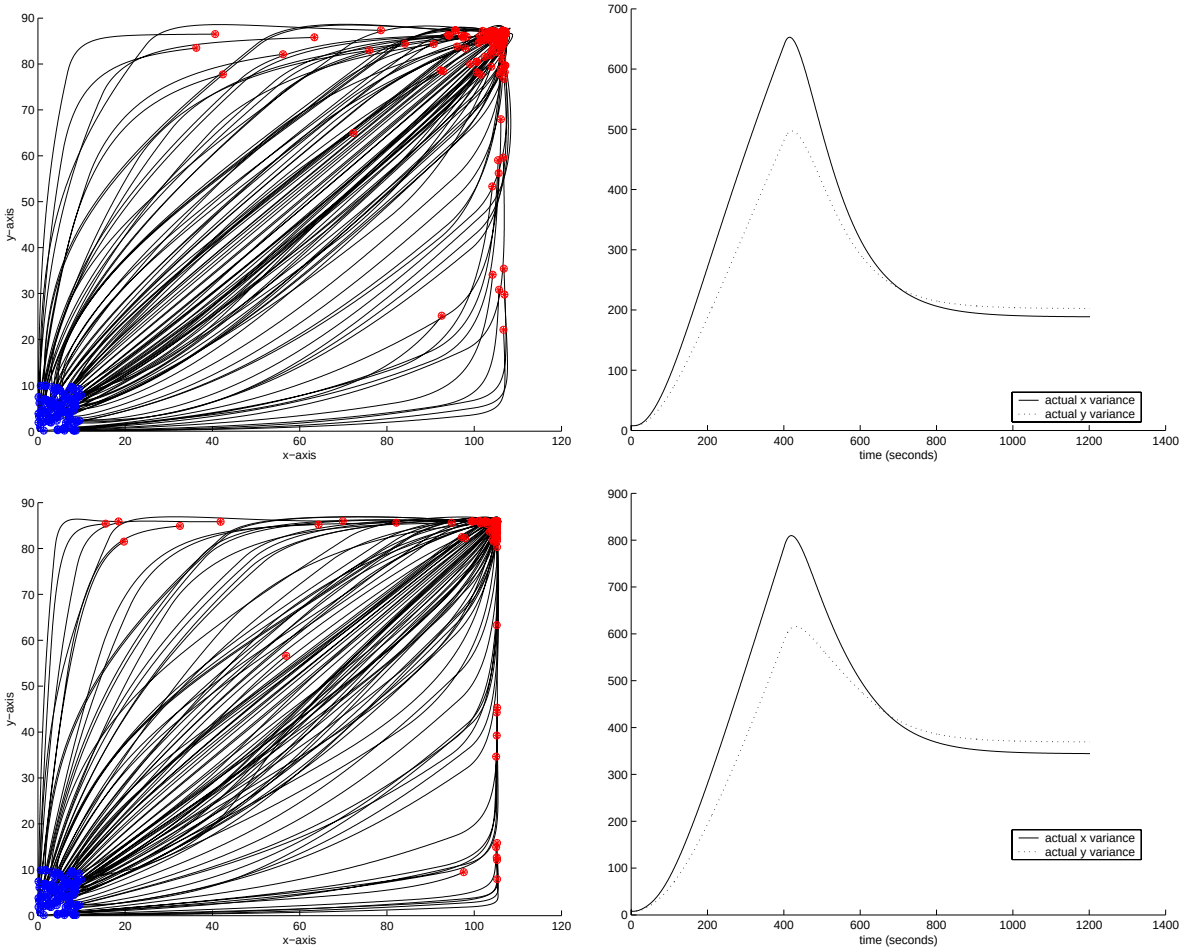

Figure 4.7: Trajectories and corresponding variance characteristics for $h^d(q) = [\phi_{2x,y}, \phi_{3x,y}]^T$, $[\phi_{2x,y}, \phi_{5x,y}]^T$, respectively

Uniform Distribution to Normal Distribution and Variations on the Platoon Function

Of great interest is a low-communication solution for *changing* from a uniform density to an arbitrary function. The indications from the previous section give hope for at least crudely approximating a *normal* density function, as well as for making some general predictions of platoon behavior for a given selection of h.

The parameters of any normal distribution are the density's mean and variance, μ and σ^2. The probability density function of a normal distribution of the random variable x is

$$f(x) = \frac{1}{\sqrt{2\pi\sigma^2}} e^{-(x-\mu)^2/2\sigma^2} \tag{4.23}$$

and the k theoretical moments comprising h^d are defined by differentiating and evaluating at zero the normal characteristic function

$$e^{j\mu\omega - \sigma^2\omega^2/2} \tag{4.24}$$

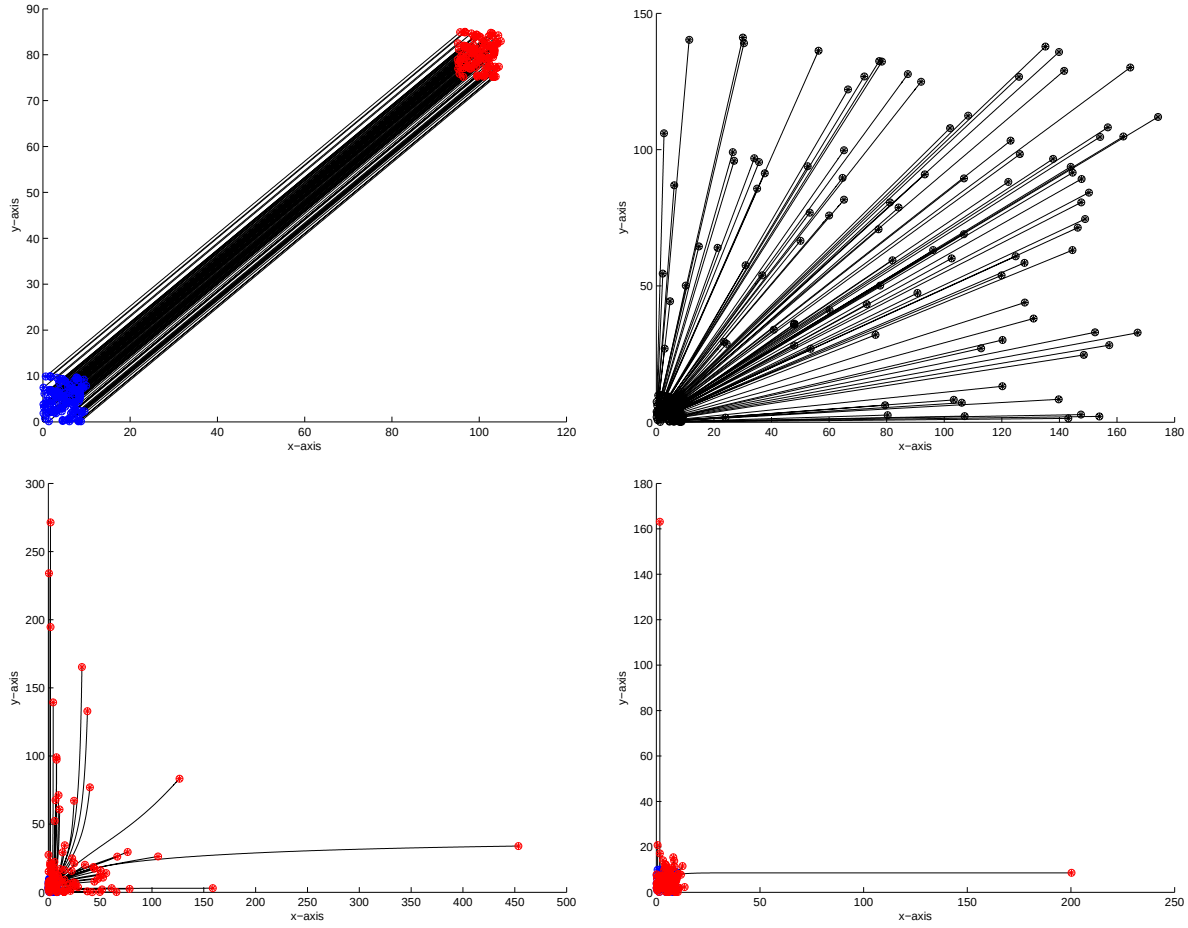

Figure 4.8: Trajectories emerging from $h^d(q) = [\phi_{1x,y}], [\phi_{2x,y}], [\phi_{3x,y}], [\phi_{7x,y}]$ (top left to bottom right)

Specifically, for a zero-mean normal random variable x,

$$E[x^k] = 0 \qquad k \quad \text{even} \tag{4.25}$$

$$E[x^k] = 1 \cdot 3 \cdot 5 \cdots (k-1)\sigma_x^k \qquad k \quad \text{odd} \tag{4.26}$$

A normal distribution is completely characterized by only its mean and variance, μ and σ^2. Scaling these parameters as functions of time guides 100 vehicles from a unifiorm distribution defined by $[a_{x,y}, b_{x,y}] = [0, 10]$ to a normal distribution with zero mean according to (4.25). Figure 4.9 shows selected results of this test. Then, to test more interesting and valuable maneuvers, $h^d(q)$ is redefined by $\mu_x = 100$, $\mu_y = 80$, $\sigma_x^2 = \sigma_x^2(0) + 2$ and, $\sigma_y^2 = \sigma_y^2(0) - 2$.

Commanding the moments of the zero-mean distribution shows promise in changing the density of position data. Even though it is characterized entirely by its mean and variance, a normal density is still not entirely *distinguishable* from other distributions. So, it is not surprising that commanding $h^d(q) = [\phi_1(x, y)]$ to zero produces an exact replica of the platoon centered about the new mean. Also, the trajectories are straight paths. Adding $\phi_2(x, y)$ and commanding σ_x and σ_y to remain constant

recreates the uniform densities of both x and y about the new mean (Figure 4.9). By adding $\phi_3(x, y)$ and commanding both σ_x and σ_y to remain unchanged, both of the final densities change; and using the fourth moment accomplishes the goal of completely altering the densities of x and y (Figure 4.9). Results are robust over a range of variance parameterizations other than $\sigma_x = \sigma_x^2(0)$ and $\sigma_y = \sigma_y^2(0)$. Additional moments only prove cumbersome in this zero-mean case. Though the command function is met for orders as high as $k = 6$, $k > 6$ produce unviable trajectories.

When consideration is broadened to maneuvers with a non-zero mean, previous success deteriorates. For $k \geq 4$, the system suffers extreme actuation demands from statistical instability. And for $k = 3$, the final histograms of x and y are approximately normal for only a small range of commanded variance values other than $\sigma_x = \sigma_x^2(0)$ and $\sigma_y = \sigma_y^2(0)$. Also, $k = 3$ does not yield viable vehicle paths, so in the case of normal densities, commanding successive higher-order moments succeeds only in limited zero-mean cases.

Uniform Distribution to Exponential Distribution and Variations on the Platoon Function

The parameter of any exponential distribution is the function's mean, β. The probability density function of an exponential distribution of the random variable x is

$$f(x) = \frac{1}{\beta} e^{-x/\beta} \qquad x \geq 0, \beta > 0 \tag{4.27}$$

and the k moments in $h^d q$ are defined by appropriately evaluating the exponential characteristic function

$$(1 - j\omega\beta)^{-1} \tag{4.28}$$

Since an exponential distribution is characterized only by its mean, the 100 vehicles are moved from a unifiorm distribution with $(a_{x,y}, b_{x,y}) = (0, 10)$ into an exponential distribution with desired means $\beta_x = 100$ and $\beta_y = 80$. Figure 4.10 shows platoon movement and final histograms of x data as a result of defining $h^d(q)$ in terms of $k = 1, 2, 3, 4$. The results in the y dimension are not shown because they represent trends similar to those illustrated by the x data. Statistical instability destabilizes the platoon for $k \geq 5$. A focus on $k \leq 4$ reveals that a successful transition to exponential densities requires a low dimension platoon function. For $k = 3, 4$ the controller generates distinctly exponential densities only after an initial period of unfeasible vehicle paths. After this, all vehicle paths are nearly straight. Also, compared to the normal distribution, this controller is more robust to parameterization.

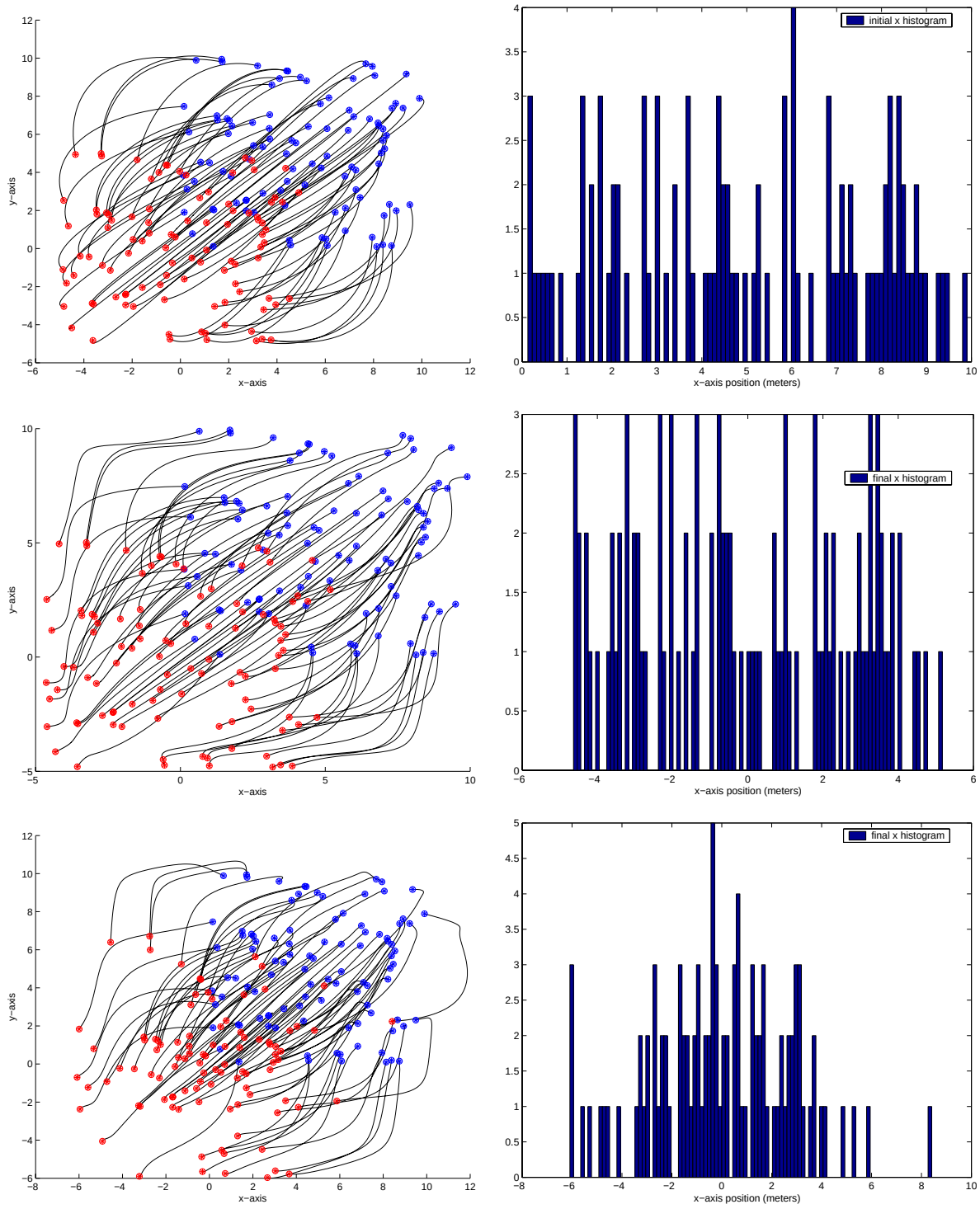

Figure 4.9: Trajectories for $k = 2, 3, 4$, initial x histogram (upper right), and final x histograms for $k = 3, 4$, uniform to zero-mean normal distribution

4.3 Investigation of Central and Spatial Moments

The central moments of a random variable x are defined as the expected value of $(x - \eta)^n$ where η is the mean of the distribution,

$$\mu_n = E[(x - \eta)^n] = \int_{-\infty}^{\infty} (x - \eta)^n f(x)\, dx \tag{4.29}$$

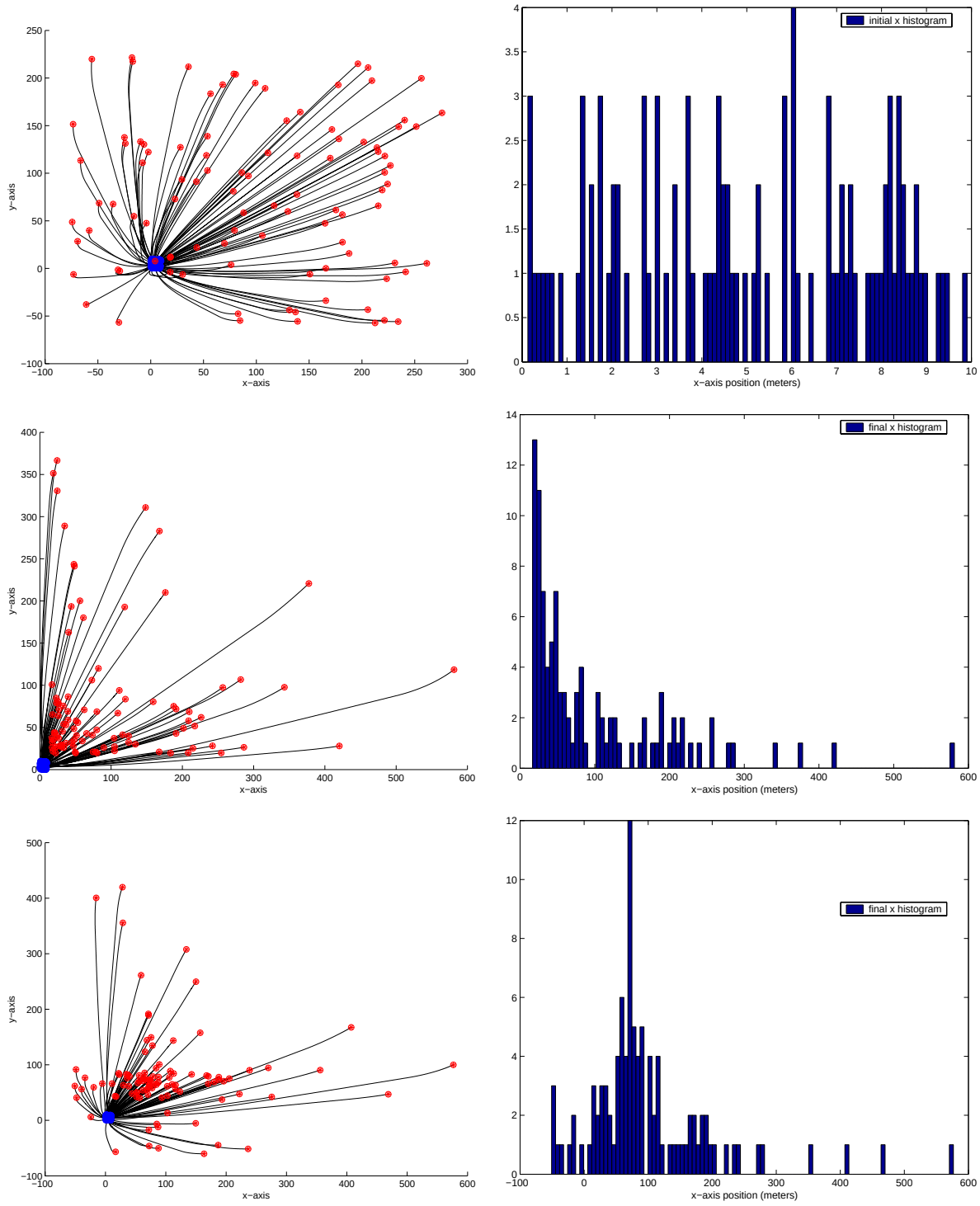

Figure 4.10: Trajectories for $k = 2, 3, 4$, initial x histogram (upper right), and final x histograms for $k = 3, 4$, uniform to exponential distribution

The first central moment is equal to zero for any distribution; and the second is by definition σ^2. Comprising $h^d(q)$ of central moments contributes only minimally to understanding the platooning problem and contributing to its generalization. Central moments are shown to produce the same

controller form as the originally proposed general moments in 4.18. Since central moments employ the difference between data points and the distribution's average, they might supposedly address the statistical instability of higher-order moments. However, the distribution average cannot be controlled by central moments and higher-order moments (including scaled and customized versions of them), when combined with $\sigma_{x,y}^2$, do not achieve new densities or useful platoon formations.

As an extension of the continuous domain $(m+n)^{th}$ moment of a joint probability density, the image processing field uses the (discrete) $(m+n)^{th}$ unscaled spatial moment for shape analysis [21]. It is defined as

$$M_U(m,n) = \sum_{i=1}^{r}\sum_{j=1}^{r} (x_k)^m (y_j)^n \tag{4.30}$$

for all pairs of 2-dimensional data. Differences between even the lower-order moments can be serveral orders of magnitude [21], so these spatial moments are scaled so that

$$M(m,n) = \frac{1}{r^{m+n}} \sum_{i=1}^{r}\sum_{j=1}^{r} (x_i)^m (y_j)^n \tag{4.31}$$

Then, by establishing the mean in each dimension, μ_x and μ_y, the scaled spatial *central* moments of a discrete image are defined as

$$U(m,n) = \frac{1}{r^{m+n}} \sum_{i=1}^{r}\sum_{i=1}^{r} (q_{i1}-\mu_1)^m (q_{i2}-\mu_2)^n \tag{4.32}$$

and can characterize position data for a platoon of robots just as they can specify image features in image processing applications. $q_i = [q_{i1}, q_{i2}]^T \in \mathbb{R}^2$ is a point on the plane, and r is the number of vehicles in a platoon. More specifically, according to the preceeding discussions of simulations in the $x-y$ plane,

$$U(m,n) = \frac{1}{r^{m+n}} \sum_{i=1}^{r}\sum_{j=1}^{r} (x_i-\mu_1)^m (y_j-\mu_2)^n \tag{4.33}$$

Now, in terming a new platoon function, note that $U(1,0)$, $U(0,1)$, $U(2,0)$, $U(0,2)$, and $U(1,1)$ are μ_x, μ_y, σ_x^2, σ_y^2, and the covariance of x and y, respectively. Since x and y are independent random variables, their covariance is zero, so any time $U(1,1)$ is included in $h(q)$, it should be commanded to zero so as not to contradict the formulation of this platooning problem, which is defined by the independence of

x and y. Of those investigated, the following platoon function is of special interest.

$$h(q) = \begin{bmatrix} \mu_x \\ \mu_y \\ \sigma_x^2 \\ \sigma_y^2 \\ U(1,1) \\ U(2,2) \end{bmatrix} \tag{4.34}$$

The command function is defined by joint uniform central moments as follows

$$U^d(m,n) = \frac{b_x b_y - b_x a_y - a_x b_y + a_x a_y}{(m+1)(n+1)} \left[(b_x - \mu_x^d)^{m+1} - (a_x - \mu_x^d)^{m+1}\right] \left[(b_y - \mu_y^d)^{n+1} - (a_y - \mu_y^d)^{n+1}\right] \tag{4.35}$$

Note that the partial derivatives of this platoon function meet the requirements of Theorem 3.4.1. Indeed, this would be true for a platoon function composed of any spatial central moments $U(m,n)$. As mentioned, $U(1,1)$ is commanded to be zero. $U(2,2)$ is also commanded to be zero, which produces the cross-shaped platoon formation illustrated in Figure 4.11. Both μ_x and μ_y are commanded to be 100; both variances are commanded to remain constant in the first case and to become 200 in the second. For ease of viewing, some paths are eliminated from the figure.

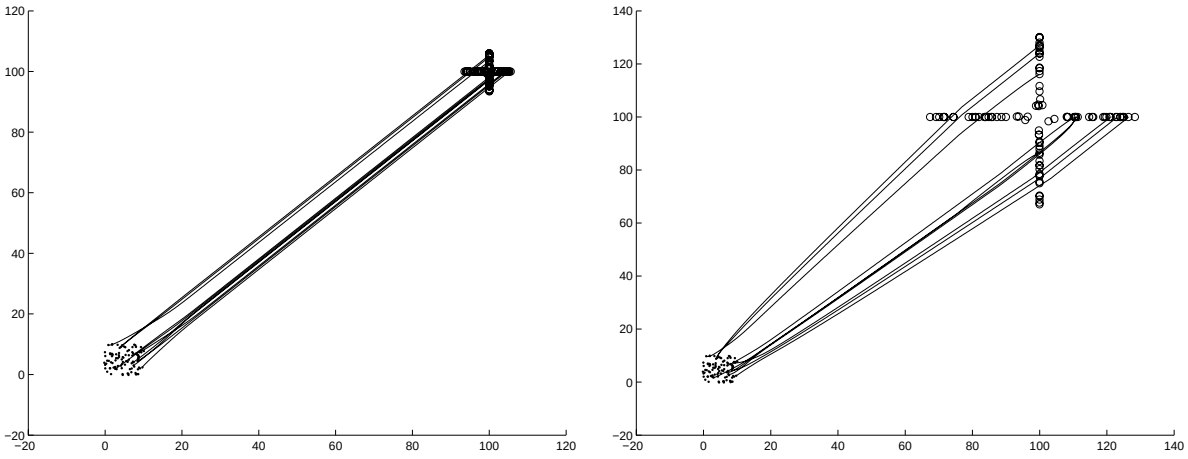

Figure 4.11: Paths generated by spatial moments: variance unchanged, variance increase to $\sigma_{x,y}^2 = 200$

4.4 Investigation of Hu's Invariant Moments

Following from the discussion of spatial moments comes a consideration of Hu's invariant moments. These are a set of compound spatial moments that are invariant in the continuous image domain to

translation, rotation, and scale change [21]. To start, consider Hu's normalization of the unscaled central moments according to

$$U_U(m,n) = \sum_{i=1}^{r}\sum_{j=1}^{r}(x_i-\mu_x)^m(y_j-\mu_y)^n \tag{4.36}$$

$$V(m,n) = \frac{U_U(m,n)}{[M(0,0)]^\alpha} \tag{4.37}$$

$$\alpha = \frac{m+n+2}{2} \qquad (m+n) = 2,3,\cdots \tag{4.38}$$

$$\tag{4.39}$$

and M(0,0) = r. The seven invariant moments are defined as follows.

$h_1 = V(2,0) + V(0,2)$

$h_2 = [V(2,0) - V(0,2)]^2 + 4[V(1,1)]^2$

$h_3 = [V(3,0) - 3V(1,2)]^2 + [V(0,3) - 3V(2,1)]^2$

$h_4 = [V(3,0) + V(1,2)]^2 + [V(0,3) - V(2,1)]^2$

$h_5 = [V(3,0) - 3V(1,2)][V(3,0) + V(1,2)][V(3,0) + V(1,2)]^2 - 3[V(0,3) + V(2,1)]^2$
$+[3V(2,1) - V(0,3)][V(0,3) + V(2,1)]3[V(3,0) + V(1,2)]^2 - [V(0,3) + V(2,1)]^2$

$h_6 = [V(2,0) - V(0,2)][V(3,0) + V(1,2)]^2 - [V(0,3) + V(2,1)]^2$
$+4V(1,1)[V(3,0) + V(1,2)][V(0,3) + V(2,1)]$

$h_7 = [3V(2,1) - V(0,3)][V(3,0) + V(1,2)][V(3,0) + V(1,2)]^2 - 3[V(0,3) + V(2,1)]^2$
$+[3V(1,2) - V(3,0)][V(0,3) + V(2,1)]3[V(3,0) + V(1,2)]^2 - [V(0,3) + V(2,1)]^2$

Employing the entire set of seven invariant moments is not possible because of the discrete nature of the platooning problem and because there is no informed starting point for understanding each moment's general value or rate of change. Even measuring all seven moments of a desirable formation and then time incrementing the initial measurements to the measured values does not work due to descritation and the apparently inappropriate application of one rate of time-variation to all seven moments. However, to help counter the problem of imaging discontinuity, more vehicles are used to test this controller. The platoon is enlarged to have 200 vehicles instead of 100. Also, based on having so little foreknowledge of each moment's behavior and knowing that they relate to shape change and orientation, the inclination was to investigate each statistic's effect on the platooning

problem by focusing on specific moments and inducing a change in them instead of maintaining their invariance. Since Hu's seven moments are simply complicated combinations of summations, they meet the requirements of Theorem 3.4.1.

The enlarged platoon initially has uniform x and y values with parameters $[a_{x,y}, b_{x,y}] = [0, 25]$. Some of Hu's moments, especially when controlled in combination with one another, generate unviable paths with tight turns at their beginning and or ends, but the second, $h_2 = [V(2,0) - V(0,2)]^2 + 4[V(1,1)]^2$, being a variation on the variance statistic, produces straight paths. Figure 4.12 displays the results of commanding the platoon to $\mu_x = 100$, $\mu_y = 80$, and h_2 to assume a value one hundred times that of its initialization, $h^d(q) = [\mu_x, \mu_y, 100h_2(0)]$. All three statistics are controlled by ramping their initial values up to the prescribed final values. Some interesting formation shapes were observed when the platoon function contained μ and Hu's first and third invariant moments. However, path viability was a concern in most tests.

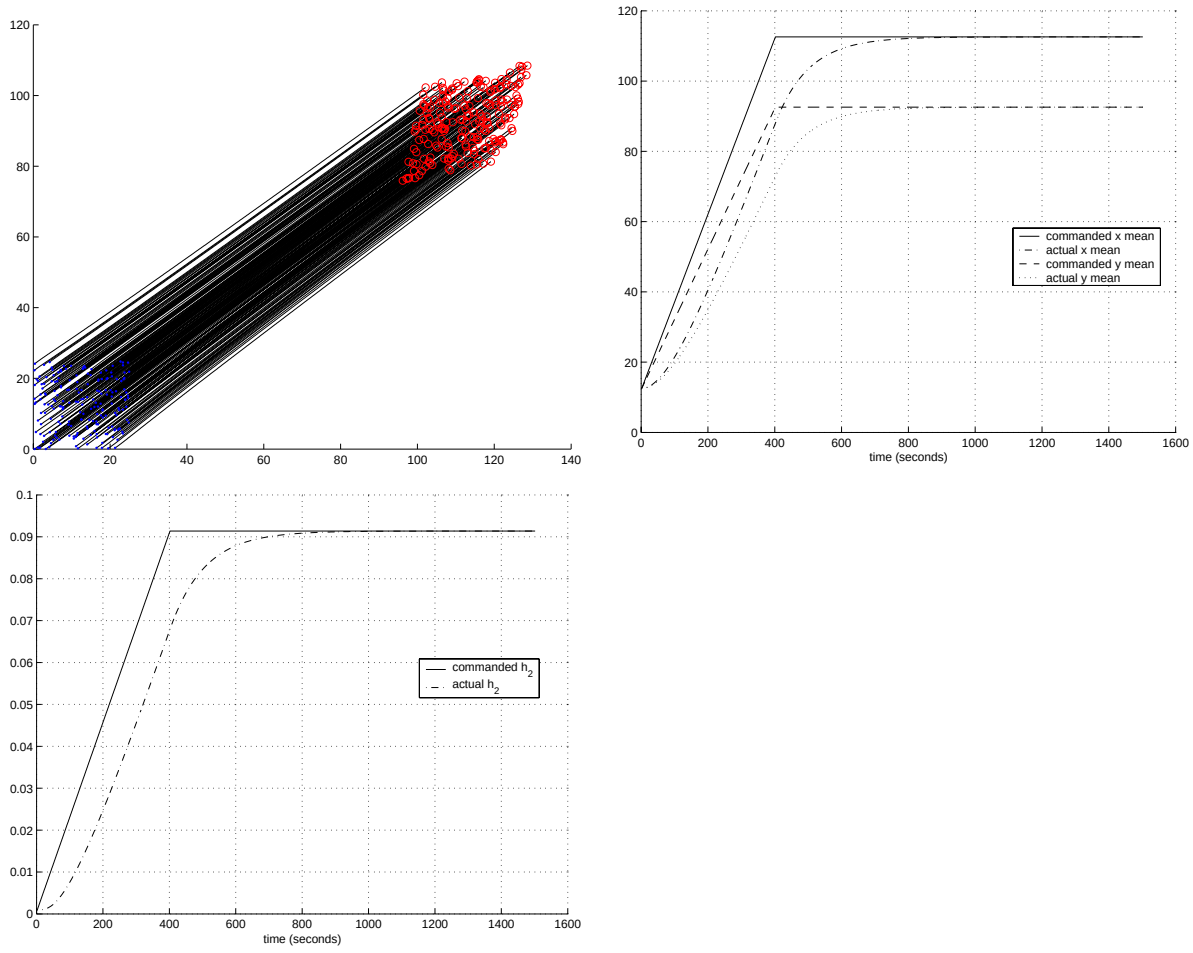

Figure 4.12: Trajectories for $h^d(q)$ containing μ_x, μ_y, and h_2

Chapter 5

Conclusions

5.1 Future Work on VT Miniature AUV Hardware

The ASCL AUV hardware design has advanced to the point of being very dependable and quite straightfoward to keep in good repair. However, two main design features remain of interest. First, there is some inclination to redesign the fins to have small bearings like those about the driveshaft [22]. Such inclusion of bearings would provide additional support to the fins, which (excluding the RF and GPS antennas) are the components most violently affected by external forces. To date, the type and extent of damage suffered by the fins indicates that bearings would eliminate some damage to both the finshaft and the finshaft housing.

The second point is not so much one of performance but one of convenience. Currently, the GPS receiver is situated such that removing the hull requires first the dismounting of the GPS receiver. Of course, removing the hull to tend to an easy repair or connection of wires would ideally not involve every time dismounting and remounting the GPS. The current design has been preferable to other propositions because of the limited space on the tail section for appending or inserting more components and because the current location of the antenna - about the evenly round hull - offers a more cooperative surface to which components can be mounted. The sloped portion of the tail, the bulkhead connector, and the desire to avoid solutions that involve drilling into the tail section's PVC walls all make the evenly round acrylic hull more structurally advantageous than propositions to date.

5.2 Statements on Low-Bandwidth Platooning Solution

All of the controllers considered and synthesized herein depend upon redundant manipulator control techniques and the meeting of the condition stated in Theorem 3.4.1 for their decentralized structure. Such adherence, as guaranteed by Theorem 3.4.1, produces decentralized controllers requiring a low-bandwidth communication network. The difference between commanding the original platoon function of mean and variance and commanding the postulated functions of approximations of specific probability distribution functions, central and spatial moments, and Hu's invariant moments indicates the value of the original formulation. Not only does $h^d = [\mu_x, \mu_y, \sigma_x^2, \sigma_y^2]^T$ require the least number of communicated scalar values for its achievement, but it also clearly indicates what can be expected of the emergent vehicle paths. Platoon mean and variance are independent of one another. In being so, viable vehicle paths always result. Clearly, though the hypothesis on higher-order moments holds true for some dimensions of h in some applications of the moments (uniform, normal, exponential distributions), the result is not very robust and is certainly not altogether directly predictable. The original platoon function should serve well the objectives of low-bandwidth communication and multi-vehicle cooperation as the ASCL moves forward to that end.

Bibliography

[1] A. S. Gadre and D. J. Stilwell, "Toward underwater navigation based on range measurements from a single location," in *Proc. IEEE International Conference on Robotics and Automation*, (New Orleans, LA), pp. 4472–4477, 2004.

[2] D. J. Stilwell and B. E. Bishop, "Redundant manipulator techniques for path planning and control of a platoon of autonomous vehicles," in *Proceedings of the IEEE Conference on Decision and Control*, (Las Vegas, NV), pp. 2093–2098, 2002.

[3] B. Siciliano, "Kinematic control of redundant robot manipulators: A tutorial," *Journal of Intelligent Robotic Systems*, vol. 3, pp. 201–212, 1990.

[4] B. E. Bishop and D. J. Stilwell, "On the application of redundant manipulator techniques to the control of platoons of autonomous vehicles," in *Proc. IEEE Conference on Control Applications*, (Mexico City, Mexico), pp. 823–828, 2001.

[5] S. B. Skaar, I. Yalda-Mooshabad, and W. H. Brockman, "Nonholonomic camera-space manipulation," *IEEE Transactions on Robotics and Automation*, vol. 8, no. 4, pp. 464–479, 1992.

[6] O. Khatib, K. Yokoi, K. Chang, D. Ruspini, R. Holmberg, and A. Cassal, "Coordination and decentralized cooperation of multiple mobile manipulators," *Journal of Robotic Systems*, vol. 13, no. 11, pp. 755–764, 1996.

[7] H. Yamaguchi, "A cooperative hunting behavior by mobile robot troops," *International Journal of Robotics Research*, vol. 18, no. 9, pp. 931 – 940, 1999.

[8] T. Balch and R. Arkin, "Communication in reactive multiagent robotic systems," *Autonomous Robots*, vol. 1, no. 1, pp. 27–52, 1994.

[9] D. J. Stilwell and J. S. Bay, "Optimal control for cooperating mobile robots bearing a common load," in *Proc. IEEE International Conference on Robotics and Automation*, (San Diego, CA), pp. 766–771, 1994.

[10] X. Yun, "Line and circle formation of distributed physical mobile robots," *Journal of Robotic Systems*, vol. 14, no. 2, pp. 63–81, 1997.

[11] C. A. Klein and C.-H. Huang, "Review of pseudoinverse control for use with kinematically redundant manipulators," *IEEE Transactions on Systems, Man and Cybernetics*, vol. 13, no. 3, pp. 245–250, 1983.

[12] J. M. Hollerbach and K. C. Suh, "Redundancy resolution of manipulators through torque optimization," *IEEE Transactions on Robotics and Automation*, vol. 3, no. 4, pp. 308–316, 1987.

[13] C. A. Klein and T.-S. Chung, "Force interaction and allocation for the legs of a walking vehicle," *IEEE Journal of Robotics and Automation*, vol. 3, no. 6, pp. 546–555, 1987.

[14] B. E. Bishop, "On the use of redundant manipulator techniques for control of platoons of cooperating robotic vehicles," *IEEE Transactions on Systems, Man, and Cybernetics, Part A*, vol. 33, no. 5, pp. 608–615, 2003.

[15] H. Singh, J. Catipovic, R. Eastwood, L. Freitag, H. Henricksen, F. Hover, D. Yoerger, J. Bellingham, and B. Moran, "An integrated approach to multiple AUV communications, navigation, and docking," in *Proceedings of IEEE/MTS Oceans*, (Fort Lauderdale, Florida), pp. 59–64, September 1996.

[16] R. Bachmayer and N. E. Leonard, "Vehicle networks for gradient descent in a sampled environment," in *Proceedings of the IEEE Conference on Decision and Control*, (Las Vegas, NV), pp. 112 – 117, 2002.

[17] E. Fiorelli, P. Bhatta, and N. E. Leonard, "Adaptive sampling using feedback control of an autonomous underwater glider fleet," in *Proceedings of the International Unmanned Untethered Submersible Technology Symposium*, (Durham, New Hampshire), August 2003.

[18] R. Bachmayer and N. E. Leonard, "Experimental test-bed for multi-vehicle control, navigation and communication," in *Proceedings of the International Unmanned Untethered Submersible Technology Symposium*, (Durham, NH), 2001.

[19] A. Papoulis and S. U. Pillai, *Probability, Random Variables and Stochastic Processes, 4th Edition*. New York: McGraw-Hill, 2002.

[20] G. Terrell, "Personal correponsdance," (Department of Statistics, Virginia Polytechnic Institute and State University, Blacksburg, VA), February 2004.

[21] W. K. Pratt, *Digital Image Processing, 2nd Edition*. New York: John Wiley and Sons, Inc., 1991.

[22] D. J. Stilwell, "Personal correponsdance," (Autonomous Systems and Controls Laboratory, Virginia Polytechnic Institute and State University, Blacksburg, VA), 2004.

Appendix A

Steps for Constructing a VT Miniature Autonomous Underwater Vehicle

The following specific steps are required to replicate the current VT miniature AUV. These steps provide details on labor, screw types and sizes, thread strengths, necessary drill bits, mixture ratios, etc.

1. Upon acquisition of acrylic tube sections, cut the six foot length into three 24 inch lengths. The Industrial Systems Engineering Machine Shop (on the first floor of Whittemore Hall) has personnel that are usually helpful enough to take the time to make these cuts. The ISE shop has a high quality band saw with three important features for this cutting process. First, the table of the saw has a long conveyor belt component to it, so the whole tube is well supported, which eliminates the risk of the awkward six foot tube moving during the cutting process. Second, the saw uses a cooling and lubricating solution that keeps the acrylic from cracking and fracturing along the surface of the cut. This is a significant problem because of how brittle acrylic is. Third, the saw table has a squaring block against which the tube is aligned, which ensures a 90 degree cut and a flush interface between each hull's ends and its corresponding tail and nose pieces. Rinse each tube; sink pressure water is sufficient to rinse away the lubricating solution. Deliver these pieces to Metal Processing, Incorporated (MPI) when a contract is negotiated to begin work on new AUV parts. As described in the above components section, MPI will use these hull pieces to ensure the proper fits of each tail and nose piece.

2. As soon as MPI completes the tail and nose pieces, visit the shop and ensure the fit between each nose and each tail for each hull. The *Parker* manual indicates that a 0.003 inch clearance

is required between the inner diameter of the hull (bore) and the outer diameter of the tail and nose pieces (plug). Translated, there should be a little wiggle between the hull and the inserted piece of PVC. Depending on the hull's exact inner diameter and circularity, tail and nose pieces may have slightly different diameters. It is important to note here that custom cutting the nose and tail should only be applied to the plug diameters of each, *NOT* the o-ring groove diameter. Doing so would significantly change the o-ring's fit in the groove, risking highly the chance of poor sealing and leakage. Even with a below average bore diameter, not cutting the o-ring groove only makes more difficult the insertion and removal of the o-ring laden tail or nose, but changing the groove diameter compromises well-developed design requirements and requires a well calculated risk to reverse engineer a sufficient o-ring seal.

3. Once the tail and nose pieces have been completed, the hull pieces must be slightly modified. After an o-ring has been installed on each tail and nose, a substantial amount of evenly applied force is required to insert the piece in its corresponding hull. To greatly catalyze the insertion process and to keep the sharp acrylic edge from damaging the o-ring (cutting or scraping the rubber can compromise a seal's integrity), create a chamfer cut on the inside of each hull. A chamfer is a cut that replaces a sharp 90 degree junction between two adjacent sides of material with an angled junction, making more graduated the transition from, in this case, the hull's inner diameter and the cut surface at each end of the hull. To create this chamfer, use a Dremel Tool with a sanding attachment to grind a chamfer on the inside edge of each hull. Of the 1/8 inch wall thickness of each hull, leave approximately 1/16 - 3/32 inch of material and cut the chamfer to be 45 degrees. Use safety goggles for this and all other Dremel work.

4. The driveshaft has a flat spot against which a set screw is screwed. Insert the driveshaft as fas possible into the driveshaft coupler. Determine a spot on the coupler that corresponds to a spot somewhere along the length of the flat spot on the driveshaft. Mark this spot with a marker or scribe. A scribe is a very sharp tool that looks much like a nail; it is used to scrape markings in materials, especially very hard materials. Use the ASCL machine to drill a hole at this point. Mount the coupler in the machine's vice such that it is parallel to the floor (the machine's vice secures firmly to the machine's x-y table). Drill the hole at the highest point on the coupler, i.e., such that the drill bit is perpendicular to the tangent at the point of drilling. Drill for a 75 percent thread depth (since the hole's depth is less than one and a half times the hole diameter). To do so, use a number 43, 2.30 mm, or 2.35 mm drill bit.

5. To tap this screw hole (tapping is the process by which a smooth hole is threaded), use tapping oil and a 4-40 tap (taps are *quite* brittle and will break if tapping oil is not used). Use the hand tap set available in the ASCL, which contains the 4-40 tap and a handle for turning it. Firmly mount the coupler in a vice (parallel to the floor) and apply a small amount of tapping oil to the hole. It is also helpful to add a bit of oil to the length of the tap that will be used for cutting. To cleanly tap a hole without breaking the tap or damaging the threads being made, turn the tap one quarter turn *in reverse (counterclockwise)* after each full forward turn (clockwise). As a tap is turned forward, it cuts the material in such a way that a small barrier develops along the inside wall of the hole. Turning the tap in reverse breaks this barrier, so periodically doing so keeps a number of barriers from cooperatively breaking the tap. Using compressed air is a good way to clean debri and tapping oil from drilled and tapped holes and off of the rest of the part. If it is not available, just strongly blow out the hole and rinse the part with water.

6. To ensure the integrity of the AUV's propulsion system, the motor shaft also requires a flat spot like that on the driveshaft in order to make the same sort of connection to the motor coupler. As the motor has no such flat spot, one must be made by tooling in the ASCL. Use a Dremel Tool with a grinding bit to create this flat spot. Use eye protection to protect against sparks and steel shards. There are two parameters on this cut. The first is that the flat spot should not be more than 1/2 inch long. The second is that it should not be more than 1/8 to 5/32 inch wide. A wider cut would end up requiring too long a set screw to reach to the flat spot.

7. Drill a 4-40 screw hole in the motor coupler, in which a 4-40 set screw will be placed. Use the same procedure as was followed to drill a screw hole in the driveshaft coupler.

8. Tap the 4-40 screw hole in the motor coupler by following the tapping process listed for the driveshaft coupler.

9. Both the RF antenna and the GPS antenna cable exit the tail section of the AUV in order to mount to the exterior. These two lengths of flexible material are pulled through two holes in the top of the tail section, both of which must be aligned with the top-most finshaft housing (directly above the bulk head connector hole made by MPI). Mount the tail section in the machine vice such that the top-most finshaft is perpendicular to the floor (in both the front view and side view directions). Drill a 1/4 inch hole that is both in the center of the flat portion of the tail diameter *and* in line with the top-most finshaft housing. Also use a hand drill and a 1/8 inch drill bit to make a hole for the GPS cable to pass through. Align this hole with the top fin. Then, mill a

10x10 mm, 1/4 inch deep square around the hole so that the RF coaxial cable can be screwed into the coaxial end of the whip antenna (Figure A.1).

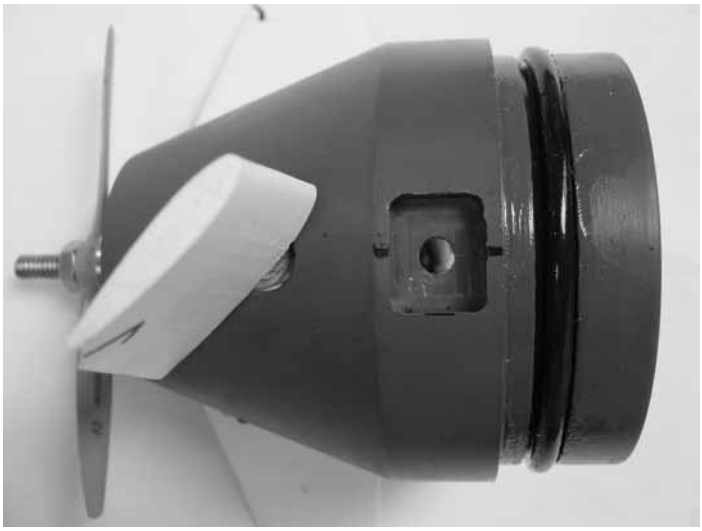

Figure A.1: Tail details, hole for RF antenna mounting

10. A similar hole must be drilled in the nose section (Figure 2.14). This hole is meant for the permanent mounting of the pressure sensor. The pressure sensor has a 7/16-20 threaded end, and the hole's depth is less than one and a half times the diameter of the hole, so use a 75 percent thread depth. To do so, use a number X, 10.00 mm, or 25/64 inch drill bit. Mount the nose section in the machine vice such that the open face is perpendicular to the floor. The hole should be drilled such that the drill bit is perpendicular to the tangent of the nose at the point of drilling (the highest point on the round nose piece). This is important because the sensor will not mount flushly inside the nose if the hole's center is on a slope. Drill at a point 1/2 inch from the edge of the nose's largest diameter, from the point of contact between the nose and the hull. Since this hole needs to be tapped, and since the PVC material is more sensitive than metals, ensure a careful and high integrity cut.

11. Since the pressure sensor has a threaded end, this hole must also be tapped. Use the 7/16-20 tap; and since tapping in the PVC, be very careful not to damage the material that immediately surrounds the hole. Use tapping oil.

12. The screws used to attach the servo bracket to the tail are tapered flat head screws and are intended to rest flush with the surface of the servo bracket. Since the screws are tapered, such a flush joint is possible only if an angle corresponding to the screw's taper is created in each of

the holes in the servo bracket. To do this, use a Number 4 center bore bit (available from the EE machine shop on the second floor of Whittemore Hall). This type of cut creates a chamfer on the nose side of the servo bracket that corresponds to the angle of the screw's taper. It will also enlarge the holes drilled by MPI. This is fine, though one must be careful not to drill down too far, as doing so could make too large the hole for a screw to connect to the bracket. Before drilling too much, test the depth of the chamfer by fitting a tapered flat head 6-32 screw into the hole to see if the head yet rests flush with the nose side of the servo bracket. The key to center boring a hole is to *not* clamp, in this case, the bracket until the bit is spinning inside the hole of choice. Usually, to drill a hole in a piece of material, the material is secured to the table prior to first being pressed by the drill. This ensures a perfectly shaped hole. However, the center bore can initialize a bit of wobble in the piece. If the piece is secured to the table when this wobble begins, the existing hole may be distorted. So, first set the bracket in the clamping mechanism. Then, holding loose the clamping mechanism with one hand and operating the drill with the other, lower the spinning tip inside the hole just enough for the center bore to wiggle the bracket into alignment with the bit. Stop lowering the bit at this point and tighten the clamping mechanism, then continue to lower the bit in order to cut the chamfer.

13. This center boring process should be repeated on all four large holes in motor bracket. The four holes that are set in a square formation are used for mounting the motor bracket to the motor. Since the servo trays mount flatly against the motor bracket, the four tapered flat head screws used in these holes must rest against a chamfer just like the one cut for each of the through holes in the servo bracket. A 6-32 screw is used here as well, so follow the same process previously described for center boring the nine holes in the servo bracket. The only difference is that the chamfer must be created on the *tail* side of the bracket.

14. The servo bracket, three servo trays, and motor bracket connect to make a solid support structure in the tail section of the AUV. This being the case, their proper alignment with one another is very important. The servo trays must align correctly with the servo bracket so that the servos will align correctly with the fins and so that none of the servo or servo linkage parts intersect the path of the drive train. Also, the motor bracket must align with the servo bracket so that the rails and electronics will stand perpendicular to the floor. Follow these steps to correctly align these parts and observe Figures A.2 - A.4 for illustrations.

    First, gather together the servo bracket, all three trays, a scribe, a measuring scale, and a tube

of VersaChem Super Silicone Type 7 instant gasket sealant. Place the servo bracket on a stable surface such that the nose side of the bracket is facing up. Use the scale and scribe to locate and mark the center of each of the straight edges. Based on the height of each servo tray being 15.5-16 mm, mark half this distance on each side of each center mark. These boundaries show where each servo tray will connect to the servo bracket (in the center of each straight edge). Consult the MainCopyPaste.dwg file in AutoCAD to clearly see the servo trays' mounting configuration. Use the scribe to texturize both ends of each servo tray, as well as the three areas of the servo bracket to which the trays are adhered. This helps the silicone sealant ensure a better hold. Spread a bit of sealant on one end of a tray. Choose one of the straight edges on the servo bracket and place the tray between its set of markers and flush with the edge. Push the tray down enough to ensure that it is sitting flatly against the tray, not tilted because of having sealant piled underneath it. Repeat this step for the other two trays and then use a book to lie across all three servo trays. If the book shifts the trays at all, do not remove the book. Rather, move the trays back into line with their boundaries. Since the sealant is clear, it is fairly easy to see markings made by the scribe if they have been made quite clear by several scrapes. Let this configuration dry in an undisturbed area (Figure A.2).

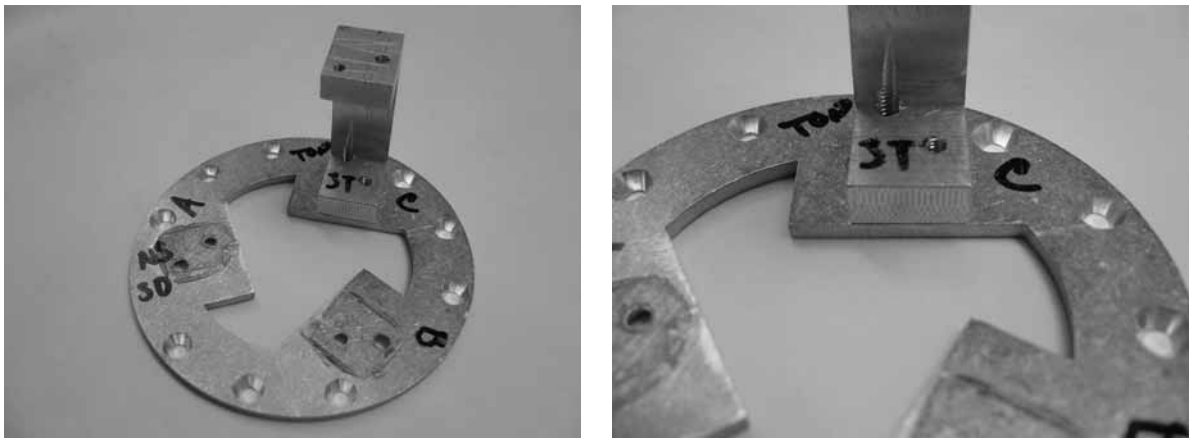

Figure A.2: Servo bracket and servo showing proper orientation and alignment for gluing process

Next, print from the AutoCAD file MainCopyPaste.dwg a one-to-one ratio plot of the servo bracket, servo trays, and motor bracket. Make a stencil from this plot that is used to see how each servo tray is positioned against the motor bracket. Cut out the u-shaped wire pass holes on the motor bracket, as well as all three servo trays. Use the u-shaped wire pass slots to align the stencil on the tail side of the motor bracket, then use the scribe to mark the spacing of the trays on the tail side of the bracket. This step ensures perfect alignment of both the drive train and

the rails and attached electronics (Figure A.3).

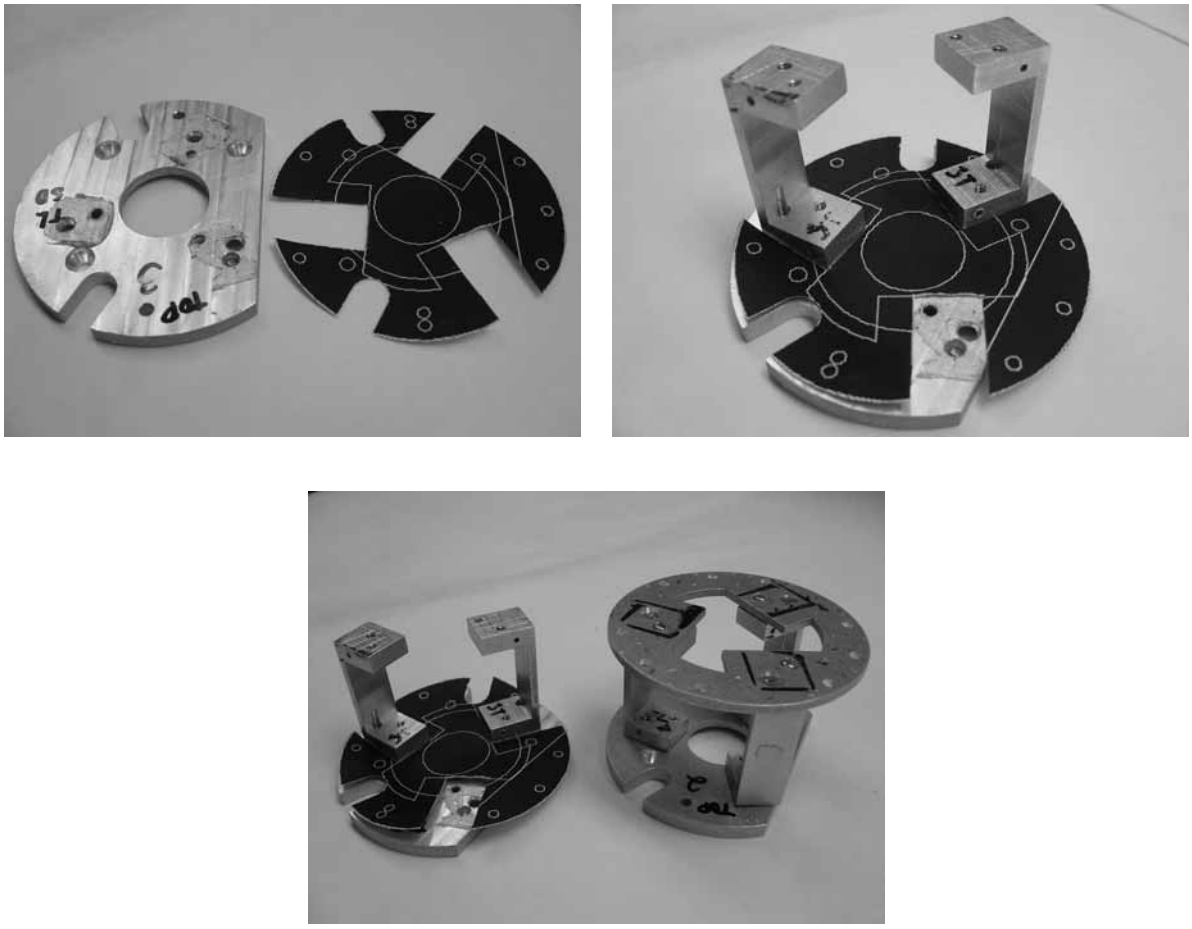

Figure A.3: Motor bracket and motor bracket stencil showing proper placement of motor bracket

Next, connect the dried arrangement of a servo bracket and three trays to the motor bracket. It is *very* important to make sure that the top of the servo tray aligns with the top of the motor bracket because the spacing of the nine servo bracket holes and that of the three servo trays makes unique the necessary orientation of these two brackets to one another. Score the area of connection on the motor bracket and use sealant to glue the servo bracket/tray assembly to the motor bracket. Let this configuration dry in an undisturbed area (Figure fig.brackets3.assembly).

Once the whole structure is dried and secure, determine where screw holes can be drilled. On the tail side of the servo bracket, use a spare servo tray to mirror each tray's position on the nose side of the servo bracket. Use a marker to show the profile of each servo tray on the nose side; this profile shows where there exists material into which a screw hole can be drilled. These same outlines are made on the nose side of the motor bracket, but they are made by observing the configuration from different angles since the servo trays cannot be seen by looking through

the center of the motor bracket in the same way that they can be seen by looking through the center of the servo bracket (Figure A.4).

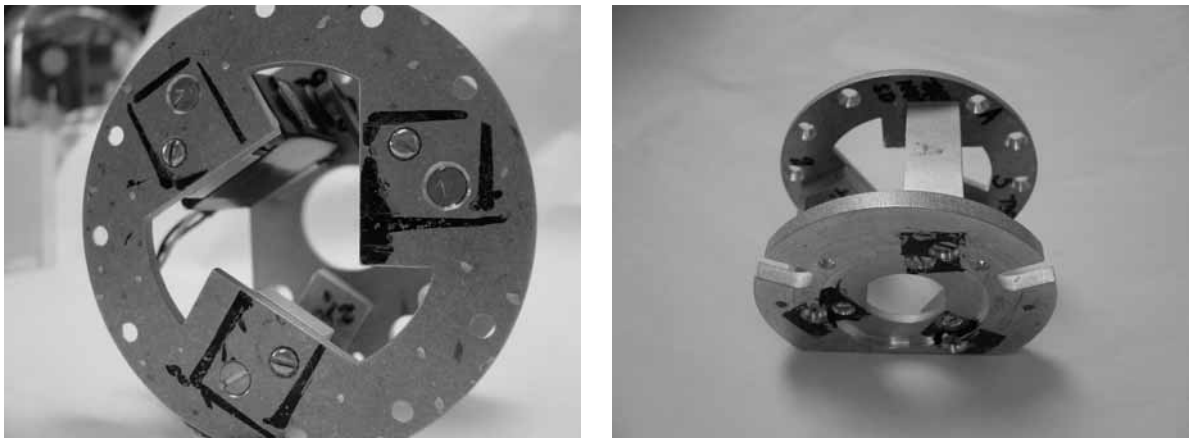

Figure A.4: Orientation of tray securing screws keeping in mind placement of servo mounting screws

15. Each servo tray is secured to each bracket by two screws. There are both a security screw (6-32, responsible mainly for holding the components together) and a stability screw (4-40, responsible mainly for stabilizing the tray relative to both brackets) on both ends of the servo tray. Consider first the motor bracket connections because they require more planning than do the screws on the servo bracket. Consider the indented portion of the motor bracket, that which has a secure keyed fit with the motor. The space composing the overlap of this indention and the servo trays is enough space for each of the 4-40 screws. In these locations, these 4-40 screws will block the passage of screws used to connect each digital servo to its tray. So, the screws used to mount the servos in the trays have to be on the back of the tray, which means that the 6-32 screws must breach the servo tray at a point low enough not to interfere with the servo mounting screws. Choose all six of these points on the motor bracket and mark them with a marker or white correction fluid. For illustration, see Figure A.4.

    Look now to the servo bracket; and consider that the servo mounting screws should be at a diagonal to one another (use two, one on the motor end and one on the tail end of the servo tray). Once the screw location is finalized for the motor end (front or back of servo tray), choose a diagonal position for the tail end of the tray. Based on this necessity, choose points at which to drill the 4-40 and 6-32 holes. For illustration, see Figure A.4.

16. Note here that the brackets are *not* to be threaded. Ensuring a seamless pass from the threads of a bracket to the threads of a servo tray can be difficult, so only the trays are threaded. A 60

percent thread depth is desired for these deeper holes, both for the 4-40 and 6-32 holes (Remember that the coupler holes used 75 percent). To achieve such, use for the 4-40 screw holes a number 42, 2.40 mm, or 3/32 inch drill bit. And for the 6-32 screw holes, use a number 33 or 2.90 mm drill bit. All of these are available in the ASCL. Again, do *not* immediately thread these holes. Rather, disassemble the brackets from the trays (just manually pull apart the sealant bonds). Mark these pieces with numbers one through three and descriptions T and N for *tail* and *nose* so that the trays will fit back with their corresponding holes.

17. Tap the holes in each tray but do *not* tap the holes in the brackets. Use tapping oil and the 4-40 and 6-32 taps appropriately.

18. In order to have all of these 4-40 and 6-32 tapered flat head screws sit flushly against each bracket, center bore the holes in the brackets. Chamfer the tail side of each hole in the servo bracket and the nose side of each hole in the motor bracket.

19. The last holes required to be drilled in the servo trays are those into which thin screws are inserted in order to hold each servo snuggly in its tray. Once the bracket/tray assembly is taken apart, see which corner of each tray has been marked to take a screw. Start with one tray by setting a Hitec servo in it and holding firmly the assembly of these two pieces. The best way to align screw holes with the mounting wings on each servo is to use an all to mark the drill point for each hole. And since the servo is taller than the tray, hold the tray so that it sits on the edge of a table or lab bench and so that the servo hangs below the surface of the table. Then, place the all down into the correct mounting hole and use a hammer to make a clear indention in the servo tray. The dimples created by the all serve to precisely guide the drill bit to the correct point of drilling. The key to this procedure is to adequately prepare the four mounting holes on each servo. Each servo includes four small rubber buffers and four small brass braces. The four mounting holes on each servo should be fitted with the rubber buffers and the brass braces. The rubber protects the plastic material used to construct the servos and the brass supports screws when they are tightly drawn into the servo trays. Assembling these pieces prior to marking drill points with the all makes it easier to hold the all straight and thus easier to accurately place each servo mounting hole.

20. Each of the servo mount holes must be tapped for a 3-48 screw. These are quite thin holes, so the tap is more delicate than larger taps. And relative to other taps used on this project, it is used a lot, so extra care should be taken when tapping the 3-48 holes. Since the holes are drilled

completely through the servo tray, one suggestion is to periodically remove the tap in order to clear the hole of oil and debris (ideally, compressed air would be available for cleaning).

21. The metal Hitec servo arm has four points at which a fin linkage can be connected. Use a hand drill to enlarge the second hole from the end of the servo arm. It needs to be slightly larger to accommodate the clevis that attaches to the arm. Use incremental changes from a 1.5 mm bit to a 1.8 mm bit or until the clevis fits in the hole.

22. MPI drills three 6-32 screw holes in each rail brace. Tap these hole using oil and the 6-32 tap.

23. The aluminum stock supplied by Lowe's hardware supply store is sold in three foot lengths; they must be cut to 20.5 inches for the current AUV specifications. Ensure 90 degree cuts on both ends of each piece. Again, the ISE Machine Shop may be helpful here.

24. In order to make rigid the pair of rails, and to mount electronics within the AUV, drill appropriately spaced holes along the rails, each point at which one of the support screws will stand. The following instructions explain where and why to drill each of the eight required holes. Also, since the support screws need to stand perpendicular to the floor, take care to ensure the spacing and centering of each hole on each rail. Use the scribe to mark all drill points, which should be measured to be along the center of the rail. These steps should ensure the screws' perpendicular orientation to the floor. There are eight holes in each rail: two for the rail brace and two for each of three sets of circuit boards.

    Start measuring from one end of the rails and work toward the opposite end. The first two holes are meant for the rail braces. The first is 20.32 mm from the end, the second 38.1 mm from the end. Drill for the clearance of a 6-32 screw. The rails are not threaded because removing the long support screws is time consuming and cumbersome since they must be unscrewed from the rail instead of just being pulled through the rail.

    Start the second set of holes by measuring 90 mm from the end. Then, for more accurate measuring and marking of these long distances, measure the fourth hole to be another 90 mm from the third (which is 180 mm from the end of origination).

    Start the third set by spacing the fifth hole 15 mm from the fourth hole; and the sixth 140 mm from the fifth.

    Lastly, set the seventh hole 20 mm from the sixth and the eighth hole 125 mm from the seventh.

    Drill one rail at a time; do not stack them and simultaneously drill multiple pieces.

25. Center bore these eight holes in the rails so that the tapered flat head support screws sit flushly with or slightly sunken into the top of the top rail. This ensures that they do not interfere with the insertion of the rails/electronics/tail into the hull.

26. Next, make the three fin linkages that connect the servo arms to their corresponding fins. The following four steps describe how to make fin linkages of relatively high integrity. Their susceptibility to breakage is described at the end of this section.

    First, acquire one primary linkage (Kavan HLFK0624) and one secondary linkage (Kavan HLFK0623), as well as the threaded brass end and nylon clevis that accompany the secondary linkage. Screw the metal clevis so that it rests halfway along its threaded post. Use wire cutters to shorten the primary linkage to a length of 95 mm, measured from the connection point of the metal clevis to the point at which the linkage is cut. Use wire cutters to *carefully* remove 17 mm of the outer two layers of stiffener, leaving an extending 17 mm length of piano wire. Note Figure A.5.

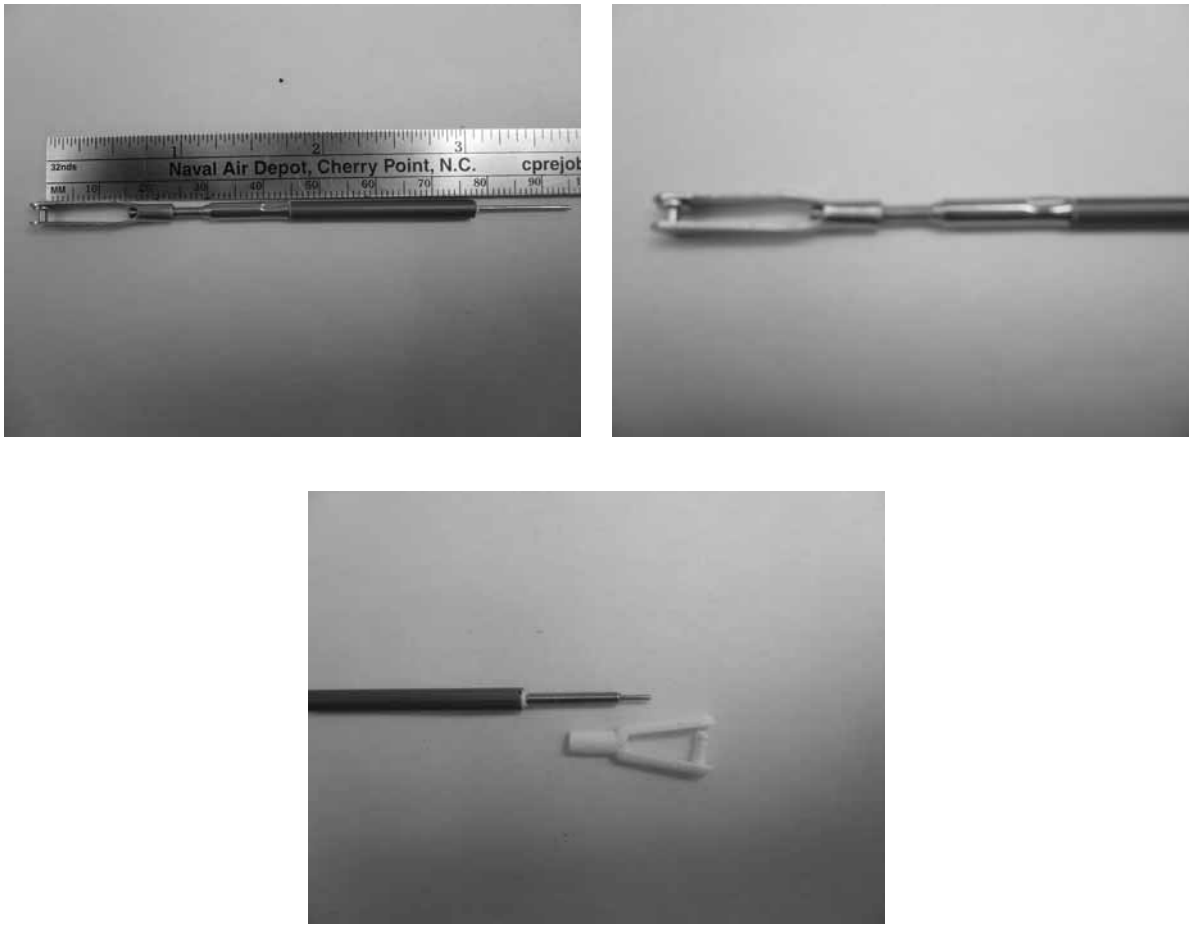

Figure A.5: Steps in linkage assembly

Second, attach the threaded brass post to the piano wire. To do so, line the exposed piano wire

with a thin line of liquid solder (available in the ASCL). Slide the brass post over the solder, coating evenly the inside of the post, all the way to the remaining stiffening layers. Solder the brass post at this point. Let the solder joint harden and cool thoroughly. Use needle-nose pliers to grip only a short length of the brass post and screw the nylon clevis onto the post. Thread it onto the brass post until the entire assembly is 101 mm long. Note again Figure A.5.

To further secure the brass post to the piano wire and stiffening layers of material, use Northeast Hobby Products Company, Incorporated Epoxy Number Five to make more secure the space between the plastic layers and the brass. Soldering melts away a bit of these plastic layers, so fill the remaining gap with epoxy.

Finally, if necessary, use a hand drill to enlarge the holes in the fin cranks to which the nylon clevis attaches. Some of the nylon pieces are too large for the small hole in the arm of the crank. It is easy to enlarge these holes with the hand drill - just be careful with the relatively thin drill bits that are required for this task.

To date, the linkages' single weakness has been that the piano wire pulls out of the primary linkage. Each time this may happen, remedy it by applying epoxy to the point of contact between the stiffening layers and the metal clevis.

27. Fins are made one at a time; they are molded from plastic that is the congealed mixture two liquid agents, one plastic, the other a hardener. Acquire the ASCL fin mold (designed and made by a previous ASCL graduate student), one finshaft, both of the PolyTek plastic ingredients, a scale, a styrofoam cup, and a cotton swab with one end removed. First, insert the finshaft in the lid of the mold so that the finshaft presses against the lid as tightly as it can. Then, insert the finshaft/lid assembly into the mold, taking care to keep the flat spot on the finshaft pointing squarely towards the thick part of the mold (the thick edge of the fin and the flat spot must point along the center of the rails towards the nose of the AUV). Once the finshaft is aligned *and* still flush with the lid of the mold, the mold is ready to be filled with plastic.

    PolyTek recommends that Part B of the mixture should have a mass that is 90 percent of the mass of Part A. Fins meet the hardness requirements of the ASCL as long as Part B of each fin has a mass of 90-95 percent of that of Part A. The higher the percentage, the harder the fin. Place the cup on the scale and tare the scale. Add about 10 grams of Part A to the cup. Calculate 90 percent of this mass, tare the cup/liquid combination, and add the appropriate mass of Part B. Pour Part B slowly because it is much denser than Part A. Use the cut end of the cotton swab

to stir the mixture. Stirring is *very* important. These liquids require a substantial amount of vigorous, thorough stirring in order to evenly mix. Not ensuring a thorough mixture will result in pockets of unhardened liquid in the fin mold, which are *very* difficult to clean out of the mold. So, mix thoroughly for about 30 seconds. Then slowly pour the plastic into the mold through the pour hole in the lid. *Do NOT overfill the mold or else there will not be enough exposed finshaft to grip with pliers when the fin needs to be removed.* After 30 minutes the fin is ready to be removed and trimmed to shape. Use pliers to pull the fin out of the mold.

28. Now trim the fin into its functional shape. Mark the thick (front) edge to be 42 mm long and the sharp (back) edge to be 58 mm long. Use a straight edge (should be flexible so as to bend along the fin's surface) to mark a line along which excessive material should be removed. Use the Dremel Tool to make initial cuts, removing a large majority of plastic and defining the shape of the fin. Use the sanding tip on the Dremel Tool to shape more precisely the plastic along the bottom of the fin and to remove nearly all of the plastic from the finshaft. Take care not to sand or knick the exposed metal of the finshaft, as it needs to maintain a smooth interface with the inside of the finshaft housing. Then use a carpet knife to remove remaining plastic from the finshaft and to make finer adjustments to the plastic that immediately surrounds the finshaft at the point at which it exits the plastic fin. Some custom shaving of plastic may be necessary with the carpet knife in order for each fin to spin freely through its required range of motion without intersecting the sloped outer circumference of the tail section. Use water to thoroughly cleanse the fin/finshaft combination of dust.

29. Each electronics card is mounted with modeling plastic to a pair of support screws. Depending on which of the three electronics mounting sections in which one needs to mount a circuit board, different boards take up different distances between the screws, so the remaining distance is bridged by two pieces of mounting plastic. Use 1.5 mm thick *Evergreen Scale Models* brand sheet styrene. First, measure the length of the card (use as an example, 70 mm). Then, measure the distance between the support screws that will support the card (e.g., 90 mm). Divide the difference by two; this is the distance between each end of the card and its support screw (e.g., $20/2 = 10$ mm). To ensure there being plenty of styrene to work with, add 10 mm (for all cards) to the length of the gap (e.g., $10 + 10 = 20$ mm). And to provide enough material to mount around the support screw, add another 5 mm (for all cards). This is how long one piece of styrene should be, 25 mm; it should be exactly the width of the card. Use a carpet knife to cut two identical pieces of styrene to have these measurements.

30. Drill holes in the corners of (or along the ends of) the circuit board; these will be for mounting the card to its corresponding plastic pieces. Use a 2.5 mm bit and a hand drill to make holes that will serve as a through hole for a 4-40 screw. PCB board is difficult to drill. Be careful not to drill too far into a card's corner, lest the corner break. Hold the board flush with a table top so as not to damage the electrical components that may already be attached to it. Take care not to let the drill bit wander along the PCB surface before actually piercing the material and beginning to drill.

31. Use the same 2.5 mm drill bit to bore appropriately located mounting holes in the card's styrene pieces. Remember to correctly space the plastic so that 10 mm overlaps the card, as this length is already factored into the size of the plastic piece. And use a 2.9 mm drill bit to bore a centered and correctly located hole for mounting to the support screws. Boring in this step need only consist of holding the drill bit in hand while turning the styrene piece with the opposite hand.

32. Depending on surface mount pieces that may be near the end of a given electronics card, some custom cutting may be necessary to allow the overlapping 10 mm of styrene to extend over the surface of the card. Use wire cutters to make necessary alterations to each piece so that it can fit around a capacitor, for example.

33. Make all of the necessary electrical connectors for the AUV. A variety of Hirose single and double row connectors are used for power and data transmission throughout the vehicle.

34. Cut the 4 inch tapered flat head 6-32 support screws to an 85 mm length with the screw cutting tool available in the ASCL. Once a screw is ready to be mounted, two 6-32 nuts are used to lock it in place at the top and bottom of the screw. The top nut fits snuggly against the bottom of the top rail, keeping the screw from sliding out through the top rail. And the bottom nut fits snuggly against the top of the bottom rail, keeping the screw from sliding further through the hole in the bottom rail.

35. Acquire one of the stainless steel worm-drive clamps and use the Dremel Tool cutting tip to trim the clamp to a 12 inch length. Use a file to remove all burrs and rough edges. Then, flatten the clamp enough to mark in its center a place to drill a hole. Drill a hole large enough to pass a quarter inch tube. This is a fairly difficult job for the hand drill and bits available in the ASCL, so it is suggested to use the ASCL machine for this operation.

36. The VT miniature AUV uses a small GPS antenna that must me mounted to the outside of the

vehicle because of how easily high frequency GPS signals attenuate in water. It is set upon a short mast that keeps the antenna above the surface of the water (when the AUV is on the surface). This mast is secured to the hull by fitting a portion of it through the hole in the worm-drive clamp and tightening the clamp about the hull. The mast is made from a section of aluminum tube stock that has 1/4 inch diameter and 1/32 inch walls. First, cut a section of aluminum of desirable length. This is done easily with the Dremel Tool because of the tube's small diameter. Then, use the Dremel Tool to cut 3/4 inch slits along opposite sides of one end of the tube. The easiest way to do this is to initially cut the slits at the same time; and then cut them individually once parallel cuts have been established. These slits leave two half circle sections of aluminum at the end of the mast. To fit the mast with the clamp, create a foot of sorts on the mast by using needle-nose pliers to bend one of these semi-circle sections. Then use regular pliers to flatten this bent section. Trimming the foot section may be necessary in order to fit the foot through the hole in the clamp. The aluminum is soft enough that this can be done easily with good wire cutter. Take care not to remove too much, as the foot needs to fit tightly between the clamp and the hull.

37. The GPS antenna must somehow be connected to the mast. This connection consists of five parts. First, waterproof the GPS receiver by filling and coating all of its openings with *VersaChem* silicon sealant. Allow this application of the sealant to dry and then recoat with another layer. This has proven a very dependable waterproofing strategy. The second is a styrene (same material used to mount electronics) shelf to which the antenna adheres with *VersaChem* silicon sealant. Cut the styrene to fit over the majority of and aligned with the surface area of the receiver's bottom. Use a 2.9 mm drill bit to bore a hole in the center of this styrene piece (in the same way electronics mounting holes were bored). Through this hole is passed a nail such that the head of the nail keeps it from going completely through the styrene.

38. For this nail to orient correctly with the mast's angle of tilt, it must be bent. Use vice-grip pliers to hold the head of the nail, then use regular pliers to bend the nail so that when the nail is inserted in the mast the head of the nail is parallel to the vehicle's hull. Insert the nail in the styrene shelf, center align it, and use silicon sealant to connect the antenna to the shelf. Stacked textbooks and a bag of lead shot are good for setting up the assembly to be thouroughly pressed and dried (Figure A.6).

39. Next, put a cotton swab up through the bottom of the aluminum mast. Stand the assembly in a

Figure A.6: GPS detail, orientation of GPS receiver with respect to AUV body (this nail requires more bending)

cup and pour into the tube a correctly mixed solution of PolyTek plastic. The cotton swab keeps the entire mast from filling with plastic and minimizes necessary clean-up. Once hardened, drips of plastic are easily peeled off of the tube's exterior. Use the ASCL hand drill to bore a hole in the plastic into which the nail can be inserted. The nail should fit snuggly in this hole.

40. Lastly, swab the nail with silicon sealant before inserting it into the mast. The sealant inside the hole and that which bundles around the top of the nail servo prevent the nail from twisting relative to the mast. This relatively insecure connection between the nail and the mast is desired, as perterbations to the mast that might otherwise break a rigid structure are with this configuration more likely not to severely break the mast or the connection between the mast and the antenna (Figure A.7).

41. Once the electronics have been mounted, a GPS mast height has been selected, and the GPS antenna cable has been cut to length, secure the GPS antenna cable and the RF antenna in their corresponding holes in the tail of the AUV. Pull both lengths of material into their desired orientations in the holes, ensuring that they are free from interference with other AUV components and operations. Use *VersaChem Super Blue II* sealant to fill the GPS hole and overlap the sealant with the PVC surrounding the hole. This material requires about 24 hours to cure. Use *VersaChem Silicone* to mount the RF whip antenna - the assembly of the cable screwed to the actual antenna - firmly in the housing created by the PVC tail. Once dried, coat the exterior of the seal with *VersaChem* silicon sealant (which can be worked with after a short time).

Figure A.7: GPS detail, silicone sealed connection between mast and nail

Appendix B

Mechanical Drawings for Machining Specialists

1. Driveshaft
2. Driveshaft Coupler
3. Motor Coupler
4. Driveshaft Housing
5. Tail Section
6. Finshaft Housing
7. Finshaft
8. Fin Crank
9. Servo Tray
10. Servo Bracket
11. Motor Bracket
12. Rail Brace
13. Nose Section
14. Driveshaft Assembly

Driveshaft
Caleb A. Sylvester, Christopher J. Cannell
Material: 316 Stainless Steel
Primary dimensions in millimeters, secondary dimensions in inches.
All surfaces machine tool finish except where noted.
NOTE the fits between this driveshaft and other components.

Last Updated: 14 January 2004, CAS

NOTE - This driveshaft is held in the driveshaft housing by a small, stainless steel bearing. The specific bearing is a McMaster-Carr product:

McMaster-Carr.com
Catalog page 1010, Miniature Precision Stainless Steel Ball Bearing - ABEC-5
Part Number 57155K36: 0.25" ID, 0.375" OD, 0.125" width.

FIT - The minor shaft diameter (shown as 6.325 mm) must maintain a LIGHT PRESS FIT with the ID of the bearing. See driveshaft_assembly_2d.dwg for more detail on placement and fit.

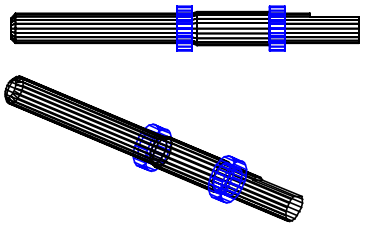

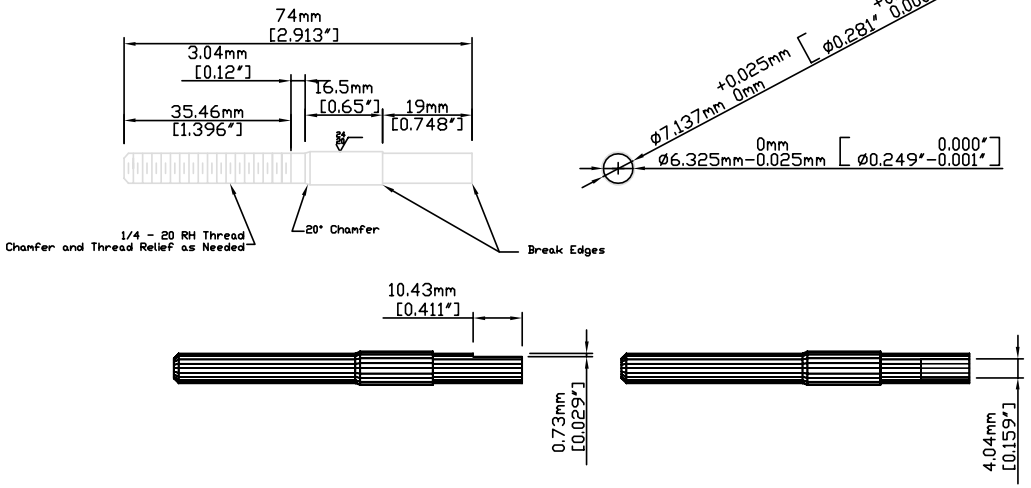

NOTE - The drive shaft requires a flat spot in order to accommodate a set screw.

Driveshaft Coupler, mounts to Driveshaft
Caleb A. Sylvester, Christopher J. Cannell
Material: 303 Stainless Steel
All units: Primary (mm), Secondary (inches)
All surfaces machine tool finish except where noted.
Break all edges, approximately .127mm[.005"]R.
NOTE the fits between this coupler and the driveshaft.

NOTE - This driveshaft coupler is used to couple the propeller on the vehicle's exterior to the motor's shaft on the interior. After placing the piece appropriately, we will drill and tap our own hole for a set screw. This set screw will secure the coupler to the flat spot on the driveshaft.

FIT - The slight lip on the ID of the coupler will keep the coupler from sliding too far onto the driveshaft. The larger ID (6.35 mm) should have a SLIP FIT with the unthreaded diameter of the driveshaft. See below as well as driveshaft_assembly_2d.dwg for more detail on placement and fit. See driveshaft_2d.dwg for dimensions on the driveshaft.

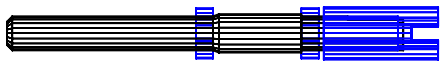

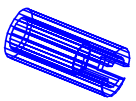

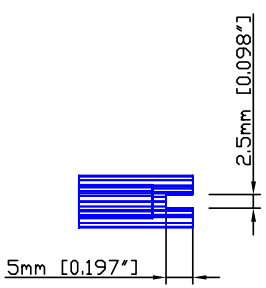

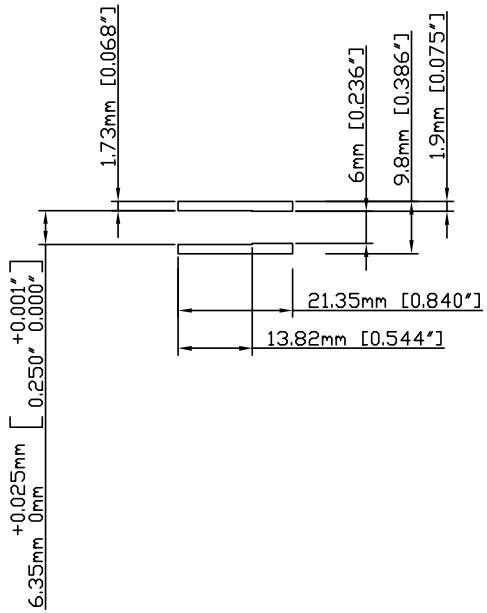

Motor Coupler, mounts to Motor
Caleb A. Sylvester, Christopher J. Cannell
Material: 303 Stainless Steel
All units: Primary (mm), Secondary (inches)
All surfaces machine tool finish except where noted.
Break all edges, approximately .127mm[.005"]R.
Updated last: 14 January 2004, CAS

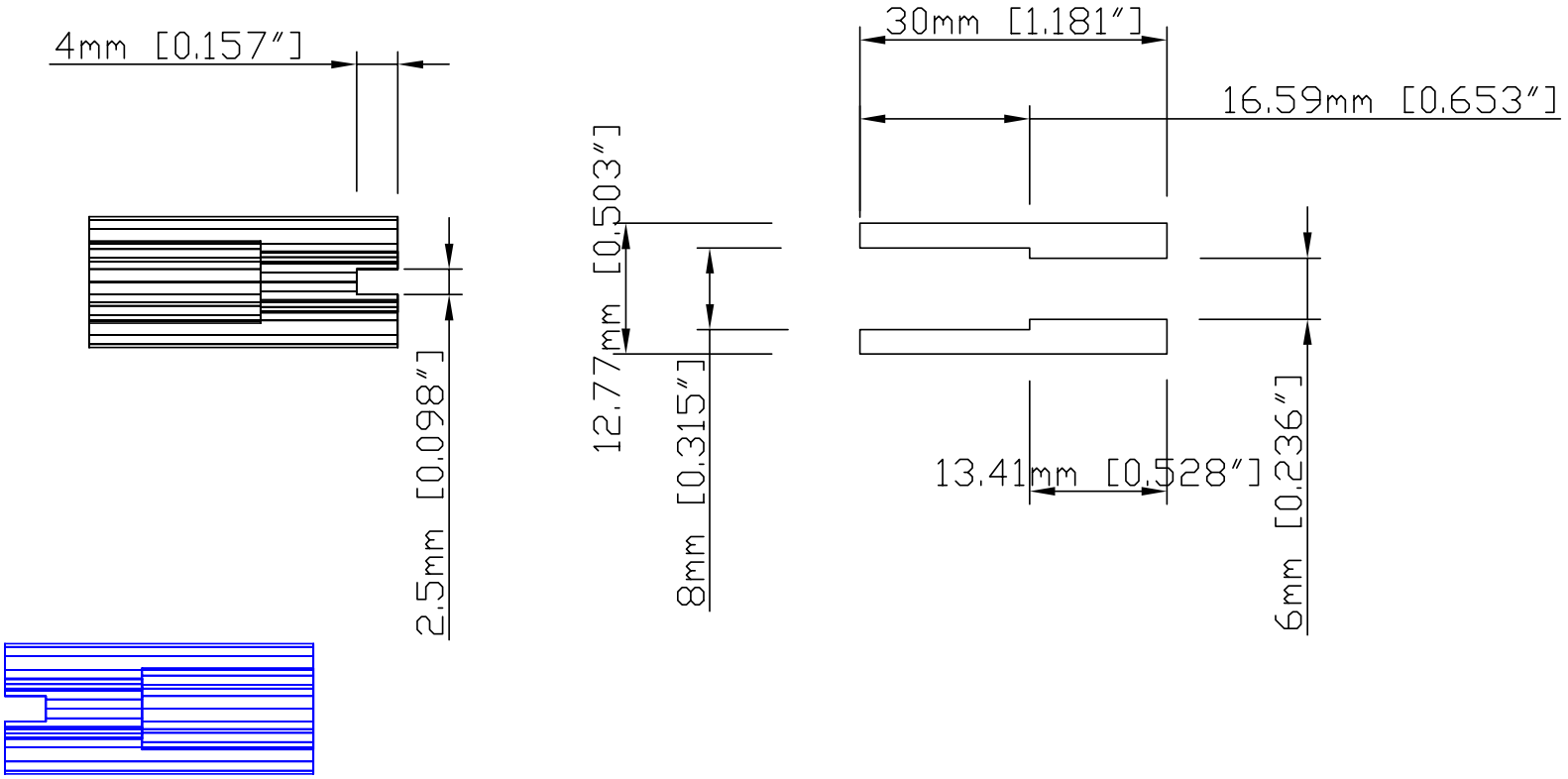

Driveshaft Housing
Caleb A. Sylvester, Christopher J. Cannell
Material: 6061 Aluminum
Primary dimensions in millimeters, secondary dimensions in inches.
Break all edges, approximately 0.127mm[0.005"]R.
NOTE the fits between this housing and other components.

FIT - This drive shaft housing fits into the large hole in the end of the tail piece. Both the ODs of this piece - the main length of the houseing (19.65mm) and the lip of the housing (3.18mm) - need to maintain an INTERFERENCE FIT tolerance with the inside of the hole in the tail. The fit between this housing and the tail piece MUST BE WATER-TIGHT. See tail.dwg for a better idea of placement.

NOTE - The bearings that stabilize the driveshaft are mounted in the ends of the driveshaft housing. The specific bearing is a McMaster-Carr product:

McMaster-Carr.com
Catalog page 1010, Miniature Precision Stainless Steel Ball Bearing - ABEC-5
Part Number 57155K36: 0.25" ID, 0.375" OD, 0.125" width.

FIT - The bearings will be mounted in the ends of the housing, so the (nominal) 9.52 mm ID at each end of the housing should maintain a LIGHT PRESS FIT with the OD of the bearings in order for the bearings to remain in place during the vehicle's operation. See driveshaft_assembly_2d.dwg for more detail on placement and fit.

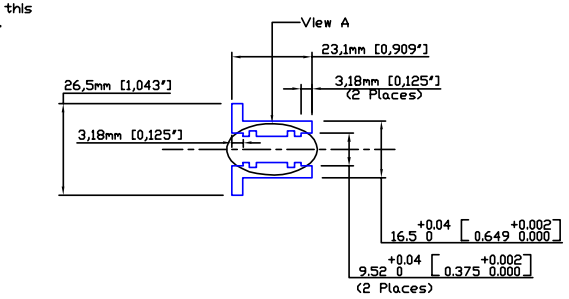

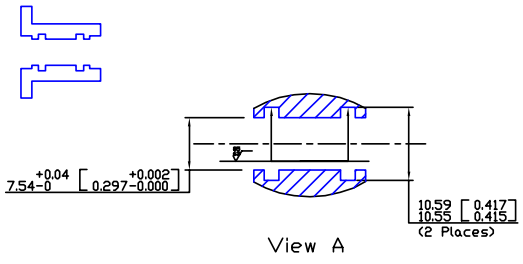

View A

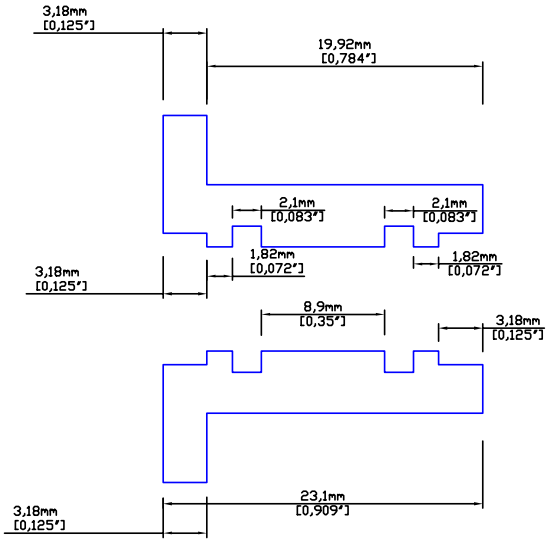

Tail Section

Material: Non-cellcore PVC or Delrin
All units: Primary (mm), Secondary (inches)
All surfaces machine tool finish except where noted.
Break all edges, approximately .127mm[.005"]R.
NOTE: the fits between this tail piece and other components.

FIT - This finshaft housing fits into the three small holes spaced at 120 degrees around the OD of the tail piece. Both the IDs of these holes - along the main length of the hole (10.44mm) and along the lip of the hole - need to maintain an INTERFERENCE FIT tolerance with the ODs of the Finshaft housing. The fit between these holes and the finshaft housing pieces MUST BE WATER-TIGHT. See finshaft_housing.dwg for a better idea of placement.
This placement and fit should be repeated for all three holes.

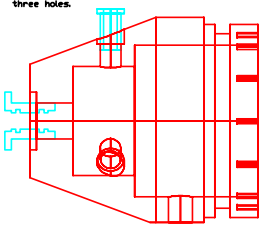

FIT - This large hole in the tail piece fits around the OD of the driveshaft housing. Both the IDs of this hole - along the main length (20mm) and along the lip of the hole (3mm) - need to maintain an INTERFERENCE FIT tolerance with the OD of the driveshaft housing. The fit between the tail and the driveshaft housing pieces MUST BE WATER-TIGHT. See driveshaft_housing_2d.dwg for a better idea of placement.

See Below, Detail A

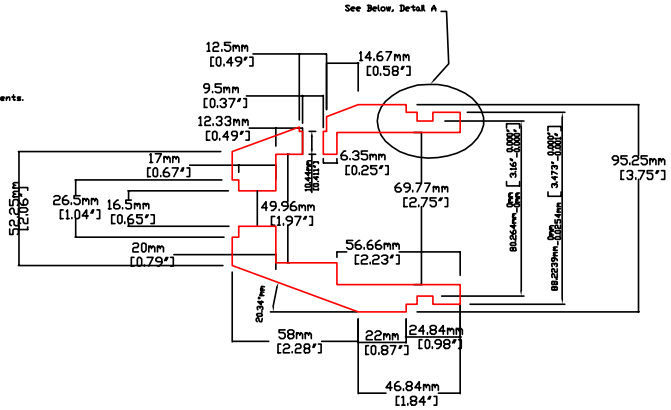

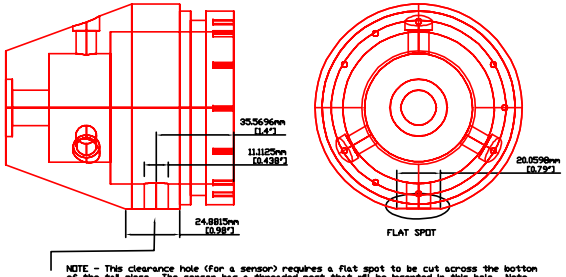

NOTE - This clearance hole (for a sensor) requires a flat spot to be cut across the bottom of the tail piece. The sensor has a threaded post that will be inserted in this hole. Note also that we DO NOT need a flat spot on the ID of the tail (we discussed needing this at our last meeting).

HOLE SPECIFICATIONS:

It is a clearance hole for 7/16" - 20 UNF-2A threaded piece of sensor.
This hole DOES NOT need to be tapped, just made to allow passage of the 7/16" threaded sensor.

Detail A

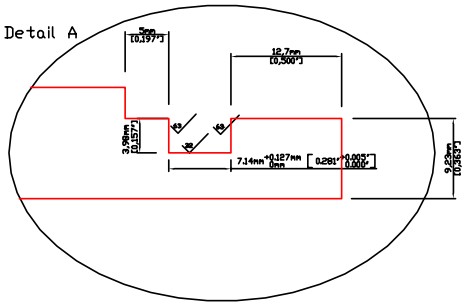

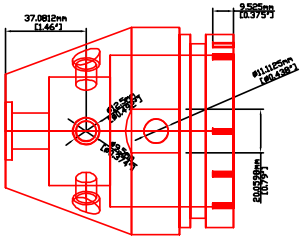

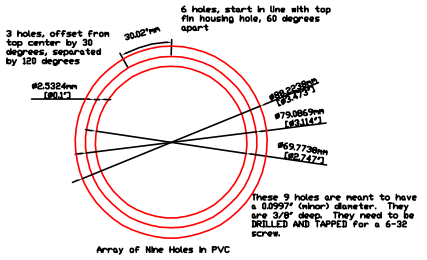

These 9 holes are meant to have a 0.0997" (minor) diameter. They are 3/8" deep. They need to be DRILLED AND TAPPED for a 6-32 screw.

Array of Nine Holes in PVC

Fin Shaft Housing
Caleb A. Sylvester, Christopher J. Cannell
Material: 6061 Aluminum
All surfaces machine tool finish except where noted.
Break all edges, approximately .127mm[.005"]R.
NOTE the fits between this tail piece and other components.

Description: The fin shaft housing is inserted into the tail and hold the fin shaft.

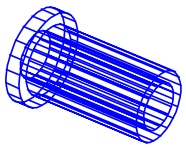

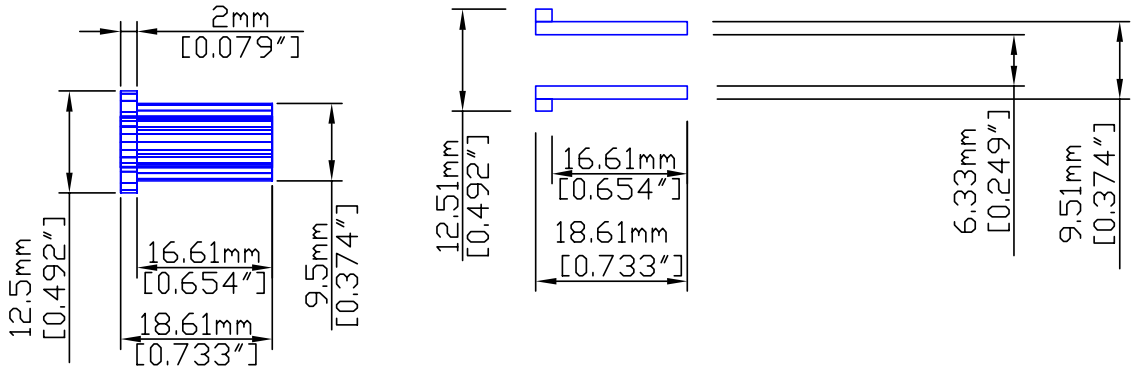

FIT - This finshaft housing fits into the three small holes spaced at 120 degrees around the OD of the tail piece. Both the ODs of this piece - along the main length of the houseing (16.61mm) and along the lip of the housing (2mm) - need to maintain an INTERFERENCE FIT tolerance with the inside of the holes in the tail. The fit between this housing and the tail piece MUST BE WATER-TIGHT. See tail.dwg for a better idea of placement.

Fin Shaft
Caleb A. Sylvester, Christopher J. Cannell
Material: 316 Stainless Steel
All surfaces machine tool finish except where noted.
Break all edges, approximately .127mm[.005"]R.

Description: Molded into the fin. Connects the fin with the fin crank.

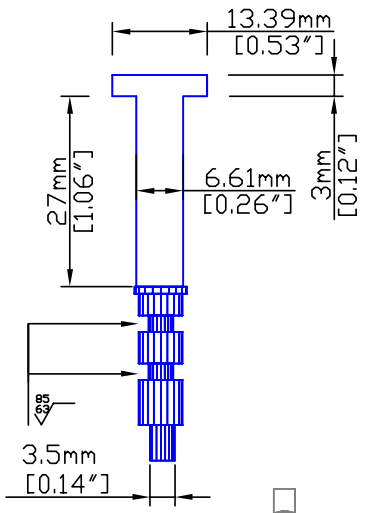

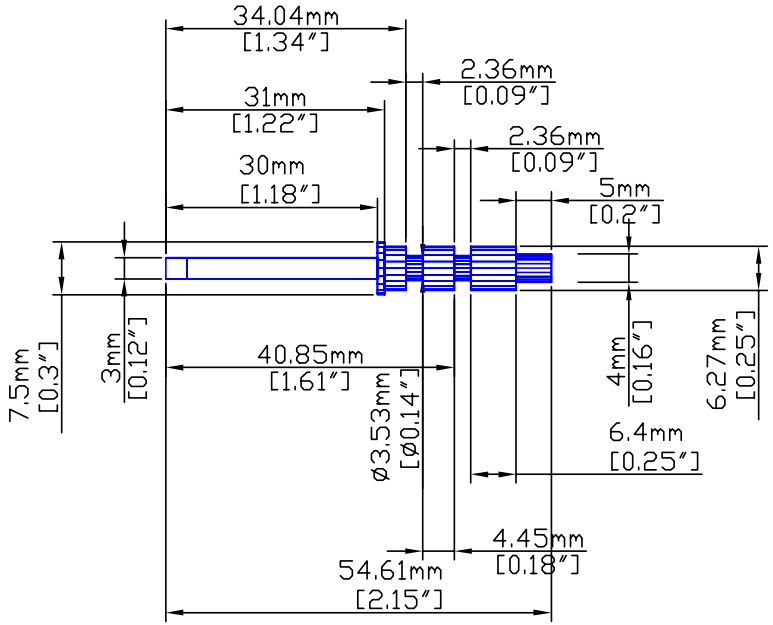

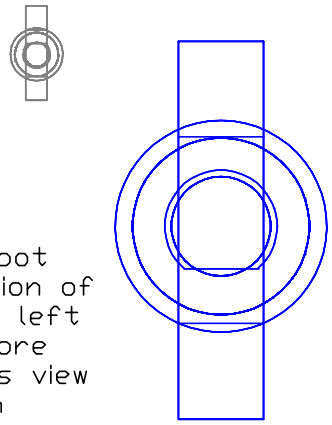

NOTE - please note the flat spot required on the end-most portion of the fin shaft. Dimensions were left off of this view in order to more easily show the flat spot. This view was achieved by scaling the fin shaft by 4 times.

Caleb A. Sylvester, Christopher J. Cannell
Material: 303 Stainless Steel
All surfaces machine tool finish except where noted.
Break all edges, approximately .127mm[.005"]R.

Description: Attaches to the fin shaft and pushrod coming from the servo.

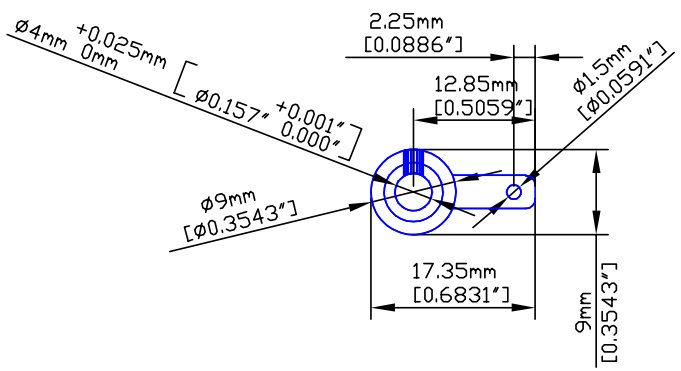

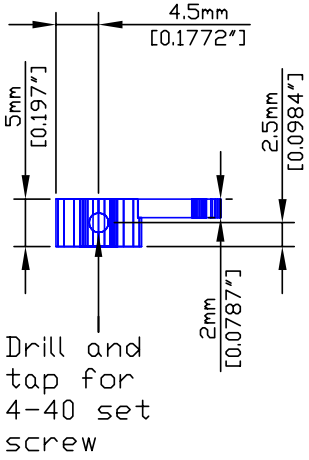

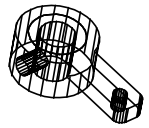

NOTE - This fin crank is used to couple the fin shaft (and fin) on the vehicle's exterior to the steering mechanism on the interior. The indicated set screw will secure the crank to the flat spot on the fin shaft.

FIT - The ID of the hole in the fin crank (4 mm) should have a SLIP FIT with the end of the fin shaft. See below for more detail on placement and fit. See finshaft.dwg for dimensions on the fin shaft.

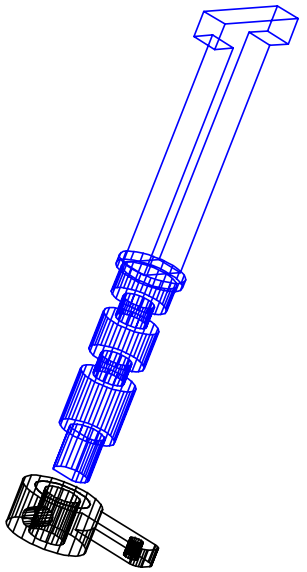

Servo Tray
Caleb A. Sylvester, Christopher J. Cannell
Material: 6061 Aluminum
All units: Primary (mm), Secondary (inches)
All surfaces machine tool finish except where noted.
Break all edges, approximately .127mm[.005"]R.

Description: The servo attaches to this piece and this joins the motor and servo brackets.

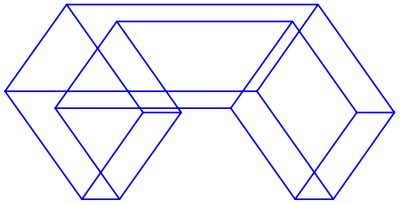

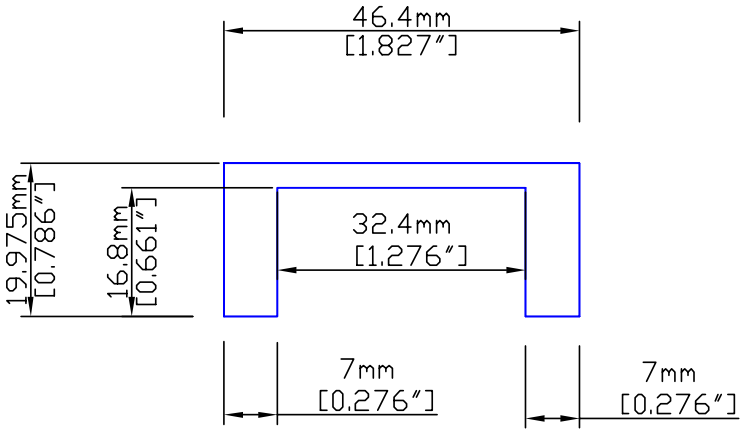

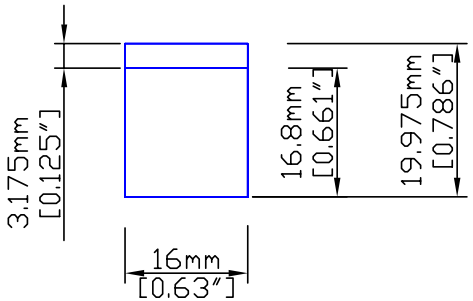

Servo Bracket
Caleb A. Sylvester, Christopher J. Cannell
Material: 6061 Aluminum
All units: Primary (mm), Secondary (inches)
All surfaces machine tool finish except where noted.
Break all edges, approximately .127mm[.005"]R.

Description: This piece attaches to the tail and the servo trays attach to it.

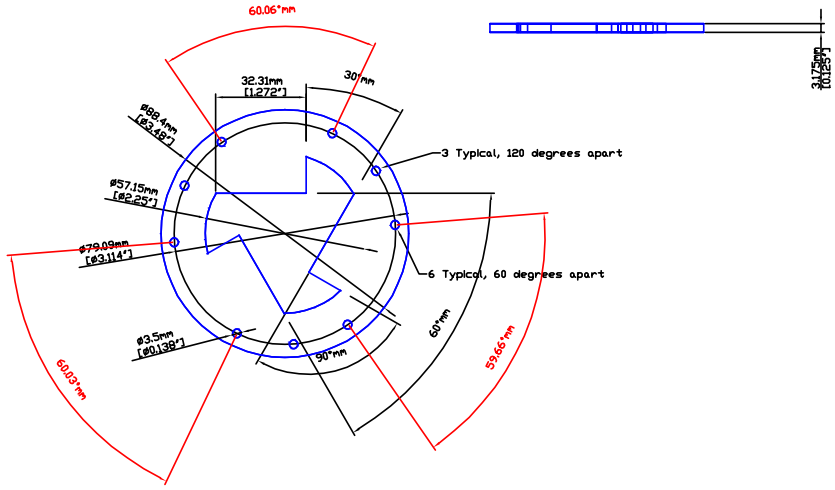

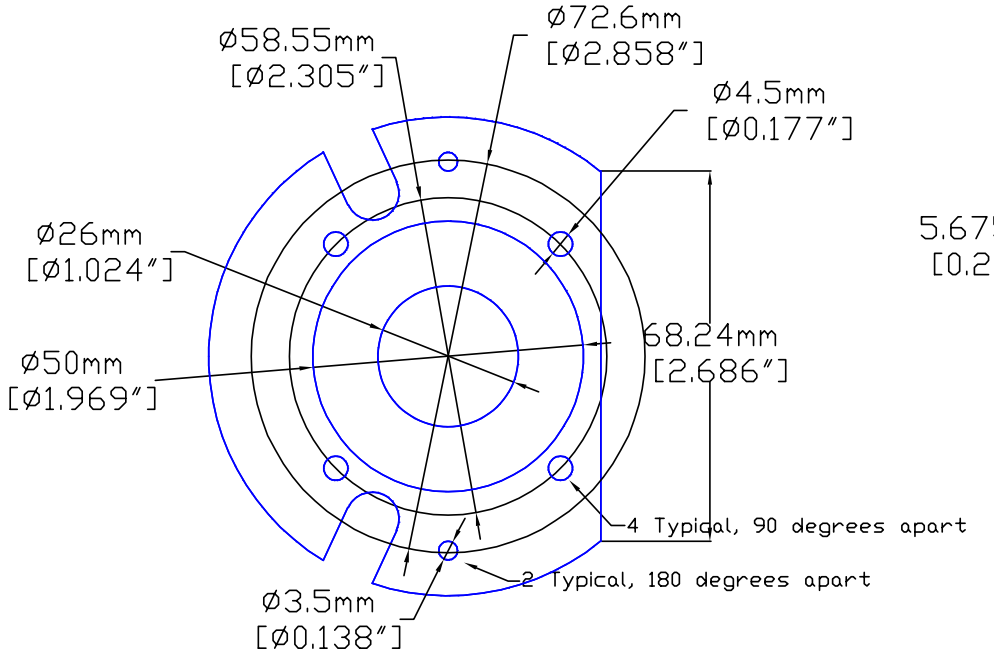

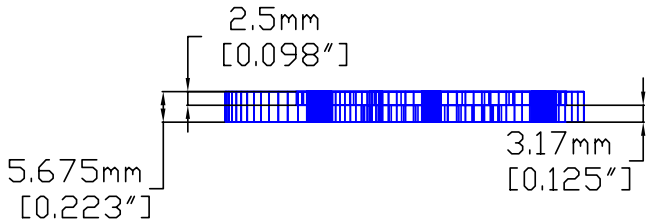

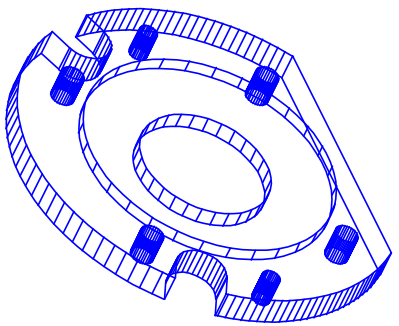

Motor Bracket
Caleb A. Sylvester, Christopher J. Cannell
Material: 6061 Aluminum
All units: Primary (mm), Secondary (inches)
All surfaces machine tool finish except where noted.
Break all edges, approximately .127mm[.005″]R.

Description: This bracket connects the motor and servo trays together. The rails mount to this as well.

Rail Brace
Caleb A. Sylvester
Material: 6061 Aluminum
All units: Primary (mm), Secondary (inches)
All surfaces machine tool finish except where noted.
Break all edges, approximately .127mm[.005"]R.

Description: The rails mount to these braces at the motor end of the vehicle.

Last Updated: 14 January 2004, CAS

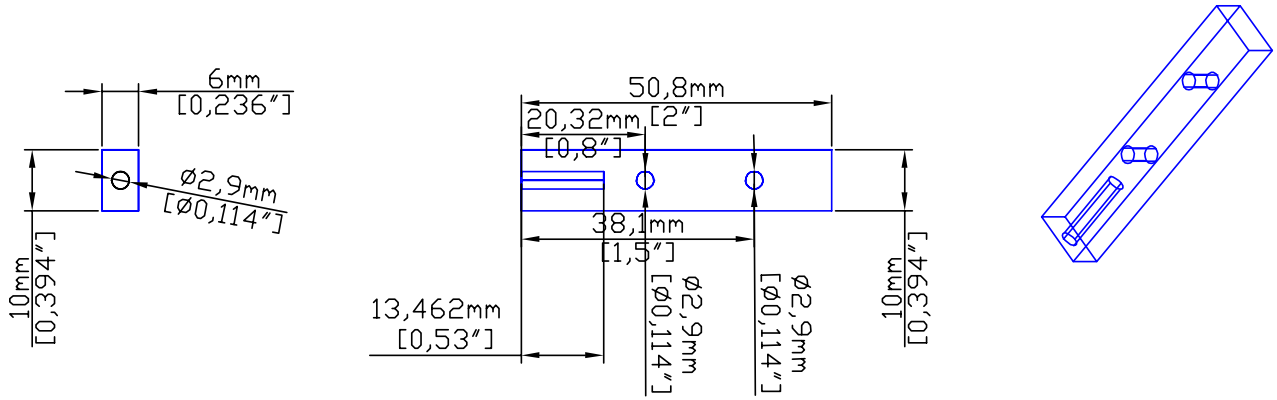

2.9mm holes are for 6-32 screws, 60% thread.
WE WILL TAP THESE HOLES OURSELVES!

Nose
Caleb A. Sylvester, Christopher J. Cannell
Material: Non Cell Core PVC
All units: Primary (mm), Secondary (inches)
All surfaces machine tool finish except where noted.
Break all edges, approximately .127mm[.005"]R.

Description: This is the front nose of the vehicle.

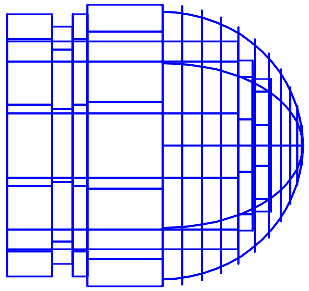

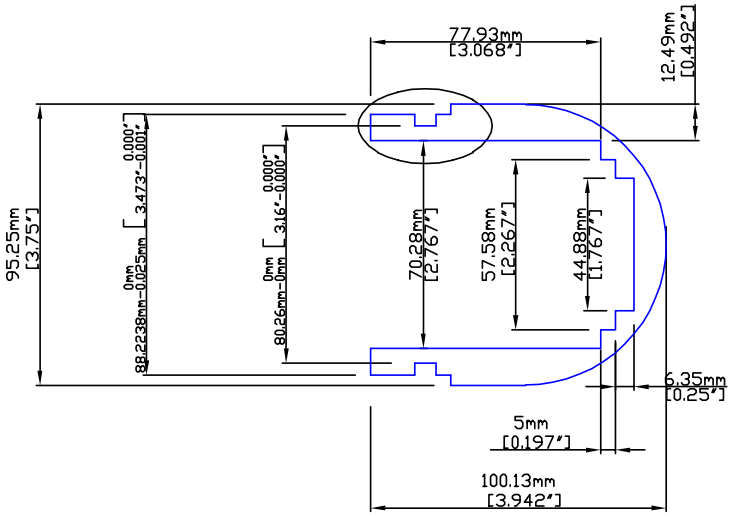

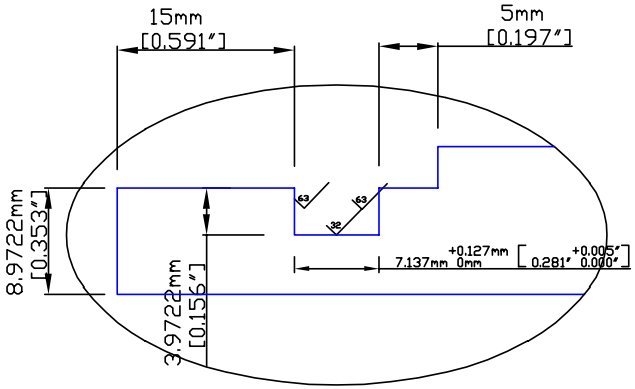

Driveshaft Assembly
Jared Mach, Caleb A. Sylvester, Christopher J. Cannell
Shows details of o-ring cuts and fits between different pieces.

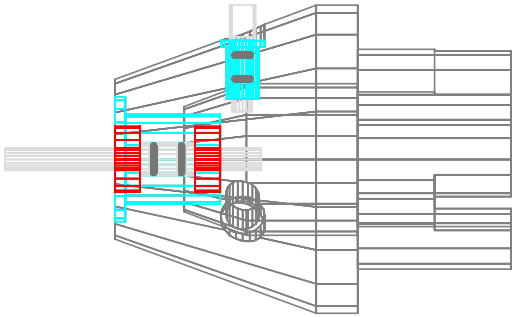

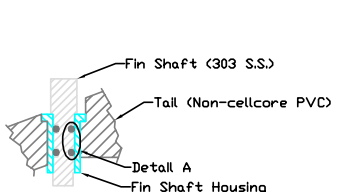

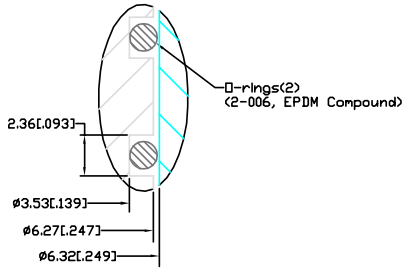

Detail A

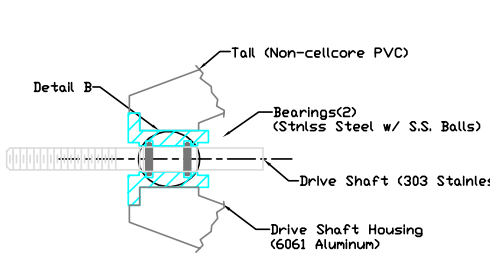

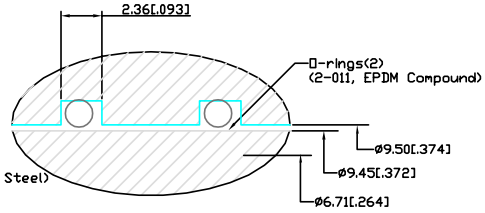

Detail B

Appendix C

Vendors and prices of VT Miniature AUV components

AUV Component	Price
driveshaft	$98.50
driveshaft coupler	$75.00
motor coupler	$75.00
driveshaft housing	$98.50
tail section	$450.00
finshaft housing	$37.50
finshaft	$112.50
fin crank	$62.50
servo tray	$37.50
servo bracket	$22.50
motor bracket	$42.00
rail brace	$10.00
nose section	$325.00

Table C.1: Parts machined by professional machinist

AUV Component	Vendor	Item Number	Price
propellor	HobbyLobby.com	5x2	$2.00
dogbone	RCModels.com	HPI 72072	$5.00
DC motor	Shinano Kenshi	LA052-040E	$112.00
Q4010, buna 70, quad ring	Pressure Seals, Inc	010BN70QR	
driveshaft bearing	McMaster-Carr	57155K36	$6.69
Q4006, buna 70, quad ring	Pressure Seals, Inc	006BN70QR	
10 pin bulkhead, 3/4" length thread	SeaCon	FAWM-10S-BC-R/A	$156.00
10 pin male dummy connector	SeaCon	FAWM-10PMPD	$76.00
10 pin connector (male)	SeaCon	FAWM-10P-MP	$150.24
nut, secures bulkhead	McMaster-Carr	91845A135	$6.31
washer, secures bulkhead	McMaster-Carr	93475A300	$5.63
servo linkages	Hobby-Lobby.com	HLFK0623	$5.90
servo linkages	Hobby-Lobby.com	HLFK0624	$8.50
3' x 3/4" W x 1/8"	Lowe's Hardware	alum stock	$3.50
support screw, 6-32, 4"	McMaster-Carr	90275A168	$10.42
1.5mm sheet styrene	Mish-Mish (art supply)	1, 1.5mm	$3.00
acrylic tube, 3.75" OD	Modern Plastics, Inc.	CAT3.7500DX.125	$39.90
1/2" black banding, 100'	McMaster-Carr	5188K45	$9.51
1/2" black buckle	McMaster-Carr	5188K56	$6.87
aluminum, .18" ID, 1/4" OD, .035" thick	McMaster-Carr	89965K42	$7.43
digital RC servo	ServoCity.com (HiTec)	HS-5245MG	$49.95

Table C.2: Vendors and prices of AUV components

VITA

Caleb Allen Sylvester

The author was born in Indiana and, along with five siblings, was reared mainly in Charlottesville, Virginia by his two loving parents. In May of 2002, he received his Bachelor of Science Degree in Electrical Engineering from Virginia Military Institute in Lexington, Virginia. He transitioned directly from VMI to Virginia Tech to pursue a Master's Degree in Electrical Engineering with a focus on control theory. Though he will dearly miss the town, people, and surrounding hills of Blacksburg, he is excited about his marriage and move elsewhere. Caleb plans to soon start a job at the National Ground Intelligence Center, in Charlottesville.